

ผลของอุณหภูมิการเผาและ โปแตสเซียมไดออกไซด์ต่อการเตรียมซิลิกา
จากถ่านแกลบเพื่อใช้เป็นสารลดการติดกันของฟิล์ม LLDPE



นายวีระศักดิ์ โมสูงเนิน

สถาบันวิทยบริการ

จุฬาลงกรณ์มหาวิทยาลัย

วิทยานิพนธ์นี้เป็นส่วนหนึ่งของการศึกษาตามหลักสูตรปริญญาวิทยาศาสตรมหาบัณฑิต

สาขาวิชาเทคโนโลยีเซรามิก ภาควิชาวัสดุศาสตร์

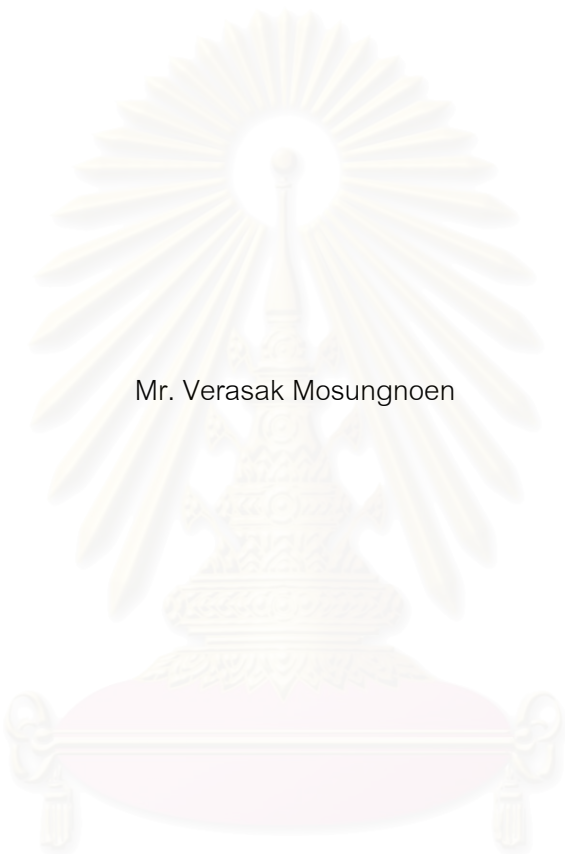
คณะวิทยาศาสตร์ จุฬาลงกรณ์มหาวิทยาลัย

ปีการศึกษา 2549

ISBN 974-14-2578-3

ลิขสิทธิ์ของจุฬาลงกรณ์มหาวิทยาลัย

EFFECTS OF BURNING TEMPERATURE AND K_2O ON PREPARATION OF SILICA
FROM RICE HUSK ASH FOR ANTI-BLOCKING APPLICATION IN LLDPE FILM



Mr. Verasak Mosungnoen

สภามหาวิทยาลัย
จุฬาลงกรณ์มหาวิทยาลัย

A Thesis Submitted in Partial Fulfillment of the Requirements
for the Degree of Master of Science Program in Ceramic Technology
Department of Materials Science

Faculty of Science

Chulalongkorn University

Academic Year 2006

ISBN 974-14-2578-3

Copyright of Chulalongorn University

Thesis Title EFFECTS OF BURNING TEMPERATURE AND K₂O ON
PREPARATION OF SILICA FROM RICE HUSK ASH FOR ANTI-
BLOCKING APPLICATION IN LLDPE FILM

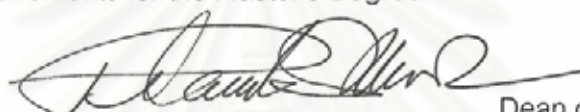
By Mr. Verasak Mosungnoen

Field of Study Ceramic Technology

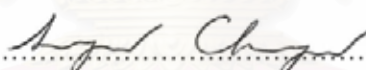
Thesis Advisor Professor Shigetaka Wada, Ph.D.


Thesis Co-advisor Wannee Chinsirikul, Ph.D.


Accepted by the Faculty of Science, Chulalongkorn University in Partial
Fulfillment of the Requirements for the Master's Degree



.....Dean of the Faculty of Science
(Professor Piamsak Menasveta, Ph.D.)


THESIS COMMITTEE


.....Chairman
(Associate Professor Saowaroj Chuayjuljit)


.....Thesis Advisor
(Professor Shigetaka Wada, Ph.D.)


.....Thesis Co-advisor
(Wannee Chinsirikul, Ph.D.)


.....Member
(Associate Professor Supatra Jinawath, Ph.D.)


.....Member
(Assistant Professor Sirithan Jiemsirilers, Ph.D.)

วีระศักดิ์ โมสูงเนิน : ผลของอุณหภูมิการเผาและโปแตสเซียมไดออกไซด์ต่อการเตรียมซิลิกาจากเถ้าแกลบเพื่อใช้เป็นสารลดการติดกันของฟิล์ม LLDPE. (EFFECTS OF BURNING TEMPERATURE AND K_2O ON PREPARATION OF SILICA FROM RICE HUSK ASH FOR ANTI-BLOCKING APPLICATION IN LLDPE FILM) อ. ที่ปรึกษา: ศาสตราจารย์ ดร. ชิกพาทะ วาดะ, อ.ที่ปรึกษาร่วม : ดร.วรรณิ์ ฉินศิริกุล 107 หน้า. ISBN 974-14-2578-3.

ซิลิกาอสัณฐานในเถ้าแกลบสามารถเปลี่ยนไปเป็นผลึกคริสโตบาไลต์และมีทริโดไมท์เกิดร่วมด้วยในปริมาณเล็กน้อยที่อุณหภูมิสูงกว่า 900 องศาเซลเซียส โดยในเถ้าแกลบมีปริมาณของโปแตสเซียมไดออกไซด์ประมาณ 2 เปอร์เซ็นต์โดยน้ำหนัก ซึ่งทำหน้าที่ลดจุดหลอมเหลวของซิลิกาในเถ้าแกลบและ เกิดเป็นผลึกคริสโตบาไลต์ที่อุณหภูมิต่ำ เถ้าแกลบดำสามารถเผาสังเคราะห์ได้ คริสโตบาไลต์และทริโดไมท์ที่อุณหภูมิต่ำ 1200 องศาเซลเซียส เป็นเวลา 4 ชั่วโมง เมื่อนำตัวอย่างที่ได้มาบดด้วยเครื่องบดที่ใช้ลม หลังจากนั้นนำไปผสมกับพลาสติกประเภทพอลิเอทิลีนชนิดความหนาแน่นต่ำเชิงเส้นตรง (แอลแอลดีพีอี) ด้วยเครื่องอัดรีดแบบเกลียวคู่แล้วเป่าขึ้นรูปเป็นฟิล์มแอลแอลดีพีอี ด้วยเครื่องเป่าฟิล์ม เมื่อเปรียบเทียบสมบัติของฟิล์มพลาสติก ที่ใช้สารลดการติดกันระหว่าง คริสโตบาไลต์เกรดทางการค้าและคริสโตบาไลต์ที่สังเคราะห์ได้จากเถ้าแกลบพบว่า มีสมบัติแรงดึงเชิงกลและสมบัติทางแสงใกล้เคียงกัน อย่างไรก็ตามรายงานการศึกษาบางฉบับในต่างประเทศได้ระบุว่า คริสโตบาไลต์เป็นสารก่อมะเร็งชนิดหนึ่งซึ่งควรมีการระมัดระวังในการนำไปใช้ ส่วนซิลิกาอสัณฐานนั้นยังคงเป็นอีกหนึ่งตัวเลือกที่สามารถใช้เป็นสารลดการติดกันในฟิล์มพลาสติกได้ซึ่งสามารถขึ้นรูป ด้วยกระบวนการชนิดเดียวกันและลดอุณหภูมิในการเผาลงมาเป็น 650 องศาเซลเซียสเป็นเวลา 1 ชั่วโมง เมื่อเปรียบเทียบสมบัติทางแสงและสมบัติแรงดึงเชิงกลโดยทั่วไปพบว่า มีค่าไม่แตกต่างจากฟิล์มพลาสติกที่ใช้คริสโตบาไลต์เป็นสารลดการติดกันของฟิล์ม

จุฬาลงกรณ์มหาวิทยาลัย

ภาควิชา.....วัสดุศาสตร์.....ลายมือชื่อนิสิต.....*ว.ศักดิ์ โมสูงเนิน*
 สาขาวิชา.....เทคโนโลยีเซรามิก.....ลายมือชื่ออาจารย์ที่ปรึกษา.....*Wada*
 ปีการศึกษา.2549.....ลายมือชื่ออาจารย์ที่ปรึกษาร่วม.....*Shinichi*

4772485323 : MAJOR CERAMIC TECHNOLOGY

KEY WORD: RH / RHA / AMORPHOUS SILICA / CRISTOBALITE / TRIDYMITTE

VERASAK MOSUNGNOEN : EFFECTS OF BURNING TEMPERATURE AND K_2O ON PREPARATION OF SILICA FROM RICE HUSK ASH FOR ANTI-BLOCKING APPLICATION IN LLDPE FILM. THESIS ADVISOR: PROF. SHIGETAKA WADA, Ph.D., THESIS COADVISOR : WANNEE CHINSIRIKUL, 107 pp. ISBN 974-14-2578-3.

Amorphous silica (SiO_2) in rice husk ash (RHA) was transformed to cristobalite with some amount of tridymite at over $900^\circ C$. The RHA included about ~ 2 wt% of potassium oxide (K_2O). The K_2O played an important role in reducing the melting temperature of SiO_2 in RHA and in re - crystallization of amorphous silica to cristobalite at lower temperature. The RHA from rice mill factory was transformed to cristobalite/tridymite by heat treatment at $1,200^\circ C$ for 4 h. Such resulting powder was ground with air jet mill and mixed to make a masterbatch with linear low density polyethylene (LLDPE) by twin-screw extruder. LLDPE film was prepared by a common film blowing extruder. Film properties containing commercial grade anti-blocking cristobalite was compared with the film containing cristobalite from rice husk, prepared in this study. It was found that transparency and mechanical tensile strength of the two film types were relatively the same. However, some reports published in other countries indicate that cristobalite is considered as a carcinogenic material. Amorphous silica is, so far, another candidate for use as anti-blocking agent in plastic films. From this study, amorphous silica could be produced by a similar process as compared to that for cristobalite, but at lower burning temperature of $650^\circ C$ for 1 h. The optical and tensile properties of the films with amorphous SiO_2 is equivalent to those containing cristobalite.

Department.....Materials Science..... Student's Signature.....*V. Mosungnoen*
 Field of Study.....Ceramic Technology..... Advisor's Signature.....*S. Wada*
 Academic Year2006.....Co-advisor's Signature.....*Wanee Chinsirikul*

ACKNOWLEDGEMENTS

I would like to thank Prof. Dr. Shigetaka Wada, my thesis advisor, for his help and valuable suggestions. My thanks are also to Dr. Wannee Chinsirikul, my thesis co-advisor for her suggestions and for providing me understanding of plastic film production process. I would like to thank Associate Professor Saowaroj Chuayjuljit for her advice and for guiding me to some important data for this thesis. I am very grateful to Thailand Graduate Institute Technology Center (TGIST), National Metal and Materials Technology Center (MTEC), Metallurgy and Materials Science Research Institute, Associate Professor Dr. Khemchai Hemachanda and Dr. Angkhana Jaroenworoluck, for all supports including raw material, equipment and in particular the financial support from TGIST and MTEC. I would like to thank Mr. Noppadon Kerddonfag for his technical assistance with blown film process.

I would like to thank Associate Professor Dr. Supatra Jinawath, Assistant Professor Dr. Sirithan Jiemsirilers and all my teachers in Materials Science Department, all my friends. I will not forget Mr. Soontorn and Mr. Nirut for guide given to me how to study and spend my life in Chula. It was a golden experience time to get many things in warm house.

Finally, I am very grateful to my family for moral and financial supports, love, encouragement and understanding.

สถาบันวิทยบริการ
จุฬาลงกรณ์มหาวิทยาลัย

CONTENTS

	Page
Abstract (Thai).....	iv
Abstract (English).....	v
Acknowledgments.....	vi
Contents.....	vii
List of tables	ix
List of figures	x
Chapter I Introduction	1
Chapter II Literature reviews	3
2.1 Background	3
2.2 Amorphous silica (Noncrystalline silica)	3
2.3 Silica in rice	4
2.4 Crystallization of silica by heat treatment	5
2.5 Effect of alkali ion and particle size of silica on crystallization of silica.....	8
2.6 Preparation and characterization of high-grade silica from rice husk	10
2.7 Use of silica from rice husk as anti-blocking agent in low-density polyethylene films	12
Chapter III Experimental procedures.....	14
3.1 Experiment on anti-blocking powder	14
3.1.1 Effect of washing and heat treatment conditions on properties of RHA	14
3.1.2 Production and evaluation of LLDPE film with synthesized powders as an anti-blocking agent	19
3.2 Water glass synthesis from amorphous silica.....	23
3.3 Analysis and heat treatment of ashes from factories and power plants.	24
3.4 Experiment on various washing conditions.	24
3.5 Experiment on low temperature calcining for RH from different sources	26
Chapter IV Results and discussions.....	27
4.1 Effect of alkaline oxide elimination by washing on the crystallization of RHA.....	27
4.1.1 Properties of starting raw materials	27
4.1.2 Crystallization of RHA	28
4.1.3 Morphology of heat treated samples by scanning electron microscope.....	34

4.1.4 Specific surface area.....	35
4.2 Application of RHA	36
4.2.1 Application of cristobalite as an anti-blocking agent.....	36
4.2.2 Application of amorphous silica as an anti-blocking agent	46
4.2.3 Water glass from amorphous silica.....	53
4.3 RHA from factories and power plants.....	56
4.3.1 Crystal phase.....	56
4.3.2 Oxidation of ashes from gasification furnaces.....	59
4.3.3 Mass loss of gasification furnace ashes after oxidation.....	60
4.4 Effect of various washing conditions on the remaining K_2O	61
4.5 RHA from two different provinces.....	63
Chapter V Conclusions.....	67
Chapter VI Future work	68
References.....	69
Appendices.....	71
Appendix A.....	72
Appendix B.....	73
Appendix C.....	82
Appendix D.....	84
Appendix E.....	92
Appendix F.....	105
Biography.....	107

LIST OF TABLES

	Page
Table 2.1 XRD analysis of heat treated samples at specified heat treatment conditions.	9
Table 2.2 Properties of RHA treated by various conditions	11
Table 2.3 Comparison data between silica from rice husk ash and aerosol OX50.....	12
Table 2.4 Comparison data between silica from rice husk ash and Sylo-1	13
Table 4.1 Chemical composition of rice husk ash (RHA) by XRF	27
Table 4.2 Specific surface area of RHA treated at different conditions	36
Table 4.3 Oil absorption and average grain size of synthesized and commercial cristobalite samples.....	39
Table 4.4 Chemical composition of rice husk ash (RHA) by XRF	48
Table 4.5 Properties of amorphous silica powder	50
Table 4.6 The crystal phase of ashes from factories and power plants.....	57
Table 4.7 Summarize the crystal phase of ashes from factories and power plants.....	59
Table 4.8 RHA from factories burnt in oxidation condition at various temperatures.	60

สถาบันวิทยบริการ
จุฬาลงกรณ์มหาวิทยาลัย

LIST OF FIGURES

	Page
Figure 2.1 Absorption and collection of silica in rice plant	5
Figure 2.2 Polymorphic transformations in silica	6
Figure 2.3 The structure “a” changes to collapsed forms “b” and “c” by displacive transformation and reconstructive form “d”.	7
Figure 2.4 XRD patterns of amorphous silica with sodium (1Na/SiO ₂) and heat treated at 500°C (a) and 800°C (b).	8
Figure 2.5 XRD patterns of amorphous silica with potassium (4K/SiO ₂) and heat treated at 500°C (a), 800°C (b) and 1000°C (c)	9
Figure 2.6 XRD patterns of 7-10 nm RH particle heat treated at 900°C	10
Figure 3.1 Flow chart of over all process of experiment	15
Figure 3.2 Flow chart of washing method and condition	16
Figure 3.3 Flow chart of incineration method and condition	17
Figure 3.4 Flow chart of producing LLDPE film with cristobalite as an anti-blocking agent	20
Figure 3.5 Blown film process.....	21
Figure 3.6 Air jet mill of the Metallurgy and Materials Science Research Institute, Chulalongkorn University.....	22
Figure 3.7 Flow chart of producing LLDPE film with amorphous silica as an anti-blocking agent	22
Figure 3.8 Flow chart of synthesized water glass from amorphous silica.....	23
Figure 3.9 Flow chart of various washing process.....	25
Figure 3.10 Flow chart of low temperature calcining	26
Figure 4.1 XRD patterns of silica glass sieved through a 100-mesh brass screen and heat treated at 1000°C and 1400°C for 2 h.	28
Figure 4.2 XRD patterns of quartz sieved through a 100-mesh brass screen and heat treated at 1400°C for 2 h.	29
Figure 4.3 XRD patterns of RHA of untreated RH not sieved and heat treated at 800°C, 900°C, 1000°C, 1100°C, 1200°C, 1400°C and 1500°C for 2 h.....	30

Figure 4.4 XRD patterns of RHA water treated RH, sieved through a 100-mesh brass screen and heat treated at 900°C, 1000°C, 1100°C, 1200°C, 1300°C, 1400°C and 1500°C for 2 h.	31
Figure 4.5 XRD patterns of RHA HCl treated RH, sieved through a 100-mesh brass screen and heat treated at 900°C, 1000°C, 1100°C, 1200°C, 1300°C, 1400°C and 1500°C for 2 h.	32
Figure 4.6 SEM photograph of untreated RHA, no sieved and heat treated at 1000°C for 2h.....	34
Figure 4.7 SEM photograph of untreated RHA, #100 sieved and heat treated at 1400°C for 2h.....	34
Figure 4.8 SEM photograph of water treated RHA, #100 sieved and heat treated at 1400°C for 2h.....	35
Figure 4.9 SEM photograph of HCl treated RHA, #100 sieved and heat treated at 1400°C for 2h.....	35
Figure 4.10 XRD patterns of B-RHA # 50 after heat treated at various temperatures and times	37
Figure 4.11 Appearance of heat treated B-RHA at various conditions, from 1000 to 1400°C for 2 h and 4 h	38
Figure 4.12 XRD patterns of B-RHA # 50 heat treated at 1200°C 4h, crushed and sieved by Air jet mill.....	39
Figure 4.13 Particle size distribution of ground and commercial grade samples	40
Figure 4.14 SEM photograph of B-RHA # 50 heat treated at 1200°C for 4 h. (before grinding).....	40
Figure 4.15 SEM photograph of synthesized cristobalite (R-3-CY).....	40
Figure 4.16 SEM photograph of synthesized cristobalite (R-4-CY).....	41
Figure 4.17 SEM photograph of synthesized cristobalite (R-5-CY).....	41
Figure 4.18 Color of masterbatches with different cristobalite powders.....	41
Figure 4.19 Blown film process.....	42
Figure 4.20 Relationship between wavelength (nm) and transmittance (%T) of plastic films with anti-blocking power of 1 and 2 wt% and control LLDPE film.	43

Figure 4.21 Percent elongation at break of plastic films with 4 kinds of cristobalite and tested in machine direction (MD) and transverse direction (TD).....	44
Figure 4.22 Tensile stress at break of plastic films with 4 kinds of cristobalite and tested in machine direction (MD) and transverse direction (TD).....	45
Figure 4.23 Flow chart of synthesizing amorphous RHA	47
Figure 4.24 XRD patterns of amorphous silica untreated and water treated and ground by Air jet mill.....	49
Figure 4.25 Particle size distribution of ground amorphous silica.....	49
Figure 4.26 Masterbatch of plastic samples.....	50
Figure 4.27 Relationship between wavelength (nm) and transmittance (%T) of plastic films with amorphous silica of 1 and 2 wt% as an anti-blocking agent.....	51
Figure 4.28 Percent elongation at break and various kinds of plastic films with 1-2% of amorphous silica tested in machine direction (MD) and transverse direction (TD).....	52
Figure 4.29 Tensile stress at break and various kinds of plastic films with 1-2% of amorphous silica tested in machine direction (MD) and transverse direction (TD).....	53
Figure 4.30 The process flow chart to synthesize water glass from (a) quartz and (b) amorphous silica.....	54
Figure 4.31 Phase diagram of $\text{SiO}_2 - \text{Na}_2\text{O} - \text{H}_2\text{O}$	55
Figure 4.32 Relationship of silica content (wt%) in RH and various washing conditions	61
Figure 4.33 Relationship of potassium content (wt%) in RH and various washing conditions.	62
Figure 4.34 XRD patterns of RHA washed by washing machine with water for 15, 30 and 45 min.....	62
Figure 4.35 XRD patterns of RHA soaked in water for 24 and 48 h.....	63
Figure 4.36 Relationship of wt% silica and various temperature following 450, 550 and 650°C compare of sources.....	64
Figure 4.37 Relationship of wt% potassium and various temperature following 450, 550 and 650°C compare of sources.....	64

Figure 4.38 XRD patterns of RHA of Nakhonratchasima province calcined at 450, 550 and 650°C.....	65
Figure 4.39 XRD patterns of RHA of Ratchaburi province calcined at 450, 550 and 650°C.....	66



สถาบันวิทยบริการ
จุฬาลงกรณ์มหาวิทยาลัย

CHAPTER I

INTRODUCTION

The world rice production as paddy is more than 550,000,000 tons/year. Thailand was the sixth in the world rice production in 2002 as shown in Table 1, Appendix A. The production of rice paddy and rice husk in Thailand are 27,000,000 ton and 5,400,000 ton in 2002, respectively. Moreover, Thailand is number one in the world rice export (10 million ton in 2004, 7.2 million ton in 2005) [1].

It is well known that silica is included in rice husk (RH) since 1983 [2]. The amount of silica in rice husk varies between 13-29% depending on geographic location. The rice husk ash (RHA) (18% from husk) is estimated as 972,000 tons per year in Thailand.

The ash contains 87-97% silica and some amount of organics, alkali oxide, and impurities [3]. The rice husk ash has been a major concern of many researchers. The applications of rice husk and rice husk silica are classified into five categories.

- 1) RH as the resource of energy and charcoal
- 2) RH as the resource of SiO_2 and activated carbon
- 3) SiO_2 as the resource of one of the component of oxide ceramics
- 4) SiO_2 as the resource of Silicon
- 5) SiO_2 as the resource of SiC and Si_3N_4 powder [4]

There are many papers on the utilities of the rice husk. However, the total amount of commercialized products might be so few comparing with the rice husk ash exhausted. Moreover, activated carbon, silicon, SiC and Si_3N_4 powders have not been produced yet from rice husk in industrial scale.

Candidates or other potential applications of RHA are as follows:

- 1) Heat insulator for tundish in steel industry
- 2) Resource of silica for manufacturing low cost building blocks and production of high quality cement [5] in cement industry
- 3) Source of silica for synthesized mullite [6], and other ceramics

- 4) Anti-blocking powder [7], and fillers for plastics and rubbers
- 5) Water glass

In order to find a new and practical application for rice husk ash, what should be known are the properties of rice husk ash and the effect of burning process on the properties. The silica from ash undergoes structural transformations depending on the conditions of combustion (time, temperature, etc). Generally, at below 800°C amorphous silica is formed and at higher temperatures, crystalline ash is formed. These types of silica have different properties and it is important to produce ash having the proper specification for the particular application [5].

The objectives of this research are as follows:

1. To find on optimal condition to synthesize cristobalite/tridymite powder from rice husk
2. To evaluate applicability of cristobalite/tridymite, and amorphous silica powder as an antiblocking agent for plastic film
3. To find an effective process to achieve or produce low cost amorphous silica

สถาบันวิทยบริการ
จุฬาลงกรณ์มหาวิทยาลัย

CHAPTER II

LITERATURE REVIEWS

2.1 Background

Rice husk (RH) is a by-product of rice production. Nowadays the RH produced more than 100,000,000 tons per year in the world. In Thailand, about 5,000,000 tons of RH are produced every year. One utility of RH is biomass as energy source. The energy of about 3600 kcal/kg is generated from RH. The heat energy is used for generating electricity [5].

2.2 Amorphous silica (Noncrystalline silica)

Vitreous silica is prepared by fusion of crystalline quartz sand and then cooled rapidly. The structure of vitreous silica is a continuous network of $[\text{SiO}_4]$ tetrahedral with lower degree of order than crystalline silica. The difference of broader distribution of Si-O-Si bond angle is observed, and Gibb's free energies (ΔG) for low temperature form of other silica are very close. (ΔG of vitreous silica = -849.05 kJ/mol, and low temperature cristobalite = -849.76 kJ/mol, low temperature tridymite = -857.08 kJ/mol.) [10].

The properties of vitreous silica are high chemical resistance, low coefficient of thermal expansion ($0.5\text{-}0.8 \times 10^{-6} \text{ K}^{-1}$), high thermal shock resistance, high electrical resistance, and high optical transmittance. The vitreous silica is difficult to produce, because the processing requires higher temperature than 2000°C [10].

The amorphous silica are composed of small particles with high specific surface area easy to agglomerate. The commercial names of the products are colloidal silica, silica gel, precipitated silica, and fume or pyrogenic silica [10].

Their surface may be substantially anhydrous or may contain of silanol (SiOH) group. They are frequently viewed as condensation polymers of silicic acid, $\text{Si}(\text{OH})_4$ [10].

Colloidal silica (silica sol) is stable dispersion of small particles in water. Commercial products contain silica particles of 3-100 nm in diameter, specific surface area of $50\text{-}270 \text{ m}^2/\text{g}$, 15-50 wt% of silica contents, and includes small amount of stabilizers (<1% sodium ion) [10].

Silica gel is composed of 3-dimensional networks of aggregated silica particle (colloidal). Within the aggregated colloidal silica, medium is filled. The examples of medium gel are hydrogen for water and alcogels for alcohol etc. The removal of liquid causes the result of extensive shrinkage, which remains on the surface extension force. Silica gel dried by this process is called as xerogels. If the liquid within pore vaporizes under the heat, a very voluminous dry silica gel is obtained [10].

Precipitated silica is in a powder form produced by the coagulation of silica particles from silicate solution in the condition of high salt concentration [10].

Silica fume is a by-product of the reduction of high-purity quartz with coal in electric furnaces in the production of silicon and ferrosilicon alloys. Silica fume is also collected as a by-product in the production of other silicon alloys such as ferrochromium, ferromanganese, ferromagnesium, and calcium silicon. Silica fume consists of very fine vitreous particles with a surface area of $20 \text{ m}^2/\text{g}$ [10].

Biogenic silicas are occurred from plant cells and small part of organism in water (diatom). Biogenic silicas are existed in amorphous phase. Dissolved silica is absorbed by the plant or diatomite to generate the silica skeleton. Diatomite is usually used as a filler. Silica in plant has very few industrial applications [10].

Opal is natural amorphous silica with a regular "lattice" arrangement of colloidal silica particle and a substantial amount of incorporated water. There is no utilization in industry. But it is used as jewel because of its beautiful rainbow reflection [10].

2.3 Silica in rice

Dissolved silica can be taken up by a root from soil and concentrates in husk, leaf-blades, leaf-sheath, and stems. When dissolved silica was absorbed by a root and transported to husk, it accumulates and turns condensed silica in epidermis to form a silica double layer. The silica in several plants has been shown to consist of a dense gel with pores of 1-10 nm diameter filled with water as shown in Figure 2.1 [7, 10].

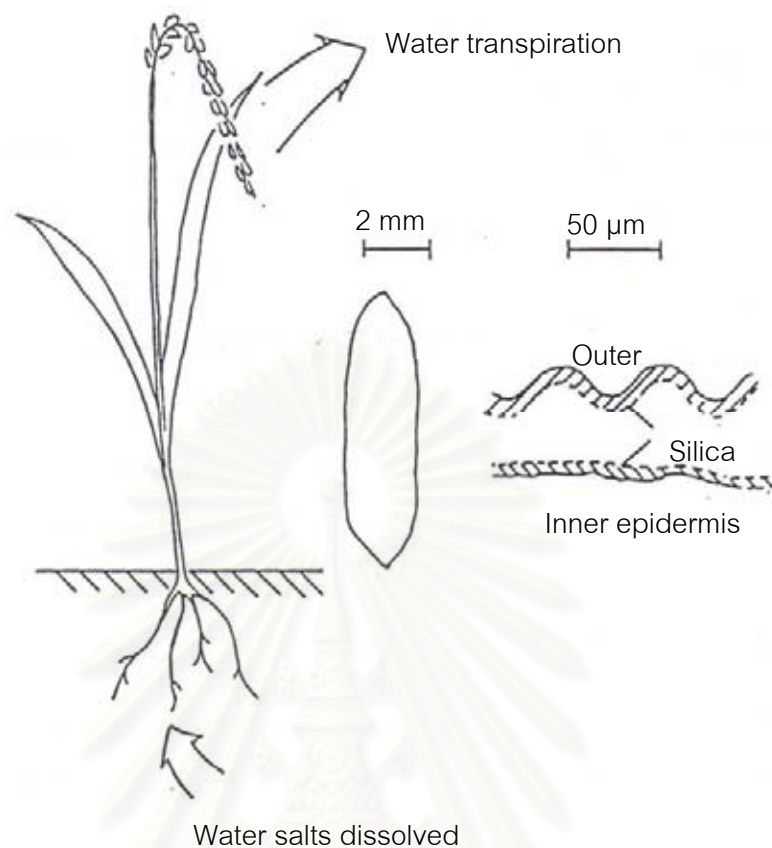


Figure 2.1 Absorption and collection of silica in rice plant [7, 10]

2.4 Crystallization of silica by heat treatment

Crystalline silica with long-range order exists in several forms (polymorphism). There are three basic crystal structures in the polymorphism of silica, quartz, tridymite, and cristobalite. Each exists in two or three modifications. The most stable forms are low quartz (below 573°C), high quartz (573 to 867°C), low tridymite (below 867°C), high tridymite (867 to 1470°C), high cristobalite (1470 to 1710°C) and liquid above 1710°C. Polymorphic transformations in silica are shown in Figure 2.2. The structures are based on $[\text{SiO}_4]$ tetrahedral link between one of silicon atom and four oxygen atoms in all of these forms [9].

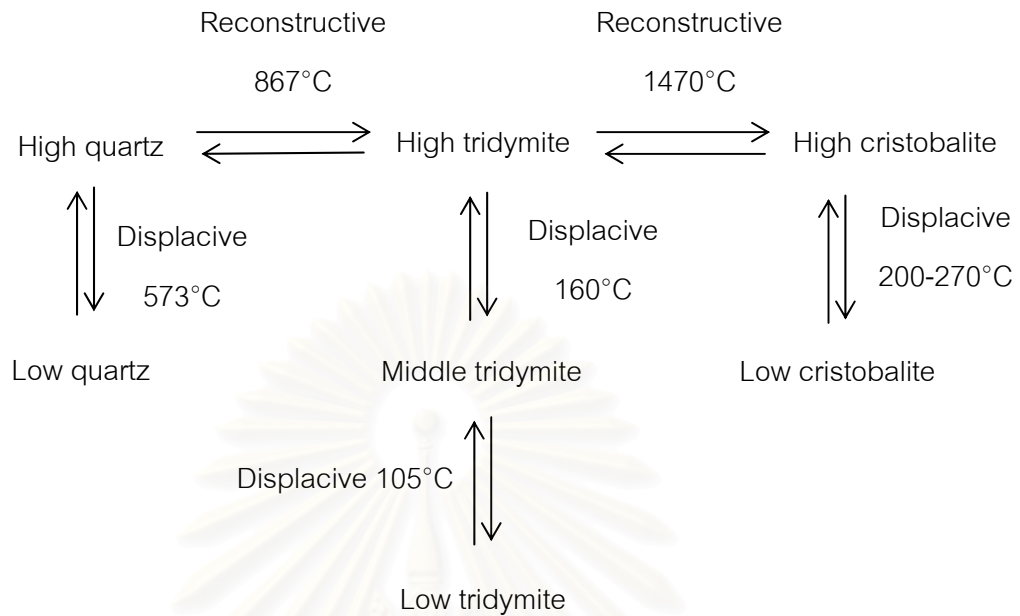


Figure 2.2 Polymorphic transformations in silica, [8]

Polymorphic transformations are classified in two types. The displacive transformation process requires lower energy than that of the reconstructive transformation. The transformation changes rapidly. The structure only distorts without breaking bond. The reconstructive transformation process requires high energy for breaking bond and rearrange a new structure. The process takes long time. These process are shown in Figure 2.3 b, 2.3 c and 2.3 d, respectively.

The vertical direction represents the quick displacive polymorphic transformation, whereas the horizontal direction represents the sluggish reconstructive transition [9].

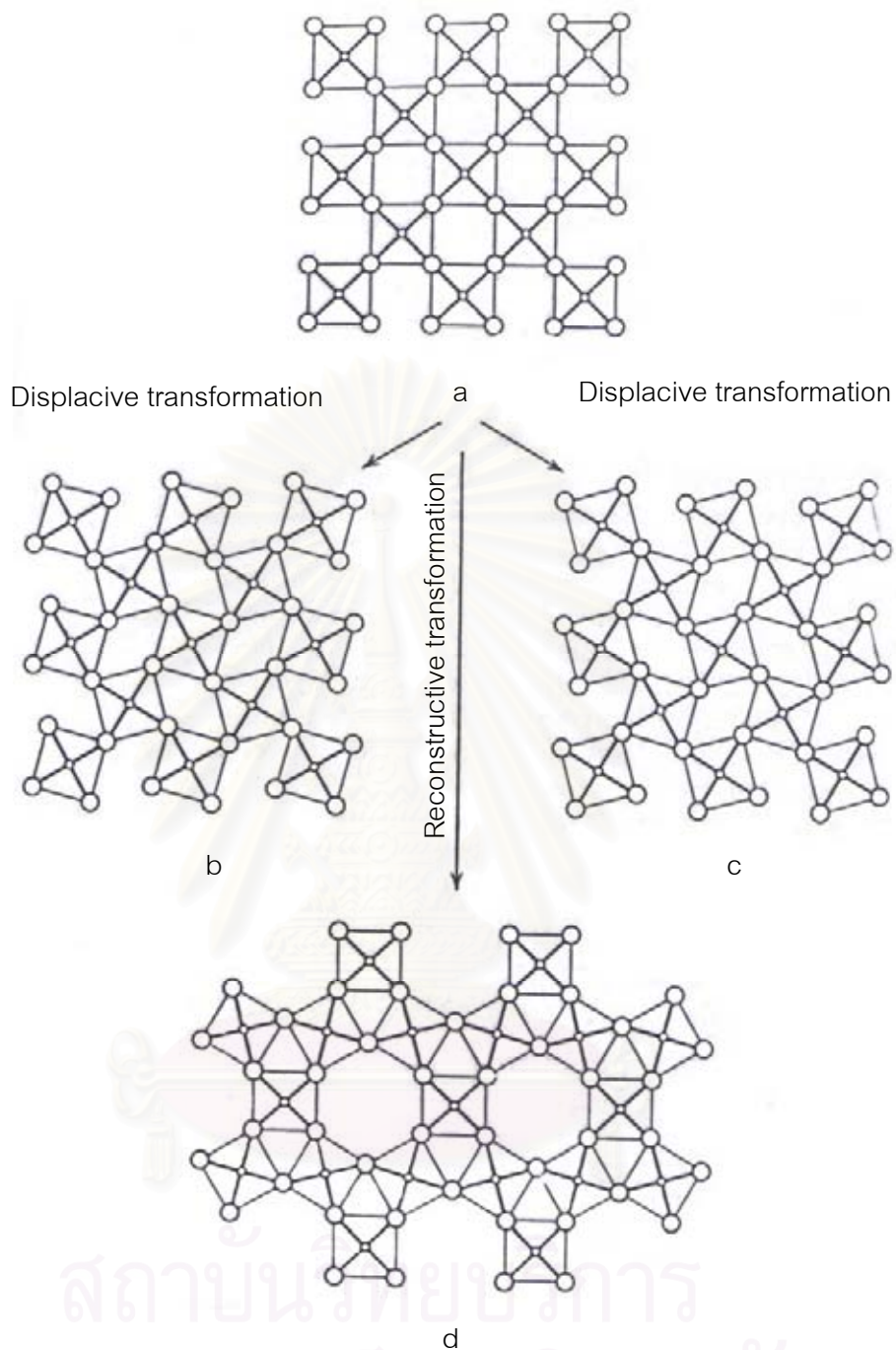


Figure 2.3 The structure "a" changes to collapsed forms "b" and "c" by displacive transformation and reconstructive form "d" [9]

2.5 Effect of alkali ion and particle size of silica on crystallization of silica

The transformation of amorphous silica to crystalline phase can be done with doping of alkali ion and heat treatment. The different alkali ion doping led to different crystalline phases e.g. Na^+ ion transformed amorphous silica to cristobalite. K^{2+} ion led to cristobalite and tridymite. The effects of Na^+ and K^{2+} on the crystallization are shown in Figure 2.4 and Figure 2.5, respectively. Effect of alkali ion on amorphous silica is considered as the solid-state reaction. The reaction between amorphous silica and different alkali oxide is depending on the physical properties of alkali ion such as size and charge. The difference drives the transition to the different crystalline phases of silicas [11, 12].

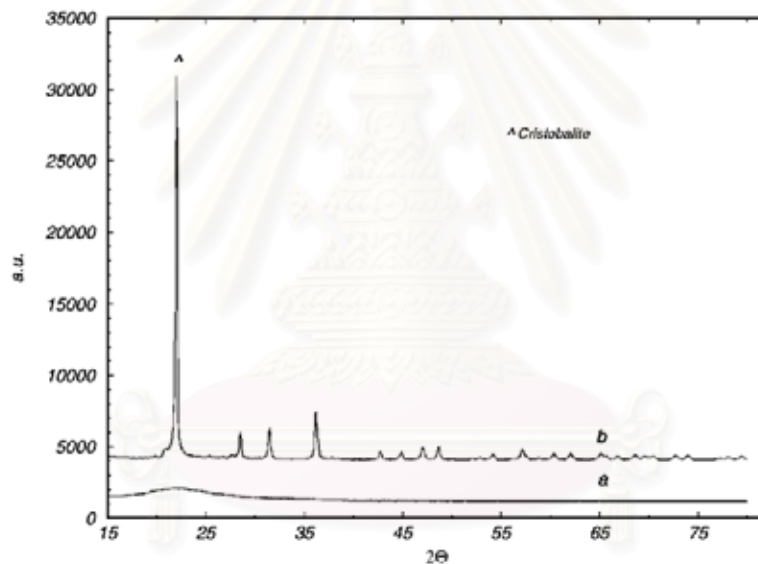


Figure 2.4 XRD patterns of amorphous silica with sodium ($1\text{Na}/\text{SiO}_2$) and heat treated at 500°C (a) and 800°C (b) [11]

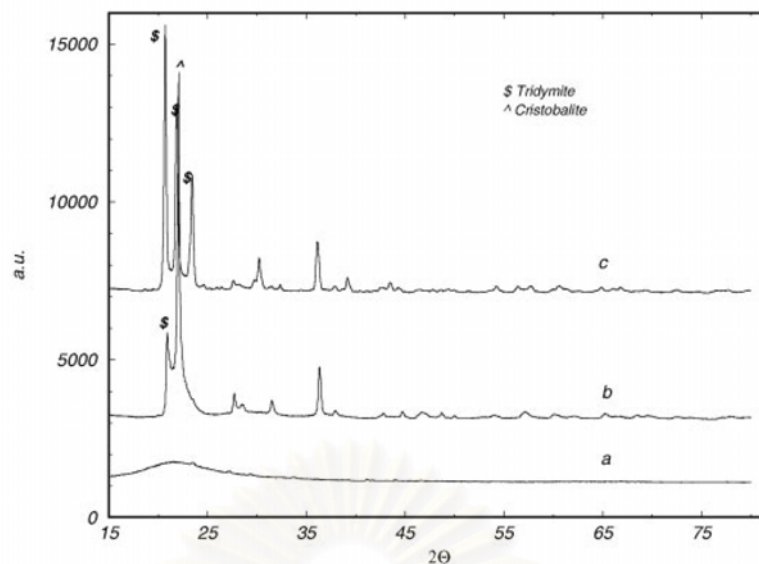


Figure 2.5 XRD patterns of amorphous silica with potassium ($4K/SiO_2$) and heat treated at $500^\circ C$ (a), $800^\circ C$ (b) and $1000^\circ C$ (c) [11]

The particle size of rice husk has strong effect on the transformation of cristobalite heated at low temperature around $900^\circ C$ for 8 hours as shown in the Table 2.1. Tridymite and cristobalite with a trace amount of alkaline oxide was formed when 7-10 nm of particle size amorphous silica was soaked at $900^\circ C$. (Figure 2.6) [13].

Table 2.1 XRD analysis of heat treated samples at specified heat treatment conditions [13]

Particle size (nm)	Heat treatment time (h)	Temperature		
		$800^\circ C$	$900^\circ C$	$1000^\circ C$
7-10	2	Amorphous	Amorphous	Cristobalite
	8	Amorphous	Cristobalite	Tridymite
	16	Amorphous	Tridymite	Tridymite
	24	Amorphous	Tridymite	Tridymite
10-13	24	Amorphous	Tridymite	Tridymite
50	24	Amorphous	Amorphous	Amorphous
80	24	Amorphous	Amorphous	Amorphous

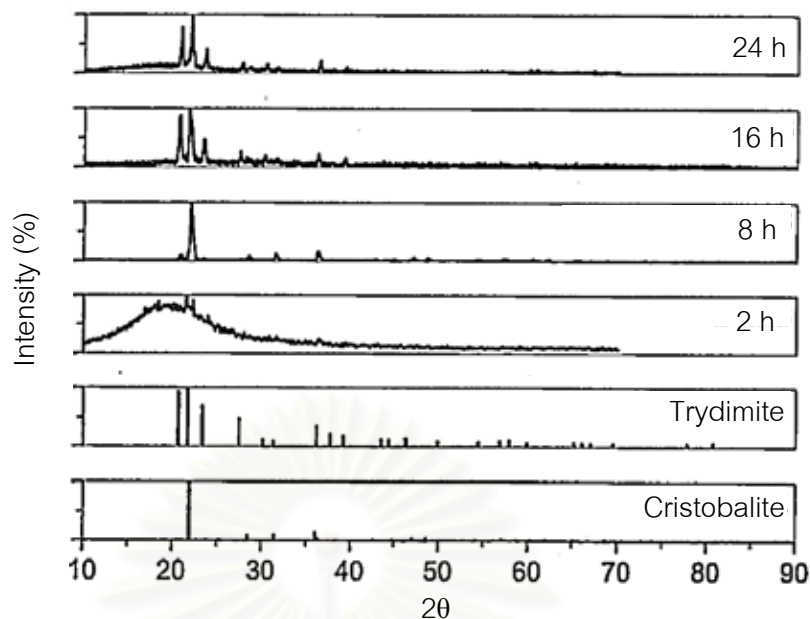


Figure 2.6 XRD patterns of 7-10 nm RH particle heat treated at 900°C [13]

2.6 Preparation and characterization of high-grade silica from rice husk, U. Leela-Adisorn, Master thesis [10]

Objective of this thesis is to make rice husk silica to a competitive source of nano-structure silica. Rice husk samples are submitted to a chemical pretreatment using cellulase enzyme and different inorganic acids. Following conditions were selected for experiment.

1. No treatment (except for washing)
2. NaOH 1 molar, 24 h. room temperature
3. HCL 1:4, boiling 3 h
4. NaOH treatment, then HCl treatment
5. H_2SO_4 1:4, boiling 3 h
6. HNO_3 1:4, 3 h room temperature
7. Enzymatic treatment
8. Enzymatic treatment, then HCl treatment
9. Enzymatic treatment, then H_2SO_4 treatment

In this study, RHA was produced by a sequence of washing, enzymatic digestion, acid leaching and packed bed incineration. Incinerating condition was 600°C

for 6 h under air atmosphere. Then rice husk ash was characterized in terms of silica content, crystal structure by XRD, particle size distribution, and specific surface area (BET, N₂). The results are shown in Table 2.2.

The rice husk ash had primary particle size of 2-3 nm, loosely coordinated secondary particle of 20-30 nm size, specific surface area (BET, N₂) of 200 to 250 m²/g, and purity of more than 99.4%.

Table 2.2 Properties of RHA treated by various conditions

Condition	% Silica content	Structure	Specific surface area (m ² /g)	Particle size (μm)
None	93.3 ± 0.6	Amorphous	107	2.4
NaOH	68.3 ± 0.2	Amorphous	60	2.7
HCl	99.37 ± 0.15	Amorphous	253	2.4
NaOH/HCl	-	Amorphous	86	2.7
H ₂ SO ₄	98.99 ± 0.07	Amorphous	217	2.3
HNO ₃	98.0 ± 0.4	Amorphous	250	2.5
Enzymatic	96.8 ± 0.15	Amorphous	223	2.5
Enzyatic/HCl	99.58 ± 0.13	Amorphous	231	2.5
Enzyatic/H ₂ SO ₄	99.56 ± 0.06	Amorphous	254	2.3

Amorphous fumed silica aerosil OX50 from Degussa was selected for comparison with rice husk ash. General properties, purity, particle size, specific surface area and nature of agglomerate were compared as shown in Table 2.3.

Table 2.3 Comparison data between silica from rice husk ash and aerosol OX50

Property	Rice husk ash (%)	Aerosil OX50
Silica content	> 99.4	> 99.9
d_0 , particle size, primary	2.4 nm	40 nm
secondary	26 nm	-
Surface area	>200 m ² /g	50 ± 15 m ² /g
Nature of agglomerate	Between globular and fractal agglomerate	Fractal agglomerate
Surface behavior	Hydrophilic	Hydrophilic

However, from the table aerosil OX50 has excellent dispersion property than rice husk ash silica, but it has a lower specific surface area than rice husk ash.

2.7 Use of silica from rice husk as anti-blocking agent in low-density polyethylene films, C Kunsawat, Master thesis [7]

Objective of this thesis is to investigate the optimum amount of amorphous silica from rice husk ash for using as an anti-blocking-agent in LDPE (Low-density polyethylene) film. The properties of LDPE with amorphous silica were compared with LDPE with commercial grade of amorphous silica (Sylo-1).

Rice husk was washed by the 0.4 molar HCl acid for 3 h, then dried completely and calcined at 600°C for 6 h. Rice husk ash was ground using a jet mill. The properties of amorphous silica are shown in Table 2.4.

Table 2.4 Comparison data between silica from rice husk ash and Sylo-1

Properties	Amorphous silica from rice husk ash	Sylo-1 (Amorphous silica commercial grade)
Particle size (μm)	4.3	6.6
Specific surface area (m^2/g)	131 ± 2	512 ± 5
pH	5.7	6-8
Oil absorption	1.92	2
Silica content (%)	99.6	99.0
Bulk density (g/cm^3)	0.68	0.32
Amount of use for film thickness less than $100 \mu\text{m}$ (ppm)	-	500-1500

These powders were mixed in various amounts such as 300, 500, 1000, 1500, 2000, 3000, 4000 and 5000 ppm. The plastic film were formed and the microstructure, blocking force, tensile strength, elongation at break, tear resistance, haze and gloss properties were characterized.

The plastic films with rice husk ash as an anti-blocking agent compared with the plastic film with Sylo-1. The conclusions are as follows:

1. LDPE films with Sylo-1 showed better result in blocking force, tensile strength, and elongation at break comparing with that of plastic films using silica from rice husk ash at same amount.

2. LDPE films with 2000 – 3000 ppm silica from rice husk ash showed same properties of LDPE film with 500 – 1500 ppm of Sylo-1 in terms of their blocking force, mechanical strength and clarity.

CHAPTER III

EXPERIMENTAL PROCEDURES

3.1 Experiment on anti-blocking powder

The main objective of this research is to study an application of silica from rice husk ash as an anti-blocking agent for linear low-density polyethylene film (LLDPE, metallocene grade). The over all flow chart of experiment is shown in Figure 3.1.

3.1.1 Effect of washing and heat treatment conditions on properties of RHA

3.1.1.1 Preparation of rice husk ash

The RH obtained from rice mill plant in Nakhonratchasima province, Thailand was used for this experiment. Firstly, the RH was thoroughly washed by tap water just to remove adhering soil and dust, then dried at 100°C. This sample was called as “untreated sample”. Secondly, the washed RH was divided into 2 groups. One was soaked in tap water for 72 h at room temperature and washed in a washing machine for 3 h, and then dried at 100°C in an oven. It is called “water treated sample”. Finally, the washed RH was leached using 1:10 / HCl:water (Analytical grade HCl solution (Merck & Co.)). Thirty-five (35) g of RH was put in 1,000 cm³ of acid solution in a glass beaker and the mixture was magnetic stirred for 3 h at room temperature. The RH sample was neutralized by distilled water and was then dried at 100°C. It is called as “HCl treated sample”. The washing process is shown in Figure 3.2. All the samples were calcined at 650°C for 1 h using an electric furnace in the air atmosphere for burning out of organic compound. Three different kinds of RHA, untreated, water treated, and HCl treated, were pulverized, ground and sieved through 100 and 325 mesh. Each sample was weighed around 5 g and put in an alumina crucible for heat treatment in as electric furnace at 800, 900, 1000, 1200, 1300, 1400 or 1500°C for 2h as shown in Figure 3.3. Moreover, two kinds of silica sand (commercial grade) and amorphous silica* were heat treated for comparison with RHA samples as shown in Figure 3.1.

*The amorphous silica is a silica glass for silicon semiconductor processing

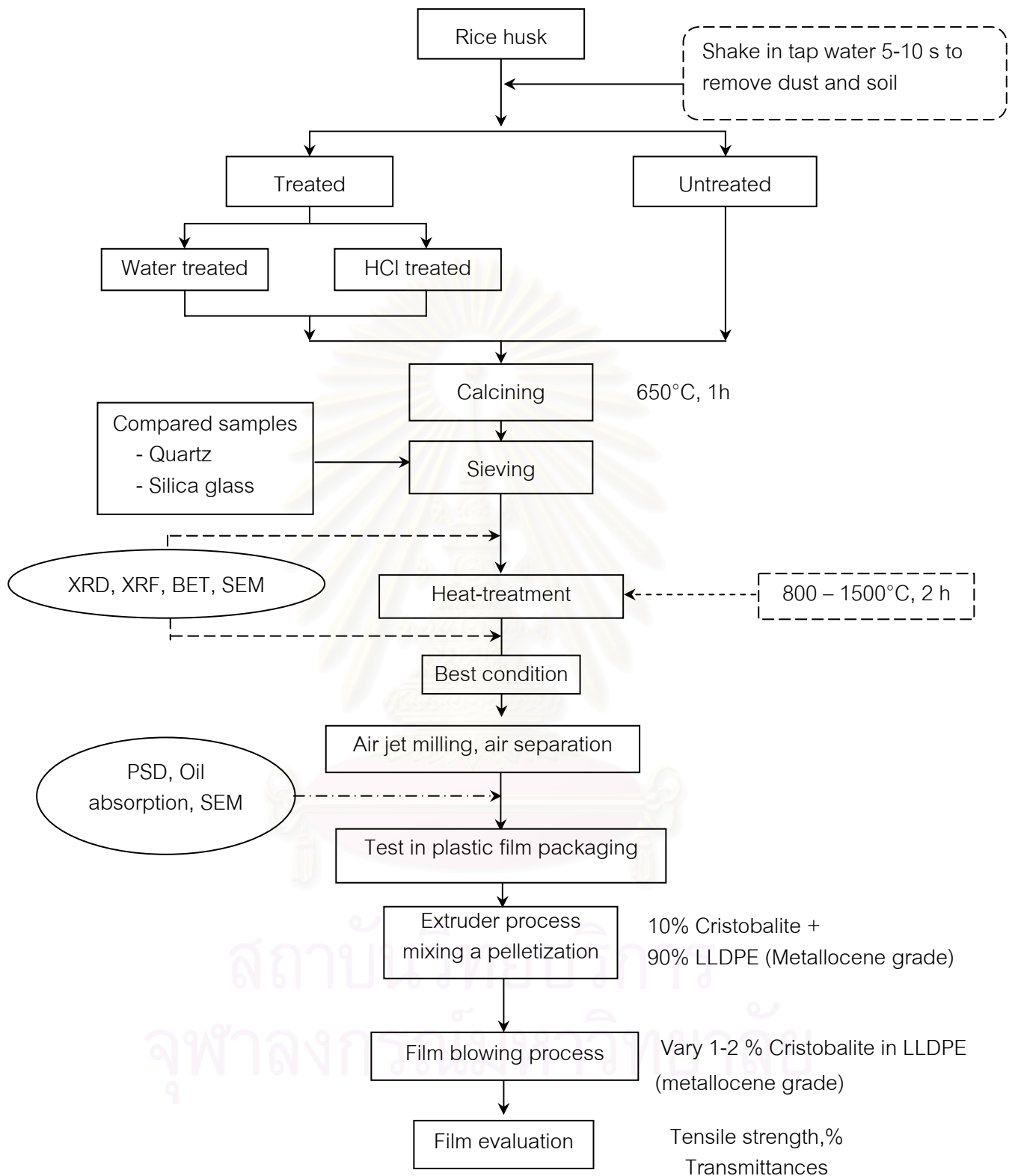


Figure 3.1 Flow chart of over all process of experiment

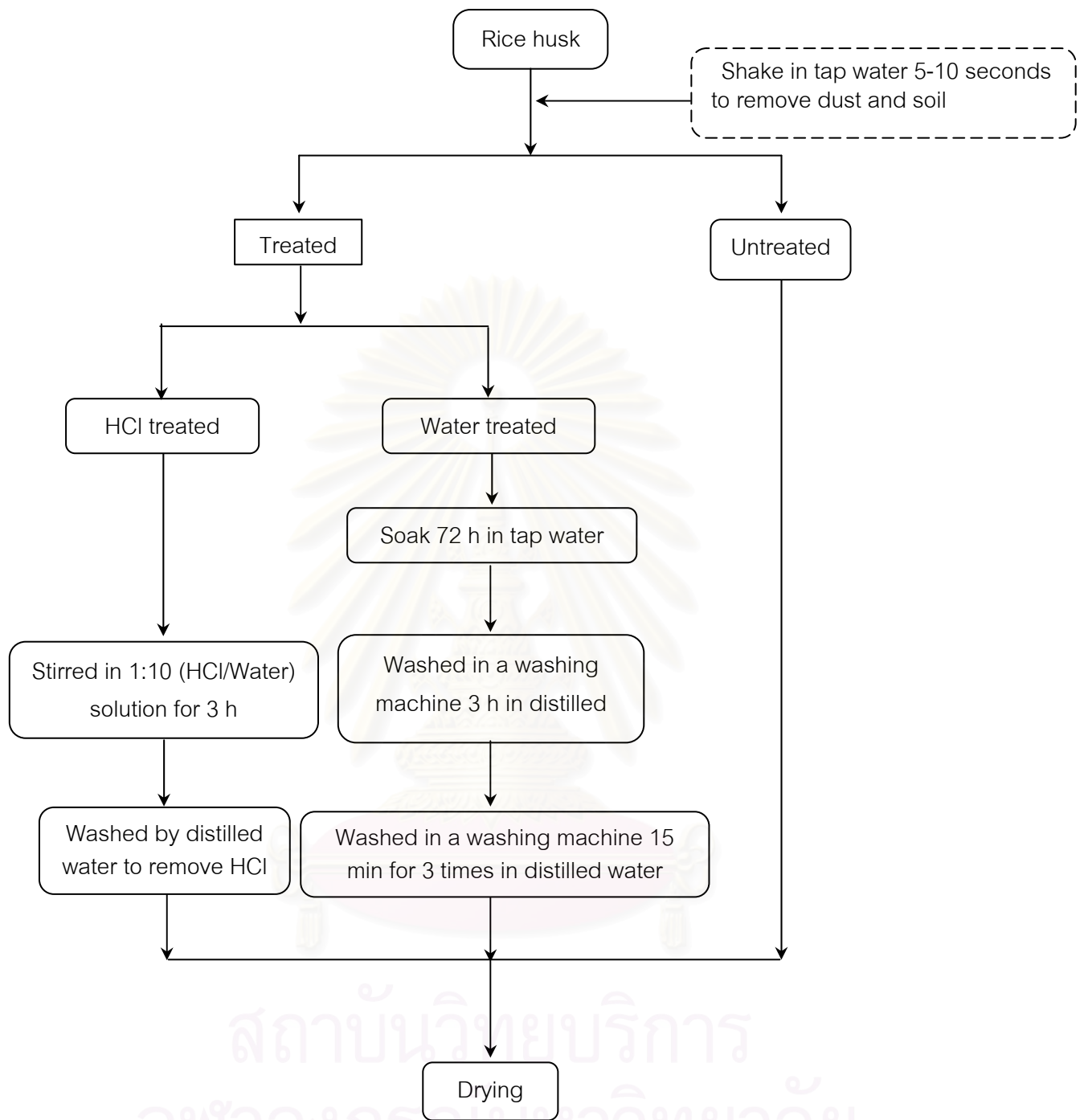


Figure 3.2 Flow chart of washing method and condition

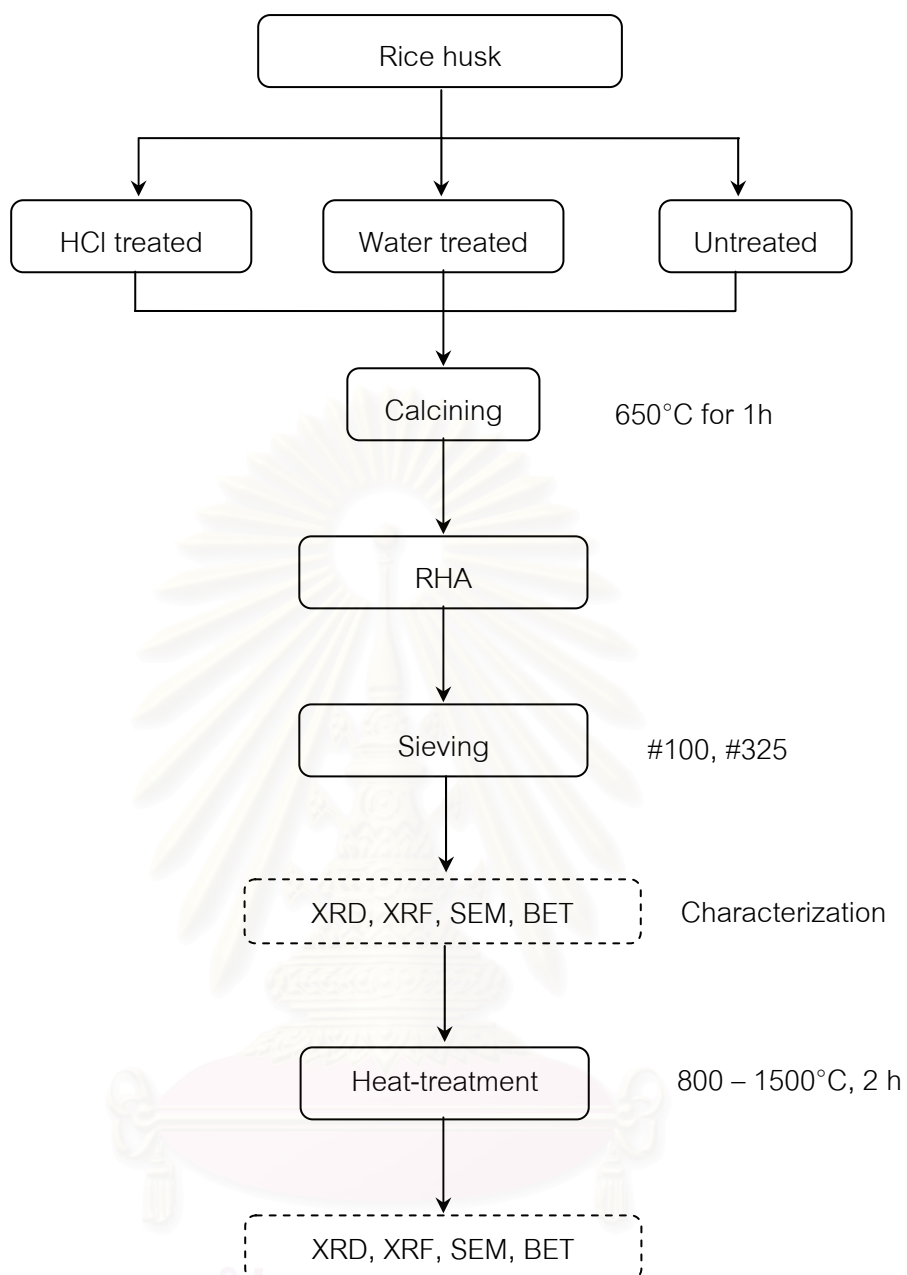


Figure 3.3 Flow chart of incineration method and condition

3.1.1.2 Characterization of rice husk ash

(1) Phase analysis

Crystalline phase of heat treated RHA samples was examined by X-ray diffraction method (X-ray detector, BRUKER Model D8-Advanced). The specimens were ground in an alumina mortar and sieved through 100 and 325 mesh brass screen. About 5 g of rice husk ash was packed in a sample holder. The conditions of XRD were Cu-K α , 40 kv, 40 mA, 2θ : 10-60°, and scanning rate of 3°/min.

(2) Chemical composition

The chemical compositions of RHA samples were analyzed by X-ray fluorescence method (XRF, BRUKER axs Model S4PIONEER). The samples were ground in an alumina mortar and sieved through 100 and 325 mesh brass screen. About 5-10 gram of rice husk ash was packed in a XRF sample holder.

(3) Specific surface area

Specific surface area was measured by BET method. The RHA samples were dried in an oven at 100°C for 24 h. About 0.1 - 0.2 g of powder was put in a cylinder tube of COULTER SA 3100 surface area and pore size analyzer.

(4) Particle size distribution

Particle size distribution of the RHA samples after grinding by an air jet mill were determined by laser diffraction method (Particle size analyzer, Mastersizer S Ver. 2.18, Malvern Instruments Ltd.). About 0.5 - 1.0 g of RHA was mixed with 20 cm³ of 0.2 wt% NaHMP aqueous solution and the mixture was then ultrasonicated for 5 min before the measurement.

(5) Oil absorption

Oil absorption of the RHA samples after ground by an air jet mill were measured following ASTM D 281-95 (Re approved 2002). The sample was sieved through a 35-mesh brass screen. About 1 g of sample was used for one test.

3.1.2 Production and evaluation of LLDPE film with synthesized powders as an anti-blocking agent

3.1.2.1 Cristobalite as an anti-blocking agent

The black RHA sample obtained from rice mill plant in Ratchaburi province was used for this experiment. Firstly, the black rice husk ash was sieved thorough 50 mesh and heat treated at various temperatures of 1000°C and 1200°C for 2 and 4 h, and 1400°C for 2 h. These heat treated samples were characterized using XRD quantitatively. The best condition (1200°C, 4 h) was then selected for heat treatment in a larger scale (2 Kg). Secondly, 2 kg of RHA was prepared by the condition mentioned above, and then the RHA was crushed by an air jet mill of HOSOKAWA MICRON, JAPAN. The samples were separated in these kinds of particles with different average particle size. Finally, the ground powders were mixed with LLDPE using a composition of 10% of ground powder and 90% of LLDPE (Metallocene grade) by extruder. This sample was called as “master batch” of plastic containing 10% cristobalite. The master batch was mixed with LLDPE (Metallocene grade). The content of cristobalite was varied between 1 and 2% for film-blowing. The flow chart of producing LLDPE film with cristobalite as anti-blocking agent is shown in Figure 3.4 and the film-blowing machine is shown in Figure 3.5.

The tensile strength of the plastic film was measured using an Instron testing machine (Model 5843, Multi Range). The transmittance (%T) of plastic film was measured by UV/VIS spectrophotometer (Perkin Elmer, Lambda 35).

จุฬาลงกรณ์มหาวิทยาลัย

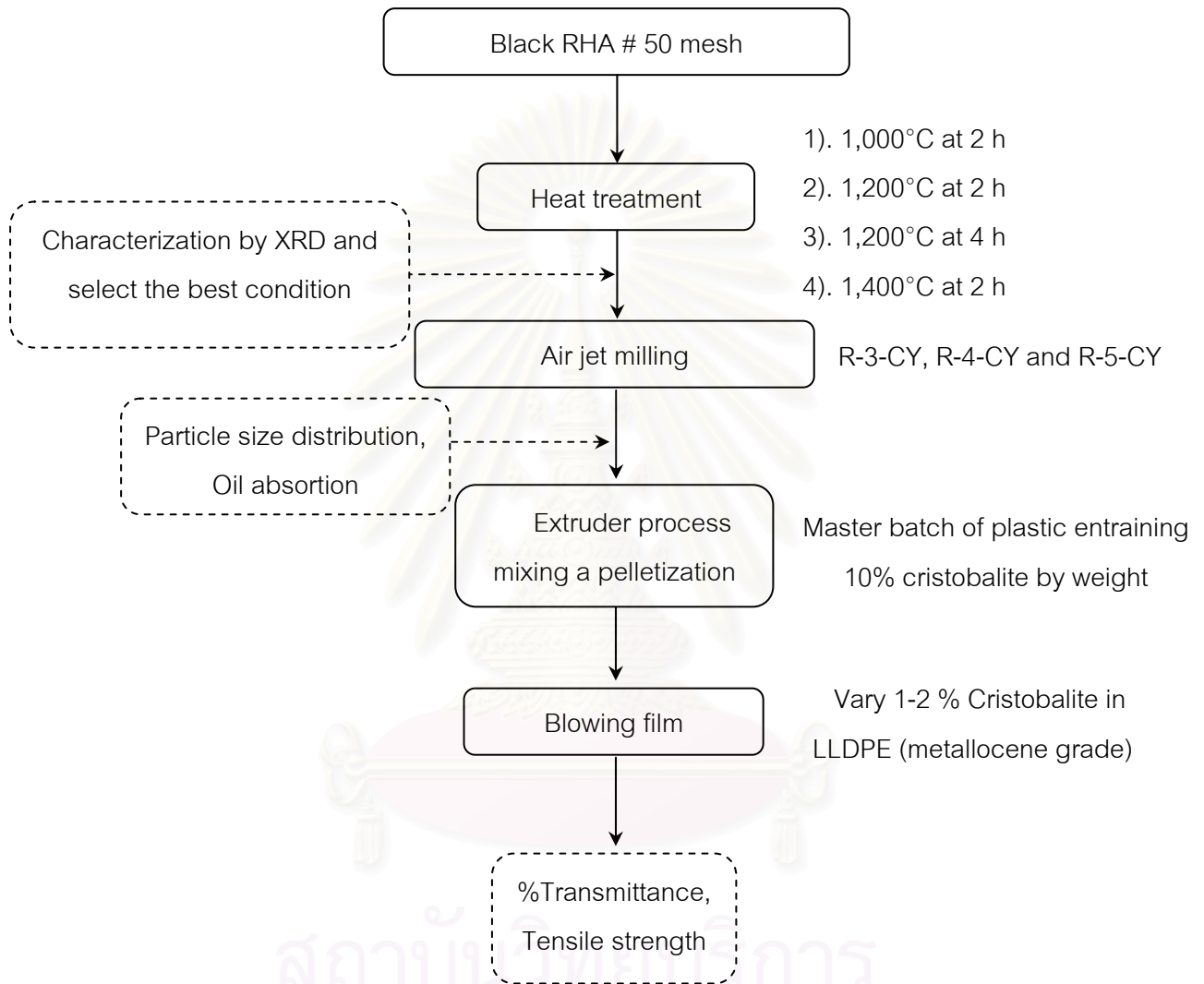


Figure 3.4 Flow chart of producing LLDPE film with cristobalite as an anti-blocking agent

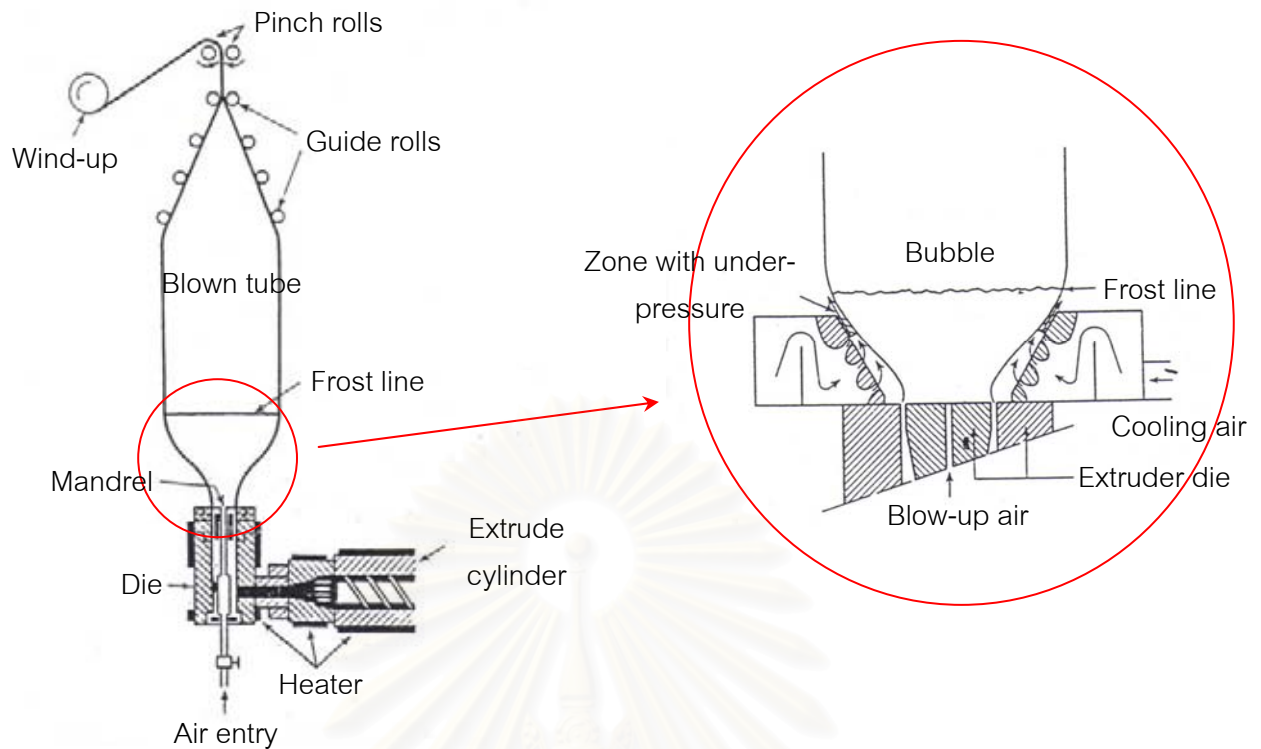


Figure 3.5 Blown film process [7]

3.1.2.2 Amorphous silica as an anti-blocking agent

The rice husk obtained from rice mill plant in Ratchaburi province Thailand was used in this experiment. The rice husk was thoroughly washed by tap water just to remove adhering soil and dust, then dried at 100°C . This sample is called “untreated sample”. The washed rice husk was soaked in tap water for 72 h at room temperature and washed in washing machine for 3 h, and then dried at 100°C in an oven. This sample is called “water treated sample”. These two RH samples were calcined at 650°C for 1 h. The RHA samples were ground by a small air jet mill as shown in Figure 3.6. After that, the sample was characterized by XRD, XRF, particle size distribution, and oil absorption as shown in Figure 3.7.



Figure 3.6 Air jet mill of the Metallurgy and Materials Science Research Institute, Chulalongkorn University

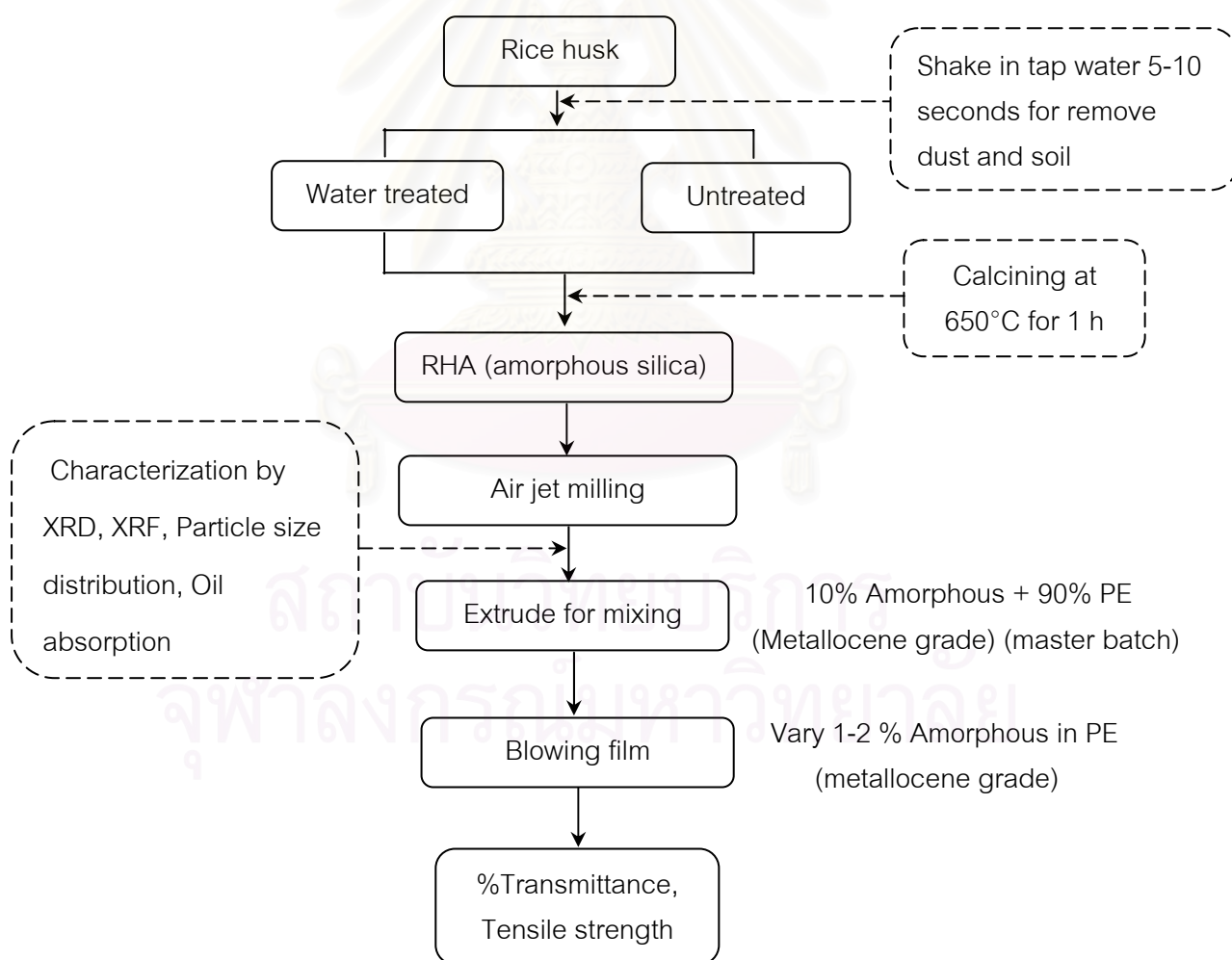


Figure 3.7 Flow chart of producing LLDPE film with amorphous silica as an anti-blocking agent

3.1.2.3 Evaluation of plastic film

(1) Transmittances

Transmittance (%T) of plastic film was measured using a double beam automatic recording spectrophotometer UV/VIS. The transmittance was measured at the wavelengths of 200 to 1100 nanometers.

(2) Tensile strength

Tensile strength of plastic film was measured following ASTM D 882-02 using an Instron tensile testing machine. The conditions are load cell of 100 N, the specimen width of 19.5 mm, and length of 150 mm. (machine direction: MD, transverse direction: TD, each 5 pieces), gauge length of 50 mm and cross speed head of 500 mm/min.

3.2 Water glass synthesis from amorphous silica

RHA was mixed in sodium hydroxide (NaOH) solution at various ratios of $\text{SiO}_2/\text{Na}_2\text{O}$ between 2.0 – 3.0, the solution was magnetic stirred for 30 min at room temperature. When the ratio of $\text{SiO}_2/\text{Na}_2\text{O}$ is in between 2.0 – 2.5 the mixtures can be prepared at room temperature. If the ratio of $\text{SiO}_2/\text{Na}_2\text{O}$ was increased to 2.5 – 3.0, the mixture need to be prepared at higher temperature on a water bath and magnetic stirred for 2 h in order to get homogeneous mixture, flow chart of process is shown in Figure 3.8.

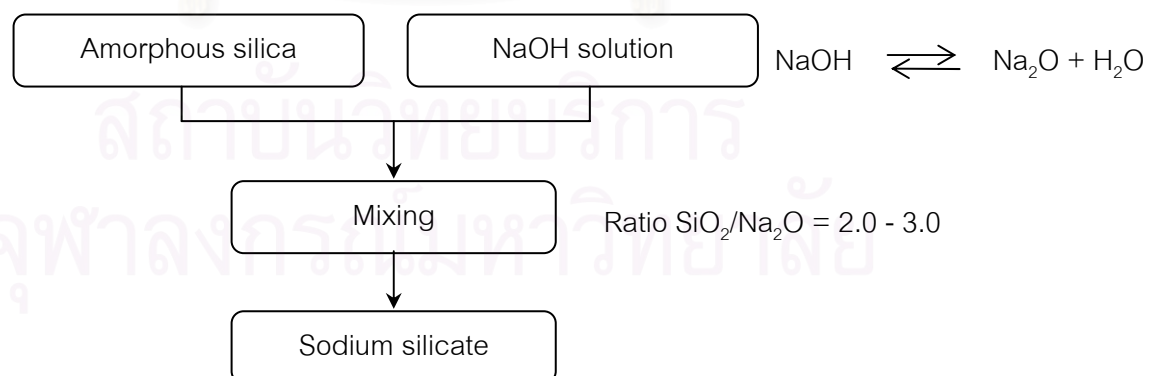


Figure 3.8 Flow chart of synthesized water glass from amorphous silica

3.3 Analysis and heat treatment of ashes from factories and power plants

3.3.1 Crystal phase analysis

Many ashes from factories and power plants are gathered. The crystal phase was analyzed by XRD. The kind of ashes and crystal structures obtained from industrial are shown in Table 4.5 and original XRD data are shown in Appendix D Figure 15 – 29.

3.3.2 Oxidation of ashes from factories and plants

The ashes were heat treated at 500 - 800°C in an air atmosphere furnace and the color of ash was observed. The heat treatment conditions are shown in Table 4.6.

3.4 Experiment on various washing conditions

The rice husk obtained from rice mill plant in Ratchaburi province Thailand was used for this experiment. The rice husk was washed by 2 conditions. Firstly, 2 kg of rice husk was put in a washing machine and soaked for 24, 48 and 72 h. Around 300 g of RH was sampling at each time and dried at 100°C. This samples were called “soaked sample”. Secondly, 2 kg of rice husk was put in a washing machine and washed for 15, 30, and 45 min. Around 300 g of RH was sampling at each time and dried at 100°C. This sample was called “washed sample”. Dried RH was calcined at 650°C for 1 h. The RHA samples were ground using an alumina mortar, then the samples were characterized by XRD and XRF as shown in Figure 3.9.

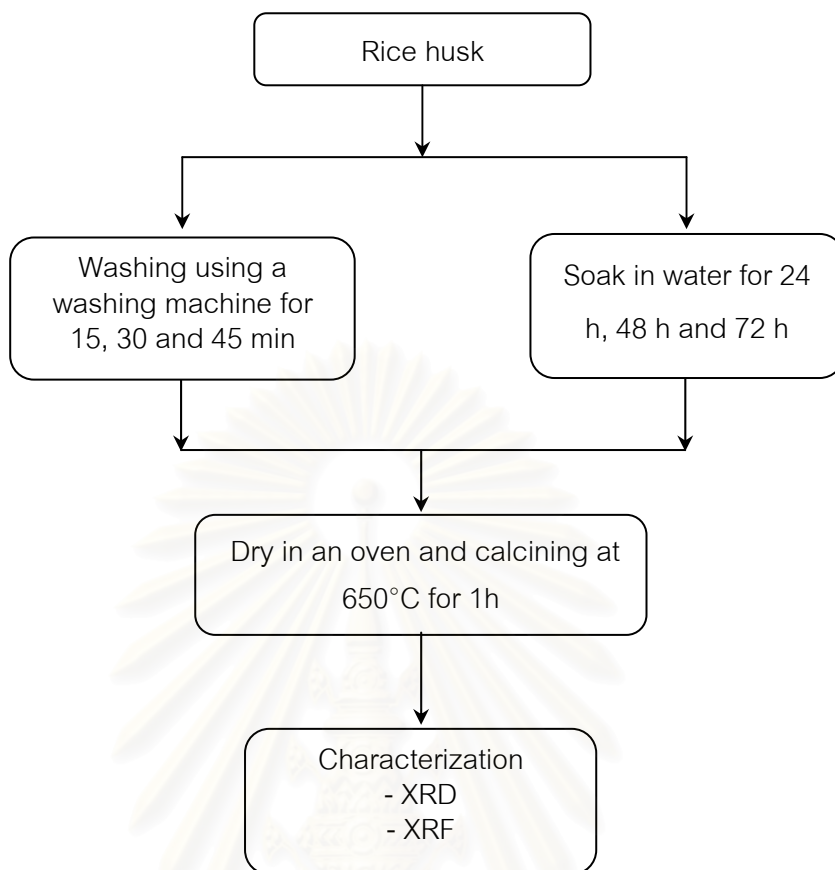


Figure 3.9 Flow chart of various washing process

สถาบันวิทยบริการ
จุฬาลงกรณ์มหาวิทยาลัย

3.5 Experiment on low temperature calcining for RH from different sources

The rice husks obtained from rice milling plant in Ratchaburi and Nakhonratchasima provinces Thailand were used for this experiment. Two kilogram of rice husk was put in a washing machine and soaked for 5 and 10 h. Each sample was washed for 15 min and dried at 100°C. The washed RH was calcined at 450, 550 and 650°C for 1 h. The RHA samples were ground using an alumina mortar, then the samples were characterized by XRD and XRF as shown in Figure 3.10.

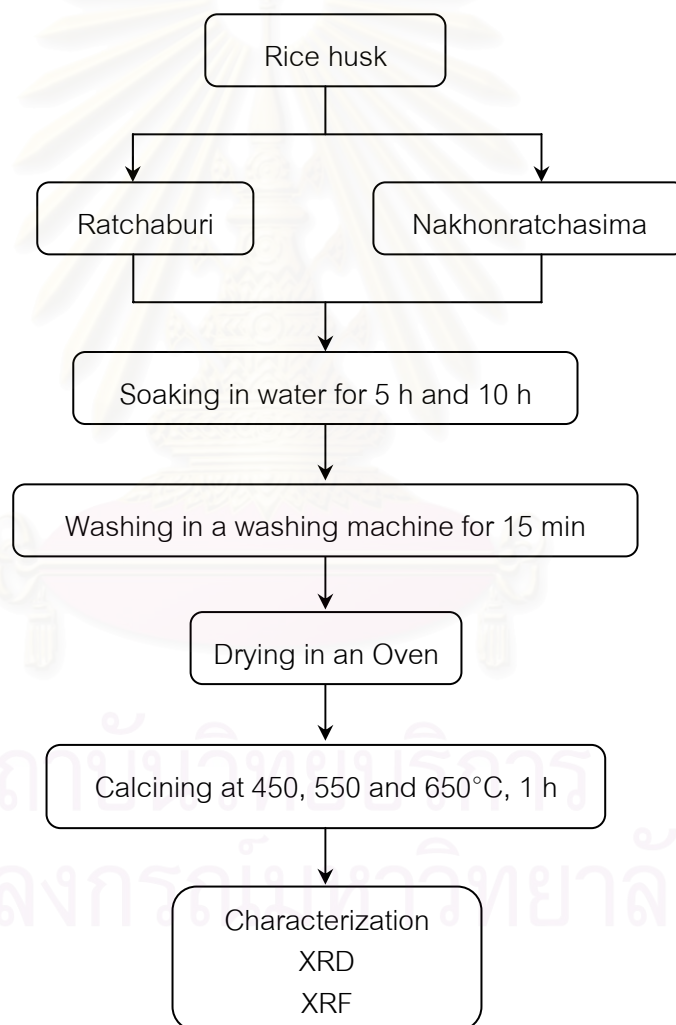


Figure 3.10 Flow chart of low temperature calcining

CHAPTER IV

RESULTS AND DISCUSSIONS

4.1 Effect of alkaline oxide elimination by washing on the crystallization of RHA

4.1.1 Properties of starting raw materials

In this experiment, the RH from Nakhonratchasima province was used as raw material (rice husk). The chemical compositions are shown in Table 4.1. Untreated sample condition contained about ~ 95 wt% of SiO_2 and other oxides such as K_2O , Na_2O , CaO and MgO . In addition, the characteristic of this sample is high concentration of potassium (~ 2 wt%). After washed by water and HCl-acid, 2% of K_2O was washed out. As a result, the SiO_2 content in these samples increased to 98.72 wt% and 99.76 %, respectively. All other impurities are also decreased.

Table 4.1 Chemical composition of rice husk ash (RHA) by XRF

Oxide	Nakhonratchasima Province		
	Untreated	Water treated	HCl treated
SiO_2	95.77	98.72	99.76
K_2O	2.11	-	0.02
Na_2O	0.18	-	-
CaO	0.53	0.75	0.06
MgO	0.38	0.06	-
Al_2O_3	-	-	0.07
P_2O_5	0.41	0.06	0.07
SO_3	0.33	0.23	-
Cl	0.12	0.03	-
Fe_2O_3	0.05	0.03	0.02
MnO	0.05	0.03	-
ZnO	0.01	0.03	-

(- = not detected)

4.1.2 Crystallization of RHA

Silica glass and quartz were heat treated to compare with RH. Silica glass is one of the typical high purity amorphous silica. Quartz is the typical crystal phase of silica at low temperature. Some general data are shown in this section. All XRD data are shown in Appendix B Figure 1 – 11.

(1) Silica glass

Silica glass heat treated at 1000°C stayed as amorphous phase and transformed to cristobalite when it was heat treated at 1400°C for 2 h. The XRD patterns are shown in Figure 4.1.

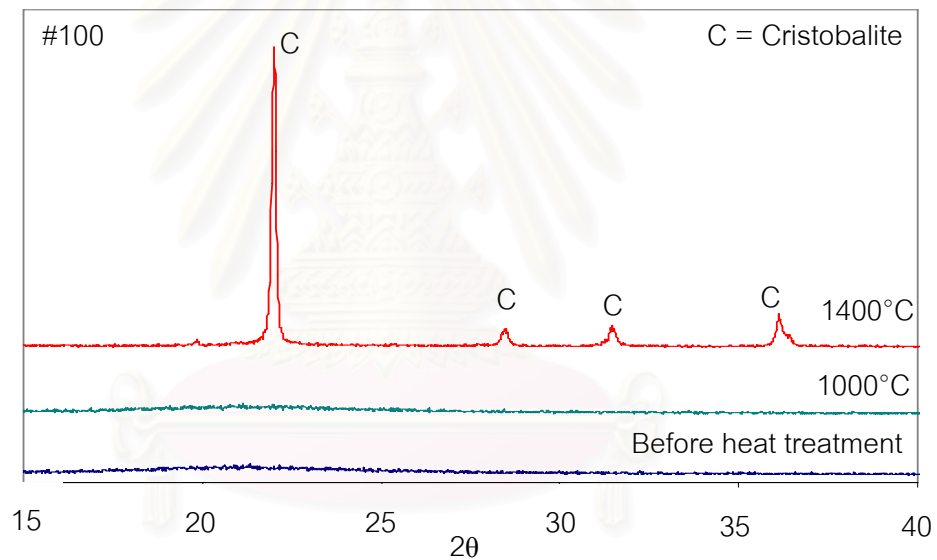


Figure 4.1 XRD patterns of silica glass sieved through a 100-mesh brass screen and heat treated at 1000°C and 1400°C for 2 h

(2) Quartz

Quartz heat treated at 1000°C stayed in quartz and transformed to cristobalite when it was heat treated at 1400°C 2 h. However, the peak of quartz remained even after heat treated at 1400°C. XRD patterns are shown in Figure 4.2.

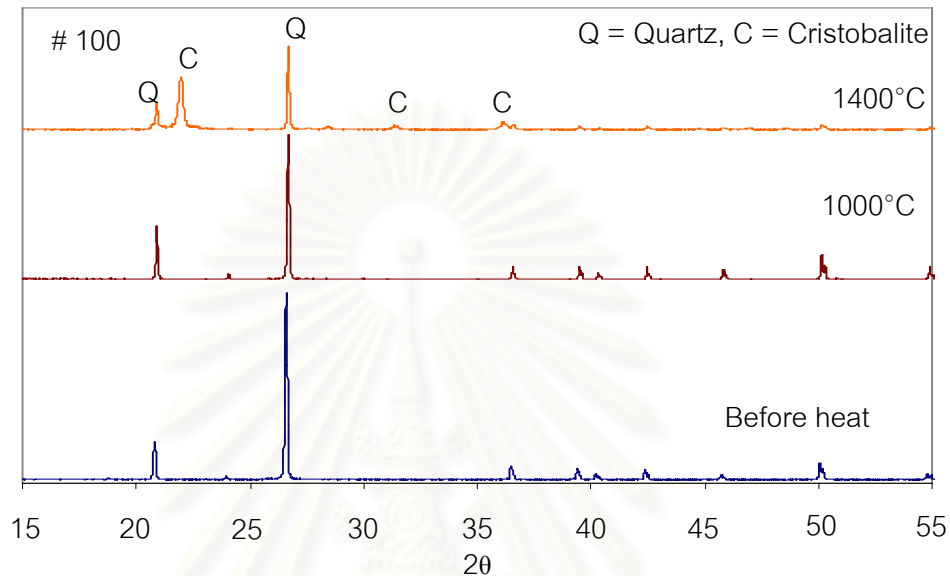


Figure 4.2 XRD patterns of quartz sieved through a 100-mesh brass screen and heat treated at 1400°C for 2 h

(3) RHA untreated RH

The RHA of untreated RH was burnt at 650°C shown broadband XRD pattern. This indicates that the silica in this material is an amorphous phase (Appendix B, Figure 5, 6 and 7).

Cristobalite was first observed above 800°C. After heating at 900°C to 1000°C, the intensity of cristobalite peak was higher and the small peak of tridymite was appeared.

The content of cristobalite decreased after heating at 1000°C to 1200°C, whereas the content of tridymite increased. When the temperature was higher than 1200°C, the content of cristobalite again increased, and the content of tridymite again slightly decreased as shown in Figure 4.3.

These results show that untreated RH can be easily transformed from amorphous silica to cristobalite and tridymite at lower temperature.

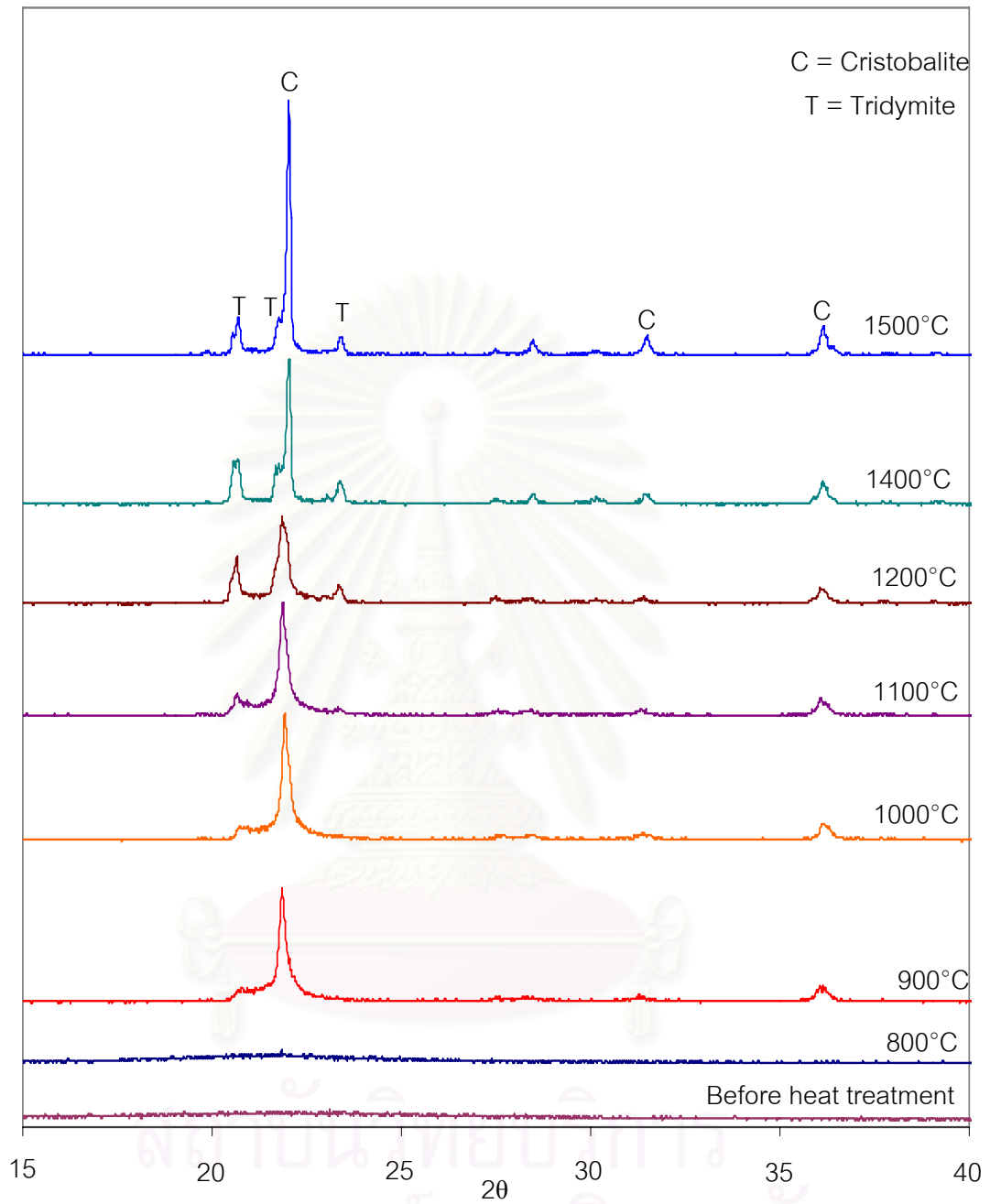


Figure 4.3 XRD patterns of RHA of untreated RH, not sieved and heat treated at 800°C, 900°C, 1000°C, 1100°C, 1200°C, 1400°C and 1500°C for 2 h

(4) Water treated RH

The RHA burned at 650°C of water treated RH also showed broadband XRD pattern. (Appendix B, Figure 8 and 9). Figure 4.4 shows the XRD patterns of heat treated RHA of water treated samples. Quartz was observed at 1000°C and amorphous phase was still remain. After heating at 1100°C to 1300°C, cristobalite peaks appeared and quartz peak decreased with increasing temperatures. After heat treated at 1400°C strong and sharp only cristobalite peak was observed. Comparing Figure 4.3 and Figure 4.4, RHA from water treated RH maintained amorphous state at 100 – 200°C higher temperature than that of untreated RH.

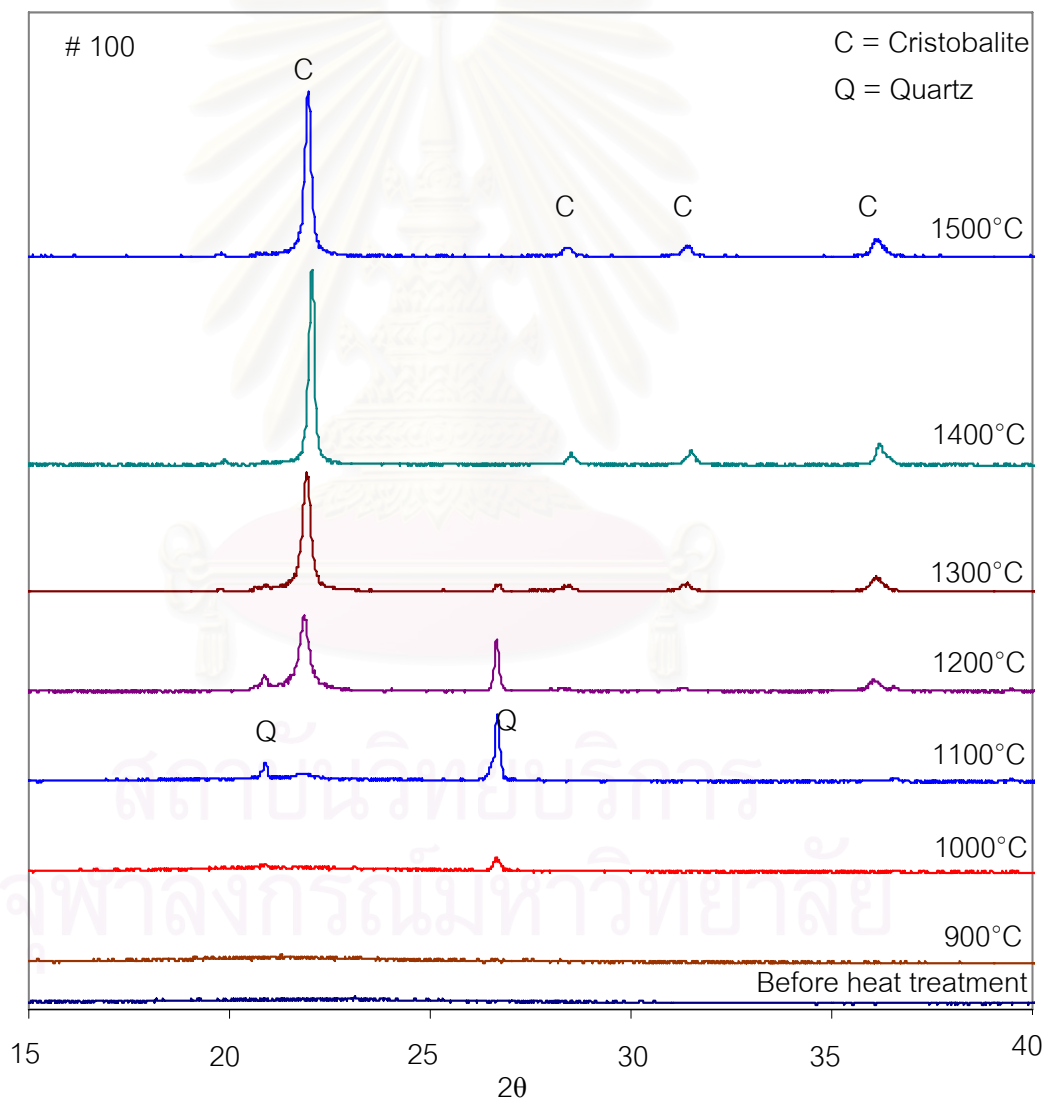


Figure 4.4 XRD patterns of RHA water treated RH, sieved through a 100-mesh brass screen and heat treated at 900°C, 1000°C, 1100°C, 1200°C, 1300°C, 1400°C and 1500°C for 2 h

(5) HCl treated RH

The RHA of HCl treated RH (#100, #325) samples before heat treatment was also showed broadband XRD pattern. (Appendix B, Figure 10 and 11).

The XRD pattern of the heat treated -100 mesh RHA from HCl treated RH sample through transformed to cristobalite at above 1200°C as shown in Figure 4.5. The XRD patterns of -325 mesh RHA show cristobalite peak at above 1300°C as shown in appendix Figure A11. The delay of the crystallization of cristobalite in -325 mesh RHA HCl treated RH compared with that of RHA-HCl treated is not clearly explained so far.

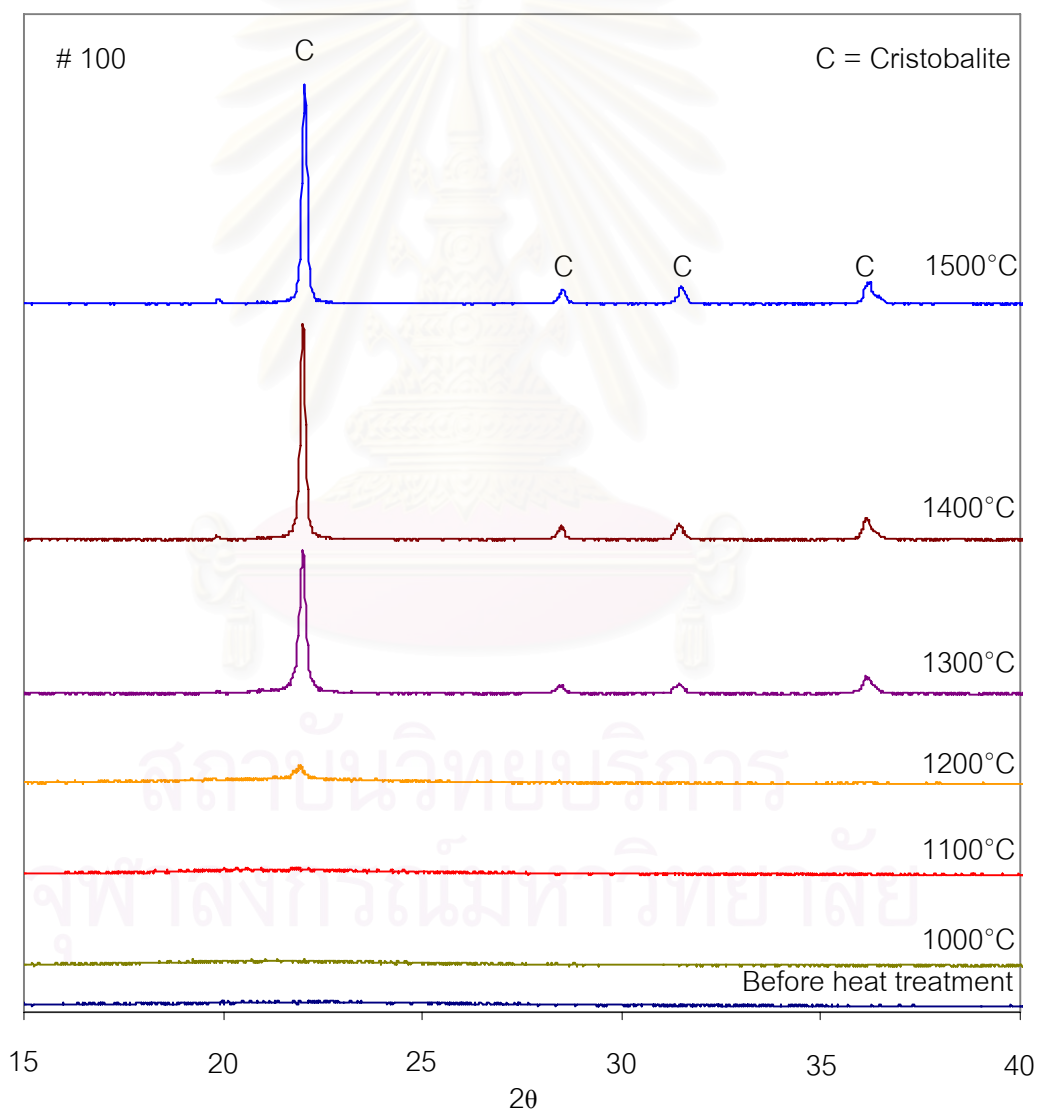


Figure 4.5 XRD patterns of RHA HCl treated RH, sieved through a 100-mesh brass screen and heat treated at 900°C, 1000°C, 1100°C, 11200°C, 1300°C, 1400°C and 1500°C for 2 h

The phase transformations after heat treatment are summarized as follows:

1. Silica glass was amorphous at 1000°C, and transformed to cristobalite at 1400°C.

2. Quartz was stable at temperature 1000°C and was not perfectly transformed to cristobalite even at 1400°C. In case of quartz, the energy required for breaking bond Si-O-Si (quartz structure) and rearrangement (reconstructive) to form new crystal structure (cristobalite structure) maybe very high as quartz transformations to cristobalite did not occur completely at 1400°C.

3. RHA of untreated RH including of ~ 2 wt% K₂O transformed to cristobalite at 900°C. K₂O played an important role as a fluxing agent. However, 100 % cristobalite could not be synthesized, this sample contains minor amount of tridymite with out prior quartz formation.

4. RHA of water treated RH sample generated quartz at low temperature (1000 – 1200°C) as well as cristobalite and transformed to nearly 100 % cristobalite at 1400 and 1500°C.

5. RHA of HCl treated RH sample showed stable amorphous phase until at 1200°C and transformed to cristobalite at higher temperature (~1300°C). The transformation temperature from amorphous to cristobalite increased with decreasing the amount of K₂O in RHA

6. The crystallization temperature was not affected by size of RH. In the literature [13], Particle size was less than 80 nm. Therefore, there are no effects on the crystallization temperature when particle size is larger than several ten-micron meter.

The refractive indices of quartz, cristobalite, and tridymite are 1.545, 1.48 and 1.47 respectively. The refractive index of LLDPE is 1.51 – 1.54 Therefore, cristobalite (C) and tridymite (T) are the candidate crystal phases as the anti-blocking powder. From the result of XRD, untreated RHA crystallized to C and T at all heat treatment temperatures. Quartz crystallized at 1000 – 1300°C in water treated RHA (RHA-W). Moreover, water treated sample transformed to pure cristobalite at 1400 – 1500°C. HCl treated RHA also transformed to pure cristobalite at over 1300°C. Only from the XRD analysis, therefore, untreated, water treated, and HCl treated RHA heat treated at 900 – 1500°C, 1400 –

1500°C and 1300 – 1500°C are the candidates for the anti-blocking powder. However, the color of untreated and water treated samples are pale pink and pale grey respectively. Only HCl treated RHA is pure white color. The specific surface area and particle size of these heat treated powders are very different with that of commercial grade (SIBELCO).

4.1.3 Morphology of heat treated samples by scanning electron microscope

The SEM photographs of various heat treated RHA are shown in Figure 4.6 and 4.9. Untreated RHA kept original morphology after heat treatment as seen in Figure 4.6– 4.7.

On the other hand, the morphologies of water and HCl treated RHA have been changed and the particle size was smaller than the untreated specimens shown in Figure 4.8 and 4.9. However, the particle size of both water and HCl treated samples are larger than the targeted particle sizes (3, 4 and 5 μm) for using as anti-blocking powder.

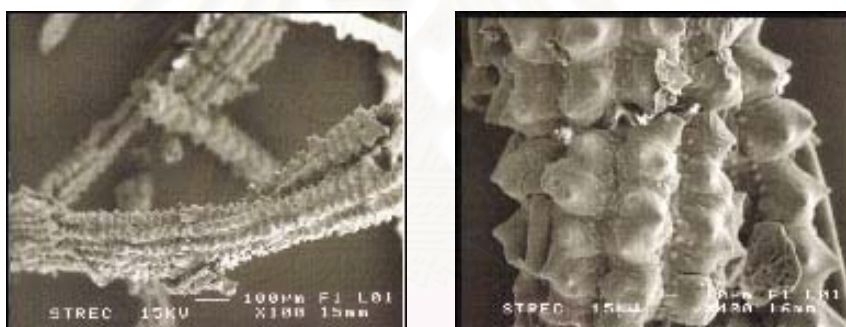


Figure 4.6 SEM photograph of untreated RHA, not sieved and heat treated at 1000°C for 2h

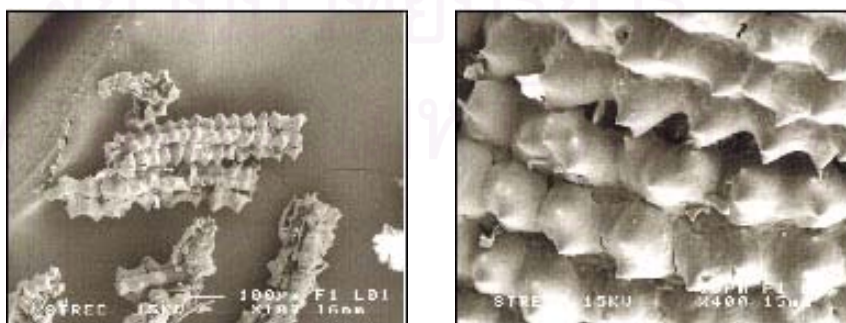


Figure 4.7 SEM photograph of untreated RHA, #100 sieved and heat treated at 1400°C for 2h

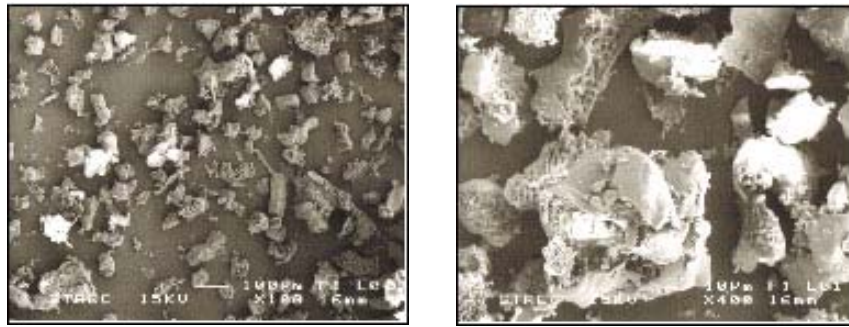


Figure 4.8 SEM photograph of water treated RHA, #100 sieved and heat treated at 1400°C for 2h

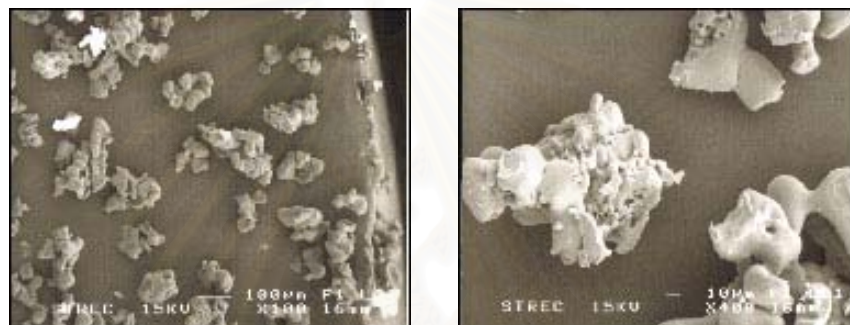


Figure 4.9 SEM photograph of HCl treated RHA, #100 sieved and heat treated at 1400°C for 2h

4.1.4 Specific surface area

As seen in Table 4.2 the specific surface area of 1-7 specimens are all less than that of commercial SIBELCO powders (8, 9 and 10 μm). Therefore, when the sample is used as the anti-blocking powder, it should be crushed to finer powder.

จุฬาลงกรณ์มหาวิทยาลัย

Table 4.2 Specific surface area of RHA treated at different conditions

Sample	Specific surface area (m ² /g)
1. Untreated no sieve, 1000°C for 2 h	0.082
2. Untreated #100, 1000°C for 2 h	0.199
3. Untreated #325, 1000°C for 2 h	0.377
4. Water treated #100, 1400°C for 2 h	0.622
5. Water treated #325, 1400°C for 2 h	0.522
6. HCl treated #100, 1400°C for 2 h	0.379
7. HCl treated #325, 1400°C for 2 h	0.225
8. SIBELCO M3000*	1.500
9. SIBELCO M4000*	3.500
10. SIBELCO M6000*	5.000

* Commercial grade cristobalite

4.2 Application of RHA

4.2.1 Application of cristobalite as an anti-blocking agent

In Thailand, cristobalite used as anti-blocking powder in polyethylene films has been imported. One of the main manufacturers of cristobalite is SIBELCO. The synthesized cristobalite from RHA was tested to see its potential as an alternative anti-blocking powder for LLDPE films.

(1) Heat treatment of black rice husk ash

In the test of anti-blocking, we need more than 2 kg of ash. To prepare 2 kg of ash, we had to burn more than 10 kg of RH. However, we do not have a good furnace to burn a large amount of RH. Therefore, we used black rice husk ash from rice milling factory in Ratchaburi province. The black-RHA (B-RHA) was sieved through a 50 mesh screen and heat treated at various temperatures between 1000 to 1400°C, as described in section 3.1.2. XRD profiles are shown in Figure 4.10. Appearance of the resulting

powder are shown in Figure 4.11. From the Figures 4.10 and 4.11, the optimum heat treatment condition to obtain cristobalite with the lowest amount of other undesired phases was 1200°C for 4h.

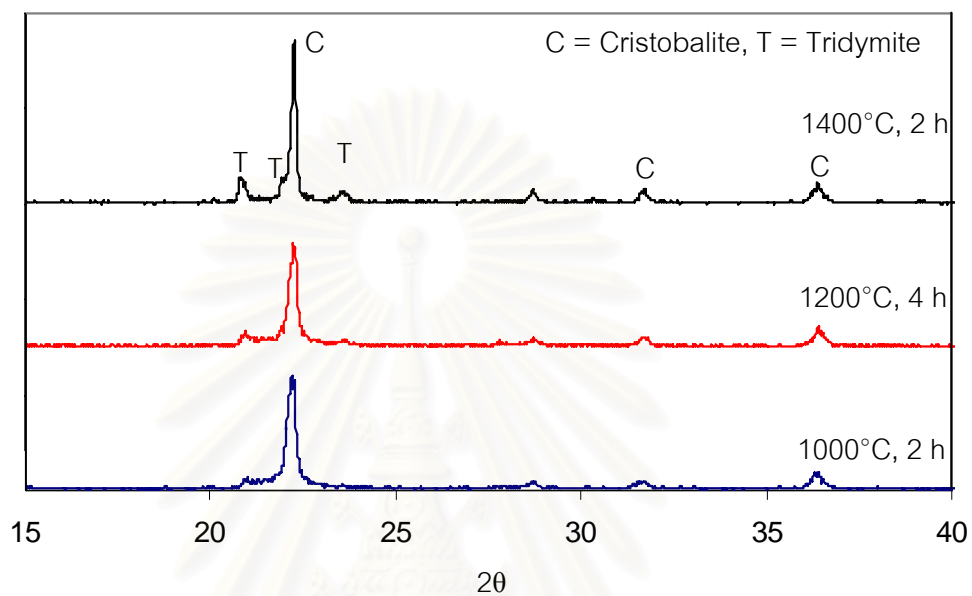


Figure 4.10 XRD patterns of B-RHA # 50 after heat treated at various temperatures and times



Figure 4.11 Appearance of heat treated B-RHA at various conditions, from 1000 to 1400°C for 2 h and 4 h

(2) Preparation of cristobalite powder

Two kilograms of the heat treated powder were ground and sieved by the air jet mill. The targeted particle sizes are 3, 4 and 5 μm . However, the average particle sizes were 3.3, 6.5 and 18.6 μm as shown in Table 4.3 and morphologies of before and after ground RHA are shown in Figure 4.14, 4.15, 4.16 and 4.17. Oil absorption and average particle size are also shown in Table 4.3. XRD patterns and Particle size distribution curves are shown in Figure 4.12 and Figure 4.13, respectively.

Table 4.3 Oil absorption and average grain size of synthesized and commercial cristobalite samples

Sample Name	Oil absorption g (100g)	D50 μm
R-3-CY	49.4	3.3
R-4-CY	46.8	6.5
R-5-CY	47.2	18.6
M4000	47.2	5
M6000	60.5	3

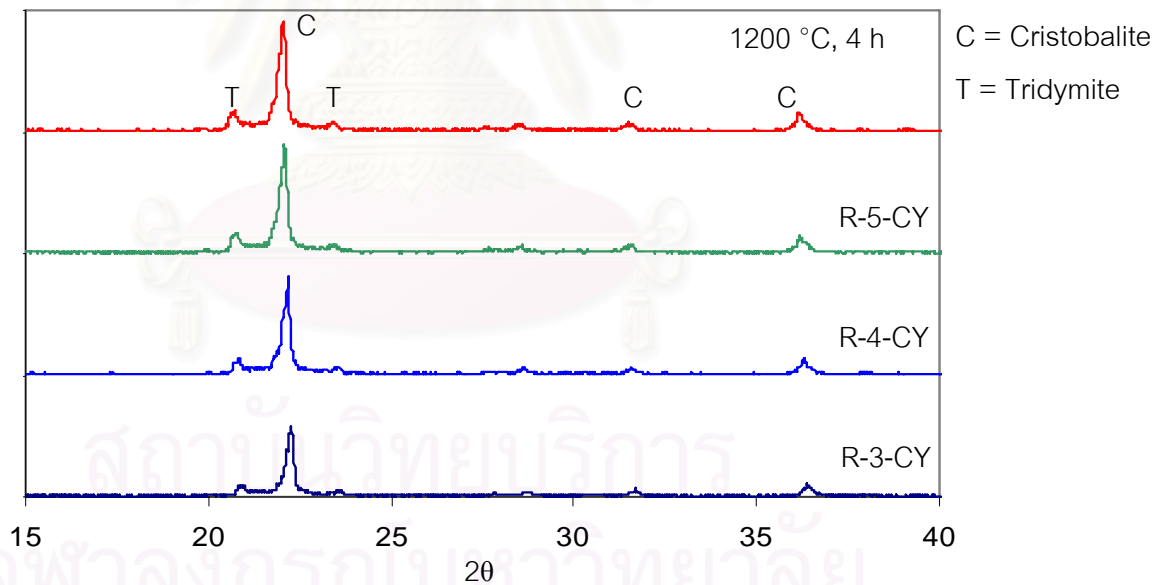


Figure 4.12 XRD patterns of B-RHA # 50 heat treated at 1200°C for 4h, crushed and sieved by Air jet mill

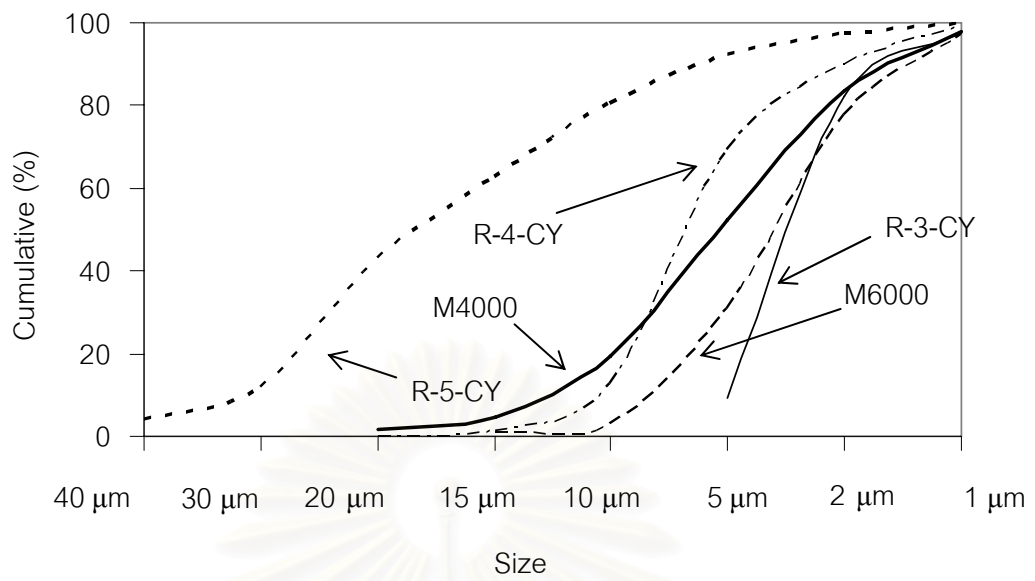


Figure 4.13 Particle size distribution of ground and commercial grade samples

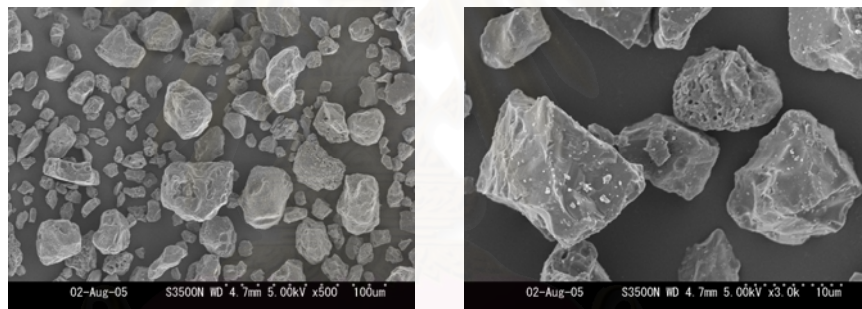


Figure 4.14 SEM photograph of B-RHA # 50 heat treated at 1200°C for 4 h.
(before grinding)

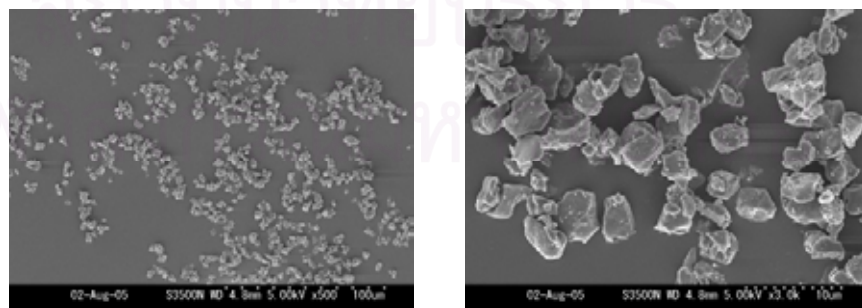


Figure 4.15 SEM photograph of synthesized cristobalite (R-3-CY)

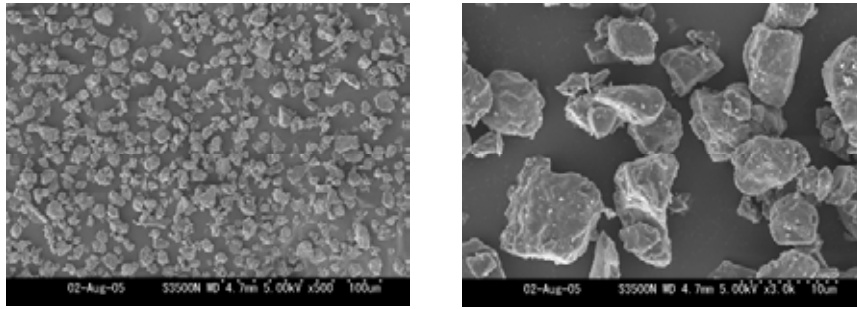


Figure 4.16 SEM photograph of synthesized cristobalite (R-4-CY)

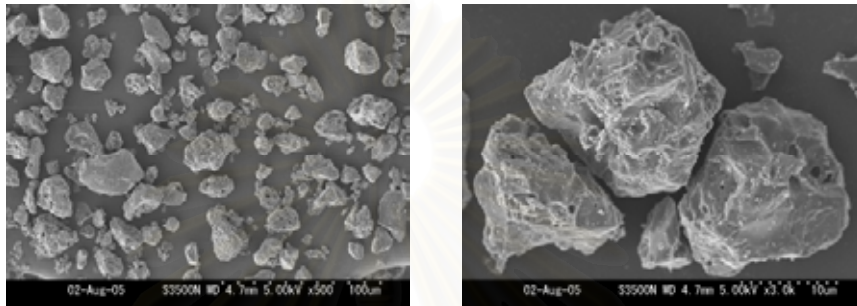


Figure 4.17 SEM photograph of synthesized cristobalite (R-5-CY)

(3) Blown films of LLDPE with various cristobalites

Synthesized cristobalite from RHA (R-3-CY, R-4-CY and R-5-CY) and commercial cristobalite (M4000) were used as anti-blocking powders for blown films of LLDPE. Ninety percent of LLDPE (metallocene grade) [15] with 10% cristobalite composition was mixed as a masterbatch. The masterbatches were extruded, chopped into pellets, and later dried. The masterbatch including synthesized cristobalite from RHA are not clear comparing with commercial grade M4000, as shown in Figure 4.18.



Figure 4.18 Color of masterbatches with different cristobalite powders

Film blowing machine used in the study is shown in Figure 4.19. The percentages of cristobalite used in LLDPE films were 1 and 2% for all batches.



Figure 4.19 Blown film process

(4) Transmittance of films

The transmittances of all blown film are shown in Figure 4.20. The transmittance values of the LLDPE films containing 1 and 2% by wt. are approximately 2.7% and 4.7% lower than that of the control LLDPE (metallocene grade). However, the differences of transmittances value of all film samples with the same amount of synthesized cristobalite and commercial grade cristobalite are relative insignificant and, see Figure 4.20.

สถาบันวิทยบริการ
จุฬาลงกรณ์มหาวิทยาลัย

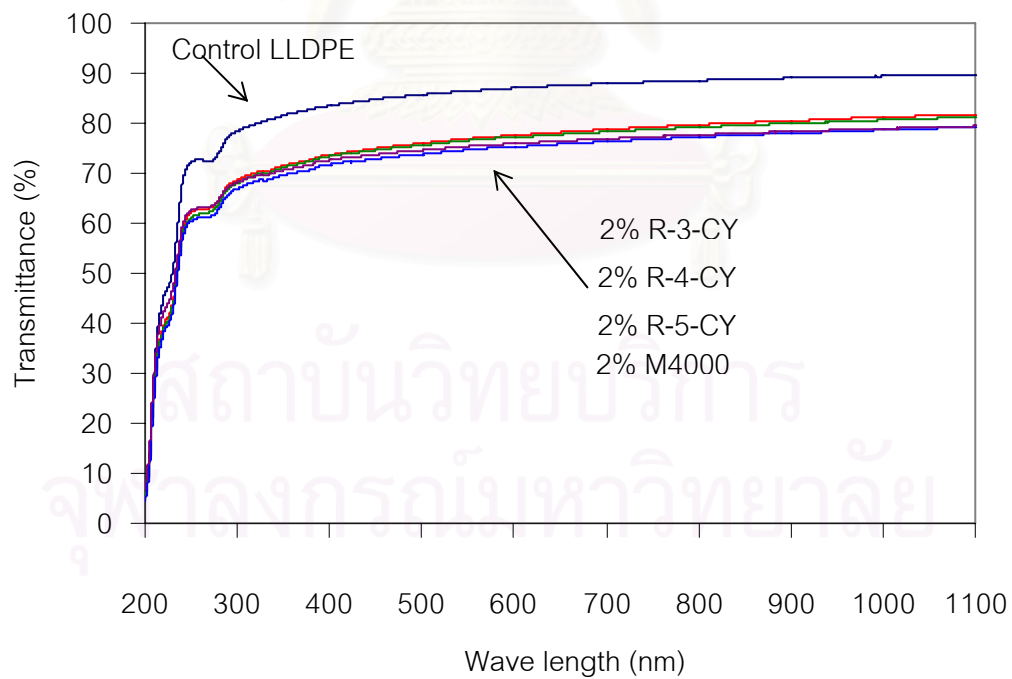
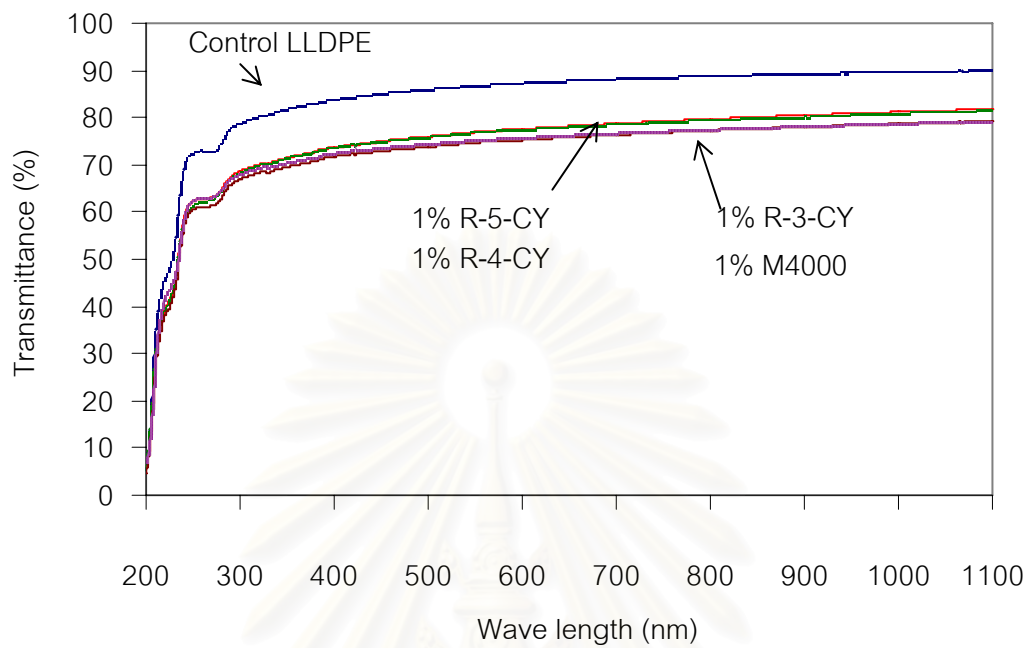


Figure 4.20 Relationship between wavelength (nm) and transmittance (%T) of plastic films with anti-blocking power of 1 and 2 wt% and control LLDPE film

(5) Mechanical properties of films

Figures 4.21 and 4.22 show the percent elongation at break and tensile stress at break of LLDPE film with 4 kinds of anti-blocking agents. Resulting properties for both R-3-CY and R-4-CY are almost the same with M4000. However, the percent elongation at break of large particle size cristobalite, R-5-CY, were lower than that of M4000. Therefore, too large particle size of cristobalite is not good from the standpoint of mechanical properties.

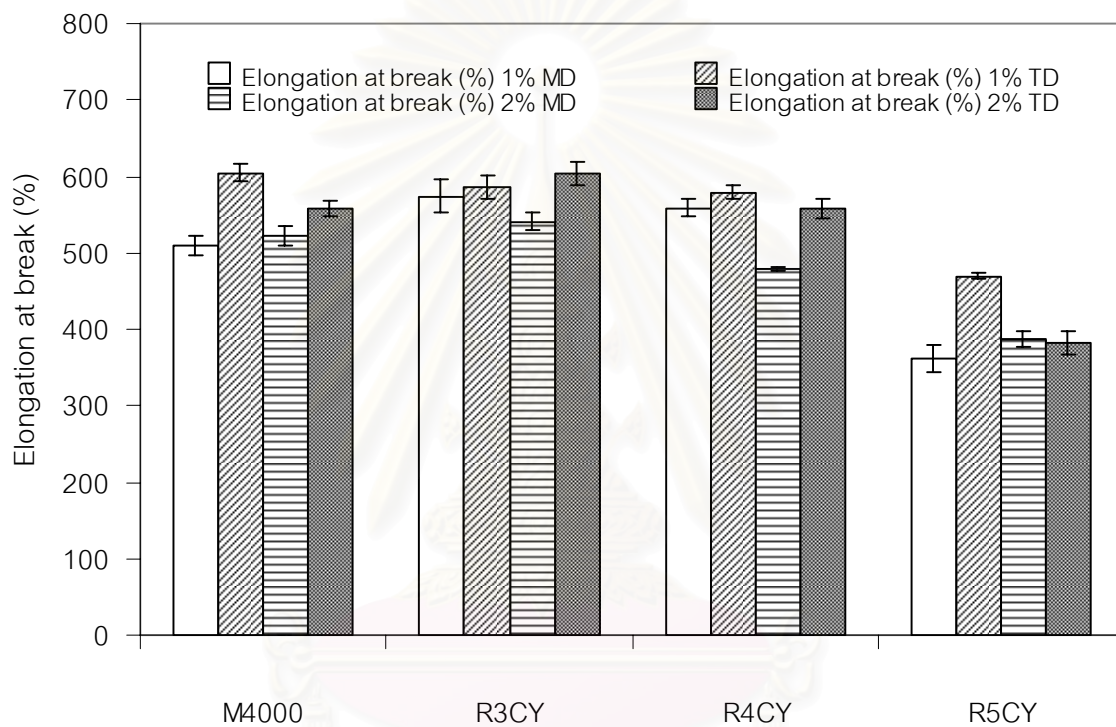


Figure 4.21 Percent elongation at break of plastic films with 4 kinds of cristobalite and tested in machine direction (MD) and transverse direction (TD)

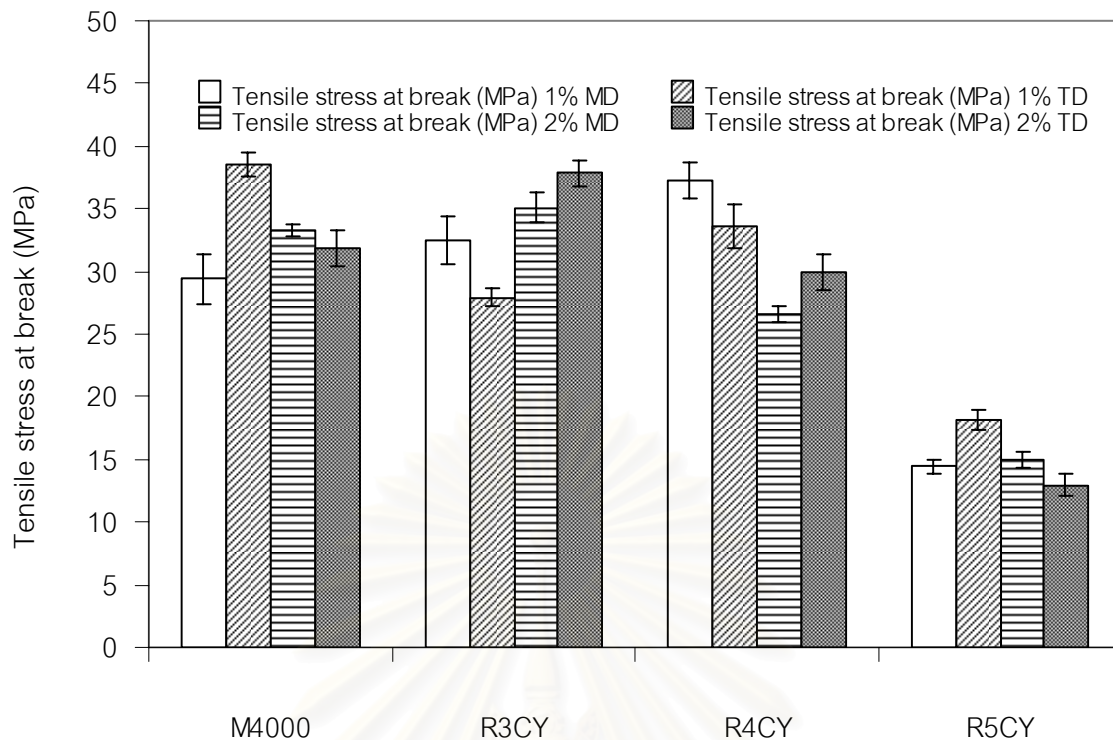


Figure 4.22 Tensile stress at break of plastic films with 4 kinds of cristobalite and tested in machine direction (MD) and transverse direction (TD)

(6) Discussion on the application of cristobalite as an anti-blocking agent

Although, a quantitative measurement of anti-blocking in plastic film using cristobalite was not conducted, the feeling of peeling off the film containing cristobalite powder prepared from RHA, R-3-CY and R-4CY, was similar to the film with commercial cristobalite such as M4000 by Sibelco. Two plies of films were easily separated with no force required.

The color of heat treated powder was pale pink as shown in Figure 4.11. On the other hand, the color of master batches are gray (Fig.4.18). The transmittance of the film with cristobalite synthesized from RHA are about 10% and 6% lower than that with M4000.

As a result, the cristobalite prepared from RHA can be applied as an anti-blocking powder in LLDPE films, however, the color of synthesized cristobalite should be improved, Otherwise this powder could be used for the film where haze is not an important characteristic.

4.2.2 Application of amorphous silica as an anti-blocking agent

(1) Chemical compositions of amorphous silica prepared from RHA

During the experimental study of utilizing cristobalite as an anti-blocking agent 4.2.1, it was found in some reports that cristobalite is currently claimed to be one of the carcinogenic materials [16, 17]. As referred in Chapter 2 [7], C. Kunsawat et. al had successfully performed experiment to apply amorphous RHA as an anti-blocking agent of LLDPE. However, RHA prepared in such investigate was washed by HCl acid. The washing process might increase the production cost. In the case of this thesis, Synthesis of RHA process is shown schematically in Figure 4.23. The chemical compositions of untreated and water treated of RHA are shown in the Table 4.4. The RH is from Ratchaburi province. Untreated RHA includes approximately 2 wt% of K_2O . However, the amount of K_2O was reduced 0.05 wt% after treated by water. SiO_2 content also increases from 89.6 wt% to 93.7 wt% after treated.

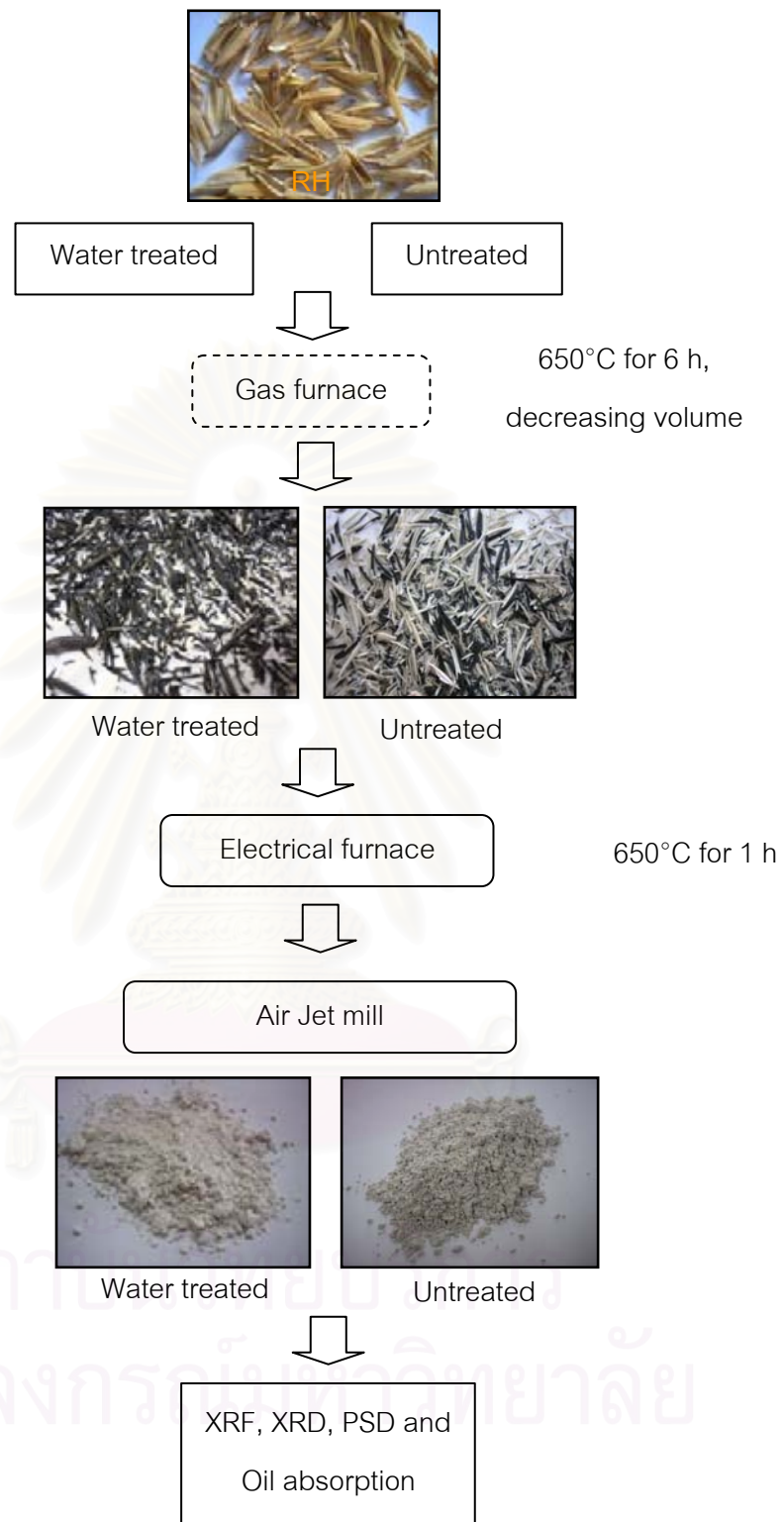


Figure 4.23 Flow chart of synthesizing amorphous RHA

Table 4.4 Chemical composition of rice husk ash (RHA) by XRF

Oxides	Ratchaburi Province	
	Untreated	Water treated
SiO ₂	89.56	93.72
K ₂ O	1.95	0.05
Na ₂ O	0.15	0.11
MgO	0.50	0.20
Al ₂ O ₃	0.30	0.04
P ₂ O ₅	0.62	0.08
SO ₃	0.21	0.19
Cl	0.23	0.15
Fe ₂ O ₃	0.12	0.02
CaO	0.87	1.09
TiO ₂	0.02	-
B ₂ O ₃	0.02	-
MnO	0.15	0.05
ZrO ₂	0.01	-

(- = not detected)

(2) Crystal structure of RHA

The RHA powders were ground and sieved using an air jet mill. The XRD patterns of RHA samples are shown in Figure 4.24. Both samples are basically amorphous. However, untreated sample shown mixture of amorphous and quartz. It may come from sand from adhering soil. Water treated sample also contaminated with quartz, but less than untreated sample. As a result, washing process was not enough to clean the RH.

Average particle size and particles size distribution of ground amorphous silica are shown in Table 4.5 and Figure 4.25, respectively. Oil absorption value of powder increased from 90.94 to 95.66 g /100g (Table 4.4) after treated by water.

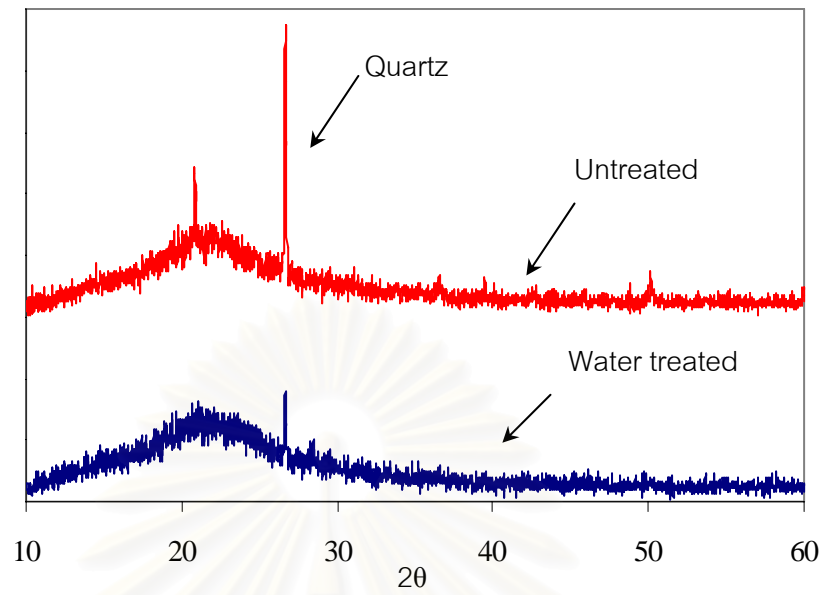


Figure 4.24 XRD patterns of amorphous silica untreated and water treated and ground by Air jet mill

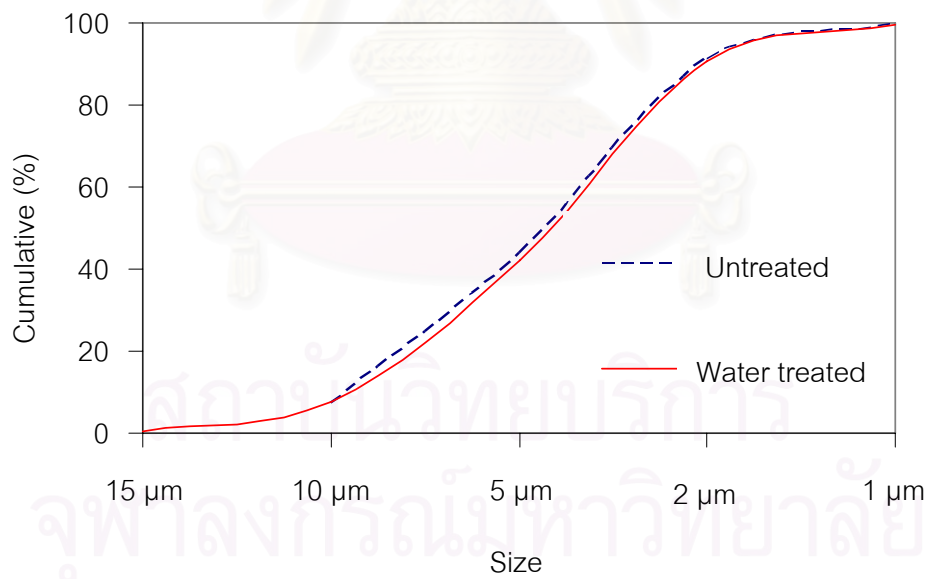


Figure 4.25 Particle size distribution of ground amorphous silica

Table 4.5 Properties of amorphous silica powder

Sample Name	Oil absorption	D50
	g (100g)	μm
untreated	90.9	5.2
water treated	95.7	5.1

(3) Film blowing process

Untreated and water treated cristobalite/tridymite powders were used for film blowing experiment. Ninety percent of LLDPE (metallocene grade) with 10% amorphous silica by wt. were mixed via twin-screw extruder to produce a masterbatch. The masterbatches were extruded, chopped into pellets which were later dried in an oven. The color of masterbatch including untreated and water treated powder RHA are not clean compared with the controlled LLDPE film sample, as shown in Figure 4.26.



Figure 4.26 Masterbatch of plastic samples

(4) Transmittance

The result of transmittances of light for plastic film containing 1 and 2 wt% of amorphous silica are shown in Figure 4.27. The transmittance values of films decreased about 10% and 14% comparing to the controlled LLDPE film (metallocene grade) with 1 and 2% amorphous powders, respectively. However, the transmittance values are not significantly different between the films having untreated and water treated powder.

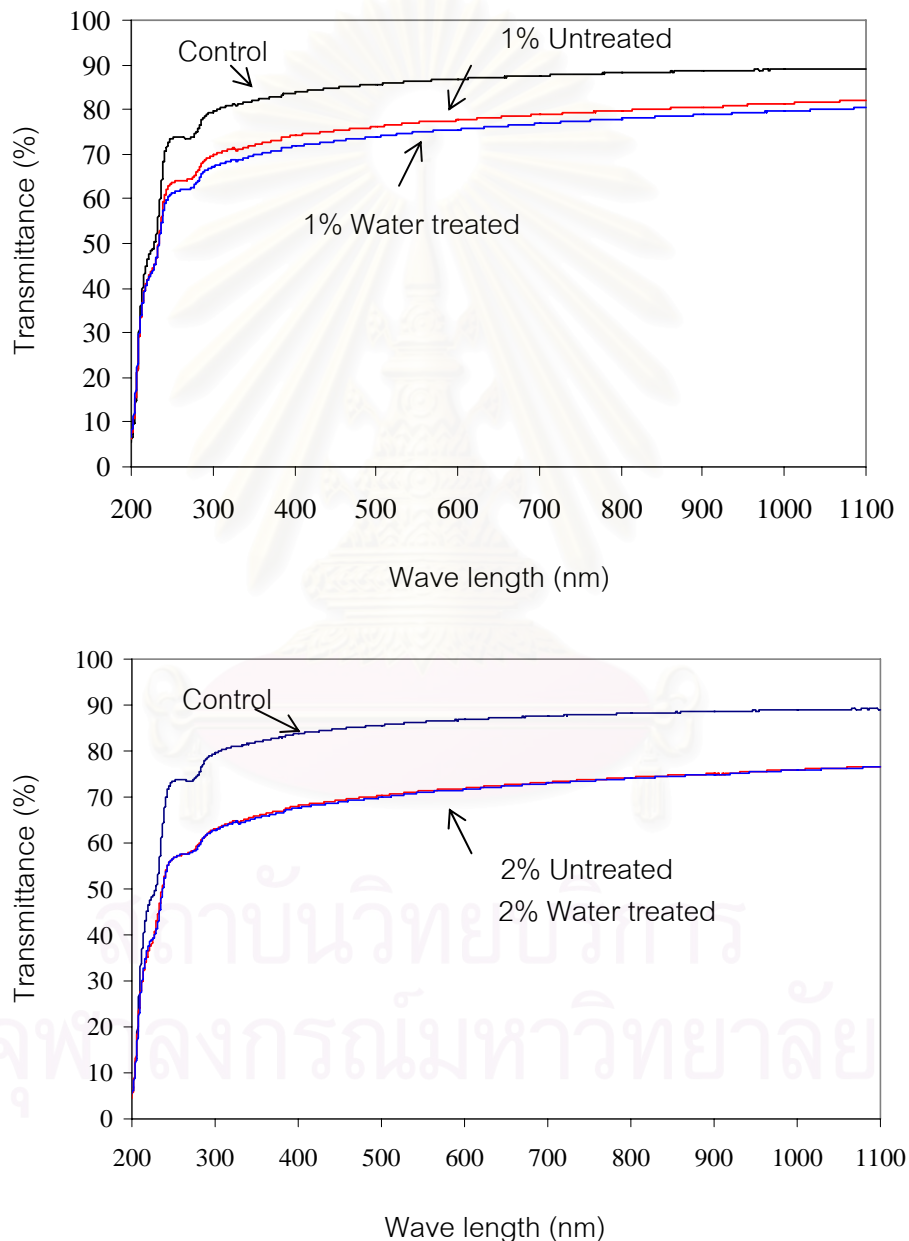


Figure 4.27 Relationship between wavelength (nm) and transmittance (%T) of plastic films with amorphous silica of 1 and 2 wt% as an anti-blocking agent

(5) Mechanical properties of films

Figure 4.28 and 4.29 Show the maximum percent elongation at break and tensile stress at break of controlled LLDPE with 2 types of amorphous silica. Both data of untreated and water treated of RHAs are slightly different with controlled LLDPE film. However, the percent elongation at break of 1% TD is different from LLDPE ~ 20%. Moreover the tensile stress at break was 7-10 MPa lower than of controlled LLDPE.

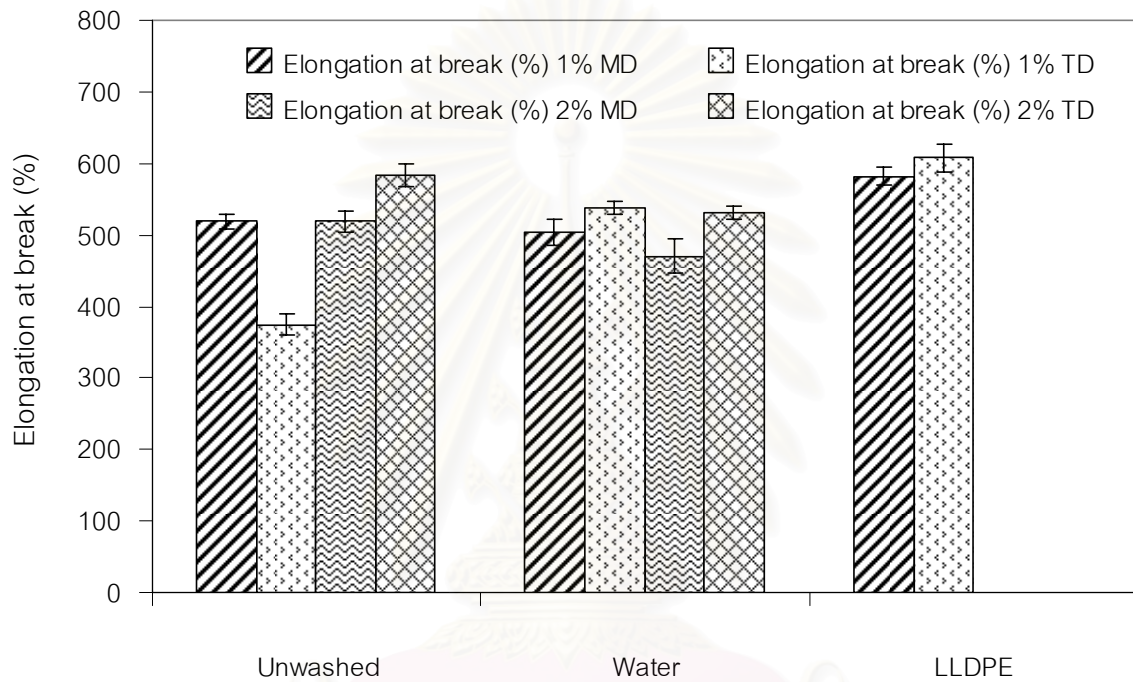


Figure 4.28 Percent elongation at break and various kinds of plastic films with 1-2% of amorphous silica tested in machine direction (MD) and transverse direction (TD)

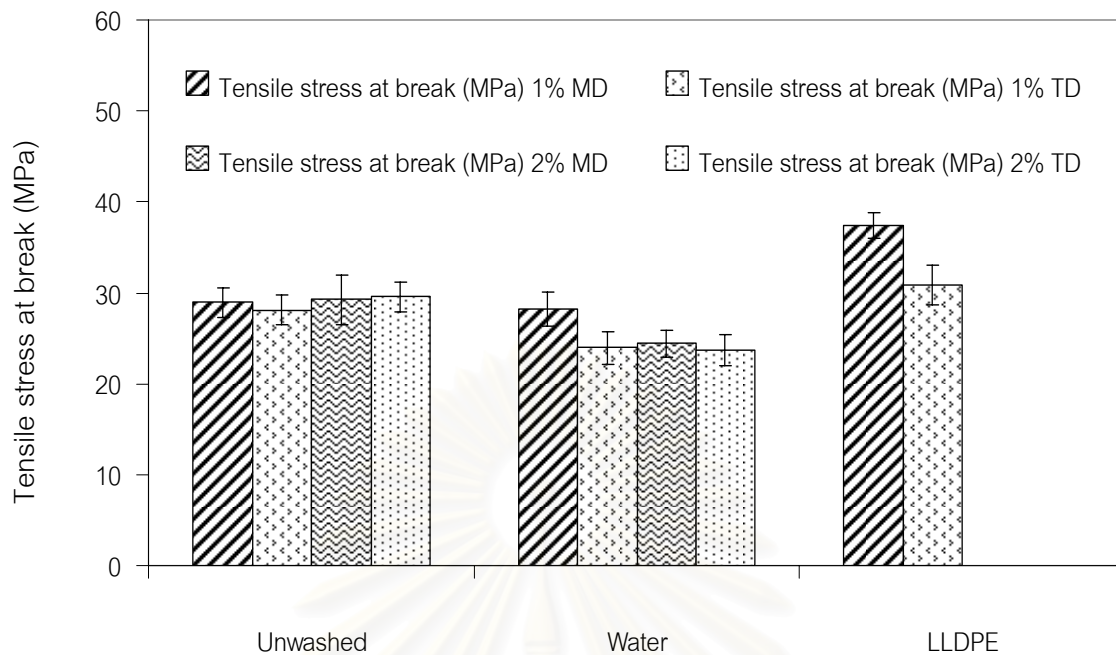


Figure 4.29 Tensile stress at break and various kinds of plastic films with 1-2% of amorphous silica tested in machine direction (MD) and transverse direction (TD)

(6) Discussion on the application of cristobalite as anti-blocking agent

Amorphous silica synthesized from RHA was crushed using a small air jet mill shown in Fig. 3.6. On the other hand, cristobalite powder from RHA was crushed by a production scale air jet mill of HOSOKAWA. As a result, the particle size distributions are similar as shown Figure. 4.3 and 4.25 oil absorption values are very different (Table 4.3 and Table 4.25), The elongation values are similar Fig. 4.21 and 4.28, but the value of tensile stress at break with amorphous silica are smaller than that with cristobalite powder. The causes of these differences were not analyzed in this experiment.

4.2.3 Water glass from amorphous silica

It has been well known that amorphous silica can react with NaOH water solution easily at less than 100°C and change to sodium silicate water solution is (“water glass”).

Water glass Na_2SiO_3 is the most widely used dispersant in ceramic industry, the soil hardening material in construction industry, the raw material for precipitated silica

and silica gel, and others. The production amount of water glass is about 600,000 tons per year in Japan.

Generally, water glass is produced as shown in Figure 4.30 (a). The process to obtain water glass using amorphous silica as raw material is shown in Figure 4.30 (b).

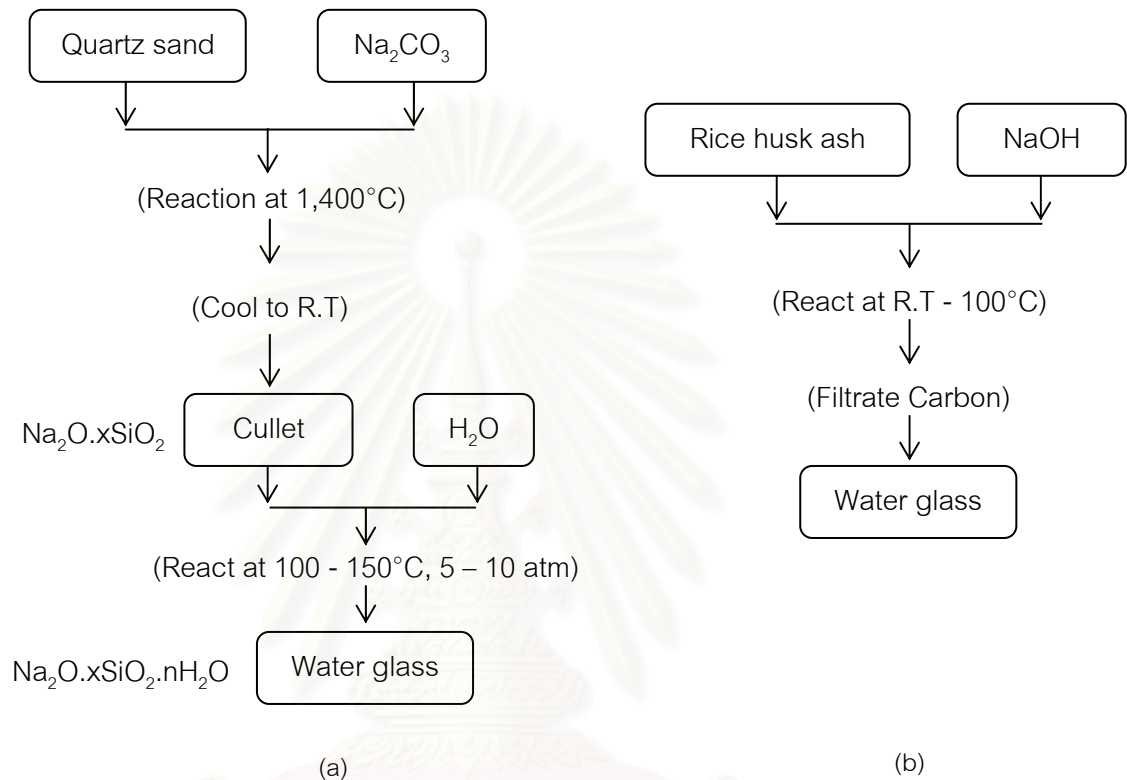


Figure 4.30 The process flow chart to synthesize water glass from (a) quartz and (b) amorphous silica

RHA includes of some amount of carbon. Therefore, filtration of carbon is essential in the process (b). Still the process (b) is simple than process (a) and does not consume much energy. As a result, RHA should be a very good raw material to synthesize water glass.

The phase diagram of $\text{SiO}_2 - \text{Na}_2\text{O} - \text{H}_2\text{O}$ is shown in Figure 4.31

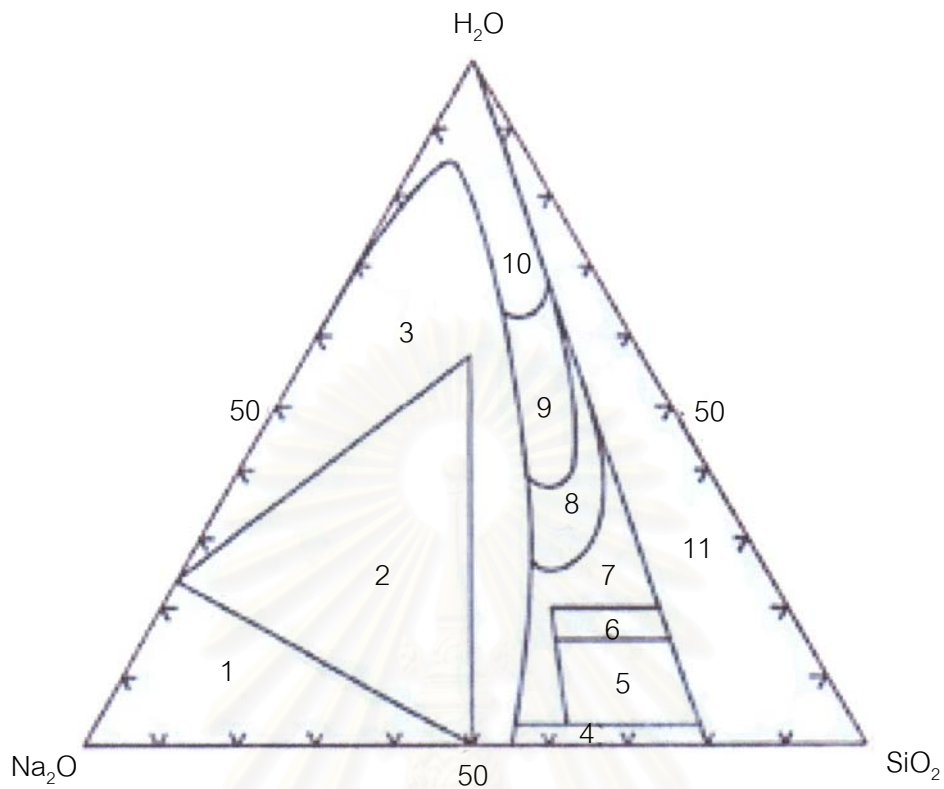


Figure 4.31 Phase diagram of SiO_2 - Na_2O - H_2O

1. Mixture of NaOH and Ortho - sodium silicate
2. Meta - sodium silicate and crystal including its hydrate
3. Mixture including crystal
4. Glassy sodium silicate
5. Glass hydrate
6. Dehydrate sodium silicate
7. Semi - solid sodium silicate
8. High viscous sodium silicate
9. Commercial sodium silicate solution
10. Thin sodium silicate solution
11. Unstable liquid and gel

As seen in Figure 4.31, stable water glass is in the region 9. RHA, NaOH, and water in the region 9 were mixed in a glass beaker. When $\text{SiO}_2/\text{Na}_2\text{O}$ mole ratio is = 2.5, silica in RHA easily changed to sodium silicate. On the other hand $\text{SiO}_2/\text{Na}_2\text{O} > 2.5$ (mole ratio), it needed to heat up to about 90°C to get sodium silicate.

RHA generally includes of 2-10 wt% carbon. Therefore, filtration of carbon after the reaction to synthesize NaSiO_3 solution was essential. The filtration sometimes needs longer time. Another disadvantage of this process is the purities of water glass. RHA includes of 3 – 5 wt% impurities such as K_2O , Na_2O , CaO , Al_2O_3 , and so on. Then the synthesized water glass also includes of these impurities.

As a result, synthesizing water glass from RHA is promising process to get water glass from the simple and a less energy consuming, however, filtration process and impurities are two process disadvantages. The industrial application of RHA as the raw material of water glass should be discussed in the difference stage.

4.3 RHA from factories and power plants

When RHA is used for some application, the cost of RHA is one of the important factors. The price of RH in the market is about 0.8–1.0 Baht/kg. The content of SiO_2 in RH is about 20%. Therefore, the cost of raw material for RHA is about 4-5 Baht/kg. If burnt RHA from factory and power plant can be used as the raw material for amorphous SiO_2 , the cost might be very low. Therefore, RHA from factories and power plants were analyzed by XRD.

4.3.1 Crystal phase

In Thailand, much amount of RHA is exhausted in many factories. Burning technology and quality of RHA from the several factories were surveyed. The properties of RHA from factories were characterized using XRD. Good properties of RHA should be amorphous silica with low carbon content for using as anti-blocking agent and sodium silicate. Crystal phase of RHA depends on the alkali ion content in rice husk before burning process, soaking temperature, and time of burning as already been reported in section 4.1.2. The burning temperature and time are different from types of different furnaces and operating conditions. RHA from various factories are shown in Table 4.6.

Table 4.6 The crystal phase of ashes from factories and power plants

No.	Factory and or Plant name	Furnace type	Crystal phase	Out look and/or color	Appendix Figure No.
1	AT Bio Power Plant (Pichit Province)	Suspension	Amorphous Quartz	Gray	A 15
2	Thai Power Supply (3 MW plant, Rice husk only)	Stoker	Cristobalite	Black	A 16
3	Thai Power Supply (Mixed bio-mass 10 MW plant)	Fluidize bed	Amorphous	Black	A 17
4	Mahaphant Fiber cement Industry	Stoker	Cristobalite	Black	A 18
5	Kong Thai Fong Ltd (fire rice mill factory)	Stationary	Cristobalite	Black	A 19
6	Saraburi Province Cooperative Ltd.(Fire rice mill factory)	Stationary	Cristobalite	Black	A 19
7	P. Saengwattana 3 Fire Rice Mill Ltd.	Stationary	Cristobalite, Quartz	Black	A 20
8	P. Saengwattana 4 Fire Rice Mill Ltd.	Stationary	Cristobalite	Black	A 19
9	Jun Kai Seng Ltd, (Fire rice mill factory)	Stationary	Cristobalite	Black	A 19
10	Song Phee Nong Rice Mill Ltd. (Fire rice mill factory)	Stationary	Cristobalite	Black	A 19
11	Satake (Pakestan plant)	Carbonizing	Cristobalite	Black	A 21

12	Satake (Suranaree university plant)	Carbonizing	Cristobalite	Black	A 22
13	KANSAI SMG 500	Carbonizing	Amorphous	Black	A 23
14	KANSAI CE/LM 600	Carbonizing	Amorphous	Black	A 24
15	KANSAI CE/DK 750	Carbonizing	Cristobalite	Black	A 25
16	KANSAI RC/DK 750	Carbonizing	Cristobalite	Black	A 26
17	KANSAI LM 900 Black	Carbonizing	Amorphous	Black	A 27
18	KANSAI LM 900 White	Carbonizing	Cristobalite	White	A 28
19	MEIWA Outer 400	Carbonizing	Amorphous	Black	A 29
20	MEIWA Inter heat	Carbonizing	Amorphous, small amount of cristobalite	Black	A 30

The ashes from small rice mill factories (Stationary furnace) are cristobalite as shown in No.5 – 10 in table 4.6. Stoker furnaces burn several thousand tons of RH in a year produces cristobalite waste as shown in No. 2 and 4. The ashes from large-scale facilities, in which more than 0.1 million tons of RH per year is burnt, are basically amorphous as shown in No.1 and 3. From the results mentioned above, stoker furnace is not good to get amorphous SiO_2 . Fluidized bed and suspension furnaces can burn RH to get RHA in amorphous state.

The ashes from No.11 – 20 are the exhaust of the gasification plant. However, ashes from gasification furnace include about 40 – 60 wt% of carbon. The ashes are amorphous, however, No.18 is the special ash stayed in the chimney.

The crystal phase of RHA from factories and power plants are summarized in Table 4.7

Table 4.7 Summarize of the crystal phases of ashes from factories and power plants

Type	Size	Scale	Phase of RHA	Crystal phase
Incineration in the field	Small	-	Amorphous, Cristobalite	X
Stationary furnace	Small	-	Cristobalite	XXXXXX
Carbonizing furnace	Small-Medium	< 1MW	Amorphous, Cristobalite	ooooΔ
Stoker furnace	Medium-Big	3 – 10 MW	Cristobalite	XXX
Fluidized bed	Big	10 – 40 MW	Amorphous	O
Suspension	Big	20 MW	Amorphous	O


























4.3.2 Oxidation of ashes from gasification furnaces

RHA from factories No. 1 – 10 included 2 – 10 wt% of carbon and the color was black. When these ashes are applied for water glass and an anti-blocking agent, white color is preferable. Selected RHA from gasification furnaces were heat treated at various temperatures between 500 and 800°C for 2 h in an air atmosphere furnace. The color of these ashes stayed gray even after heat treated at 1000°C as shown in Figure 4.11. The color fairly changed to white at very low heat treatment temperature as 500°C. However, black particles remained. It is reported that a glassy phase generated from the reaction of K_2O and SiO_2 covers the fully unburned RH, then the fully unburned RH remain as black ash. And when RH is burned slowly, the amount of the remaining is little [14]. Considering the fact, the burning speed of RH in gasification furnace was slow. Decreasing the black particles is important for the application of RHA.

4.3.3 Mass loss of gasification furnace ashes after oxidation

Table 4.8 shows the mass loss of ashes after heat treated in air atmosphere at the temperature of 500-800°C. The mass loss means the content of carbon in the ashes. Carbon combusted completely at 500°C. Kansai SMG-500 and two MEIWA's ashes included more amount of carbon than Kansai CE-LM 600 and LM-900 Black. It is thought that Kansai SMG-500 and two MEIWA's ashes have not incinerated perfectly.

Table 4.8 RHA from factories burnt in oxidation condition at various temperatures

Sample	Before heat treatment	500°C, 2h	600°C, 2h	700°C, 2h	800°C, 2h
Kansai SMG-500					
Kansai CE-LM 600					
Kansai LM-900 Black					
MEIWA Inter heat					
MEIWA Outer heat					

Samples	500°C, 2h wt. loss (%)	600°C, 2h wt. loss (%)	700°C, 2h wt. loss (%)	800°C, 2h wt. loss (%)
Kansai SMG-500	65.1	63.9	63.6	64.2
Kansai CE-LM 600	41.8	45.9	48.6	45.3
Kansai LM-900 Black	46.7	45.6	46.5	51.0
MEIWA Inter heat	59.8	60.6	62.8	60.0
MEIWA Outer heat	68.0	68.5	50.0	68.8

4.4 Effect of various washing conditions on the remaining K_2O

As seen in section 4.1.2, the crystallization of amorphous SiO_2 was strongly affected by the content of K_2O . Only one washing condition was used in experiment as shown in section 4.1. The washing condition was a complicated process and time consuming. Therefore, the effect of washing conditions was studied in this experiment.

The RHA calcined at $650^\circ C$ for 2 h was characterized by XRD and XRF. As shown in Appendix F Table 28. K_2O decreased with increasing of the washing time and soaking hours as shown in Figure 4.33. The increment of SiO_2 is shown in Figure 4.32 which almost corresponds to the decrement of K_2O .

XRD pattern of washed RH by washing machine and soaked are shown in Figure 4.34 and Figure 4.35. Quartz was strongly observed only in Figure 4.35. This must come from the adhering soil. Therefore, not only soaking in water but also washing is essential to clean the RH.

Both conditions are not sufficient to clean impurity the perfectly. The better mixing, washing, and soaking should be fast, that not too complicate, and less time consuming process.

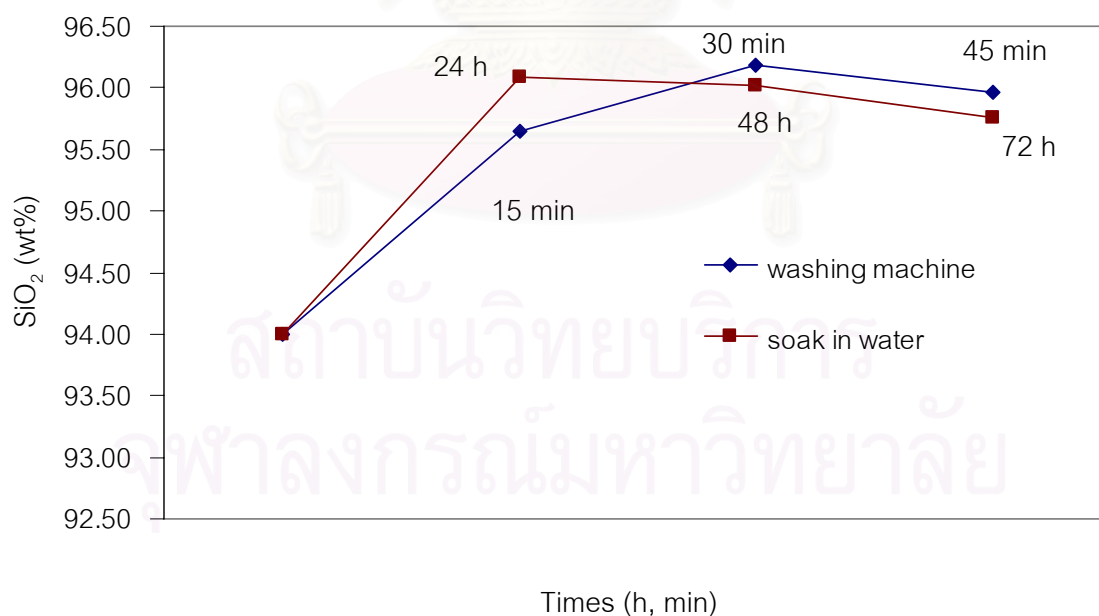


Figure 4.32 Relationship of silica content (wt%) in RH and various washing conditions

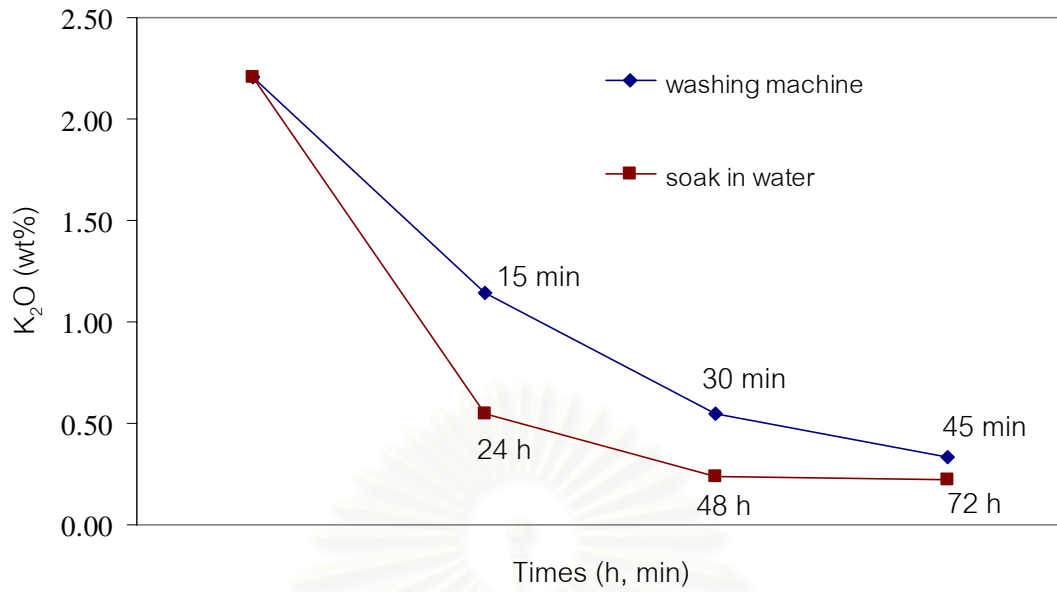


Figure 4.33 Relationship of potassium content (wt%) in RH and various washing conditions

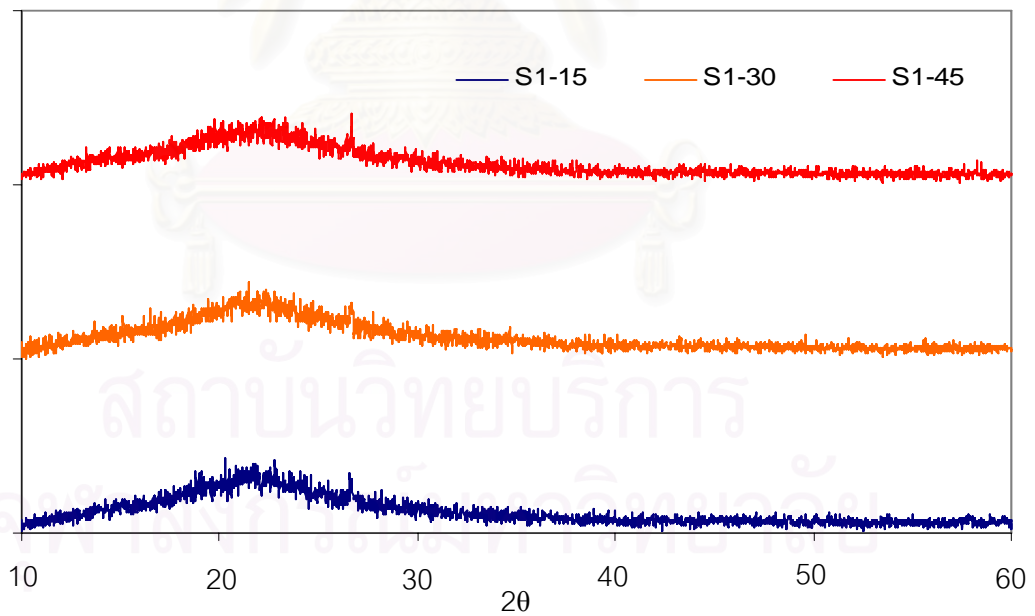


Figure 4.34 XRD patterns of RHA washed by washing machine with water for 15, 30 and 45 min

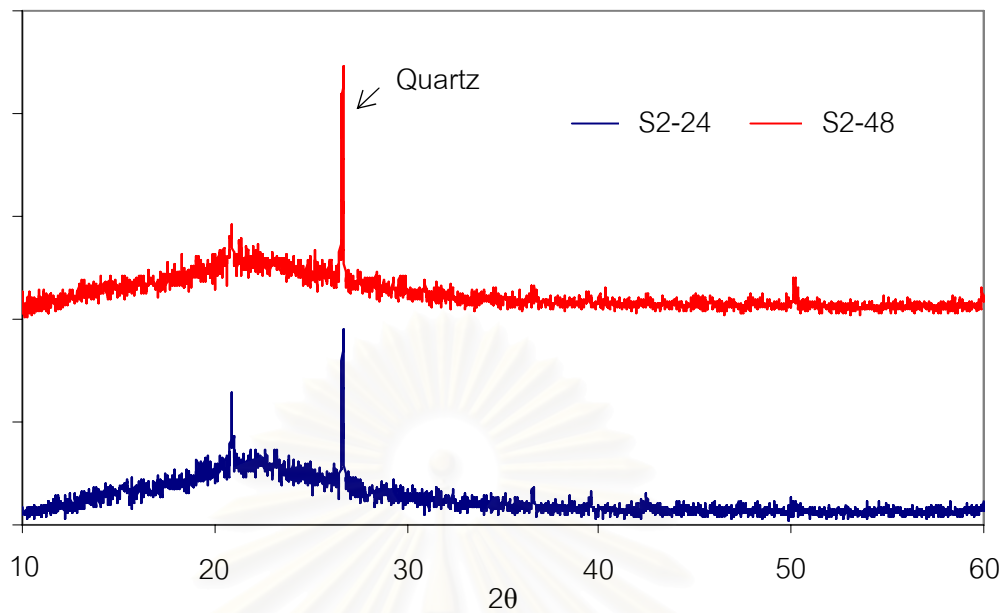


Figure 4.35 XRD patterns of RHA soaked in water for 24 and 48 h

4.5 RHA from two different provinces

RH from Nakhonratchasima and Ratchaburi were burned at 450 – 650°C and analyzed by XRD and XRF. Original XRF data are shown in Appendix F, Table 29. In this experiment, RH was soaked for 5 h and then washed by a washing machine for 15 min.

Content of silica of Nakhonratchasima source is about 1 wt% higher than that of Ratchaburi source, as shown Figure 4.36. K_2O contents of Nakhonratchasima and Ratchaburi provinces are 0.2 – 0.3 and 0.4 – 0.5 wt%, respectively, see Figure 4.37.

Partly the difference of SiO_2 and K_2O amount between the burning temperatures might be due to the deviation in analysis. The washing was efficient to clean the impurities better than the process mentioned in section 3.4 (only soak or only wash by a washing machine). The combined processes can reduce the time from 72 h to 5 h for soaking and wash by a washing machine only for 15 min.

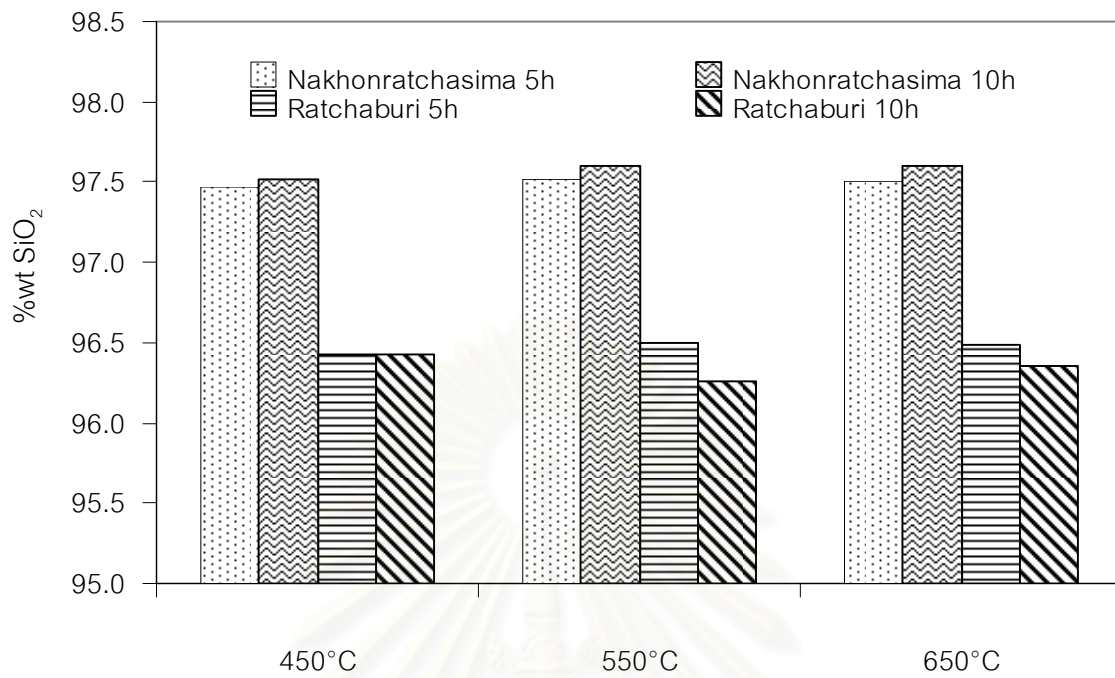


Figure 4.36 Relationship of wt% silica and various temperature following 450, 550 and 650°C compare between sources

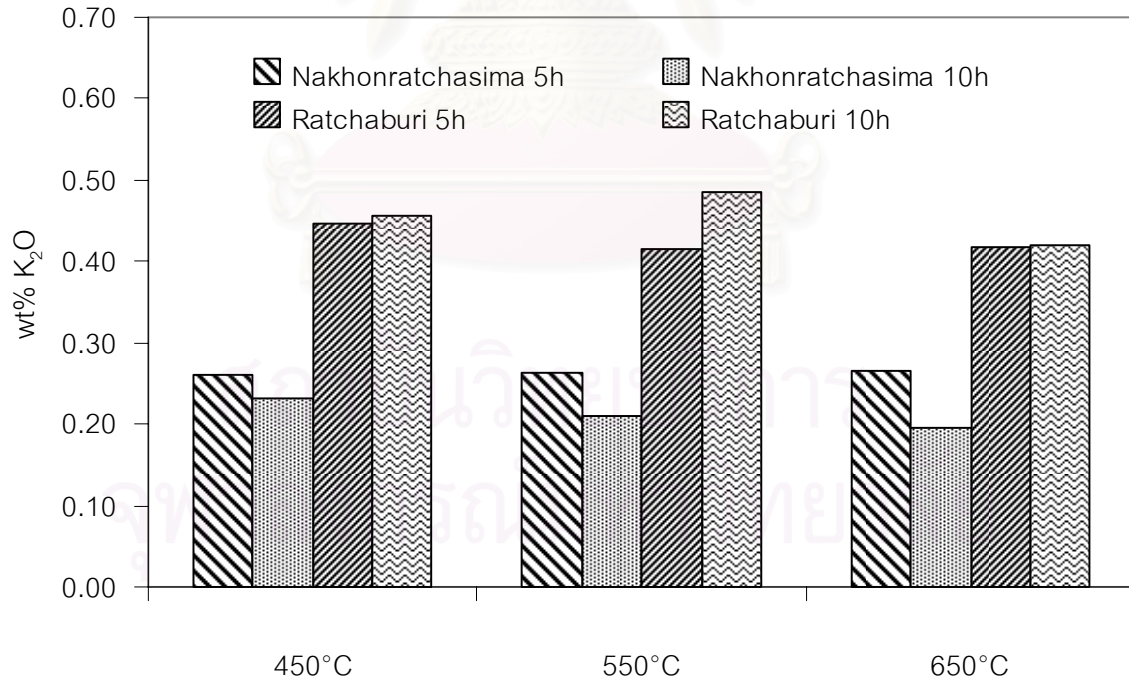


Figure 4.37 Relationship of wt% potassium and various temperature following 450, 550 and 650°C compare between sources

XRD patterns of Nakhonratchasima and Ratchaburi RHA are shown in Figure 4.38 and 4.39. The RHA was amorphous in all calcining conditions. Color of the sample at 450°C is still brown after calcined at higher temperatures the color turns to white at 550°C and completely white at 650°C.

There are insignificant differences in XRD profile and color between two RHA from Nakhonratchasima and Ratchaburi provinces.

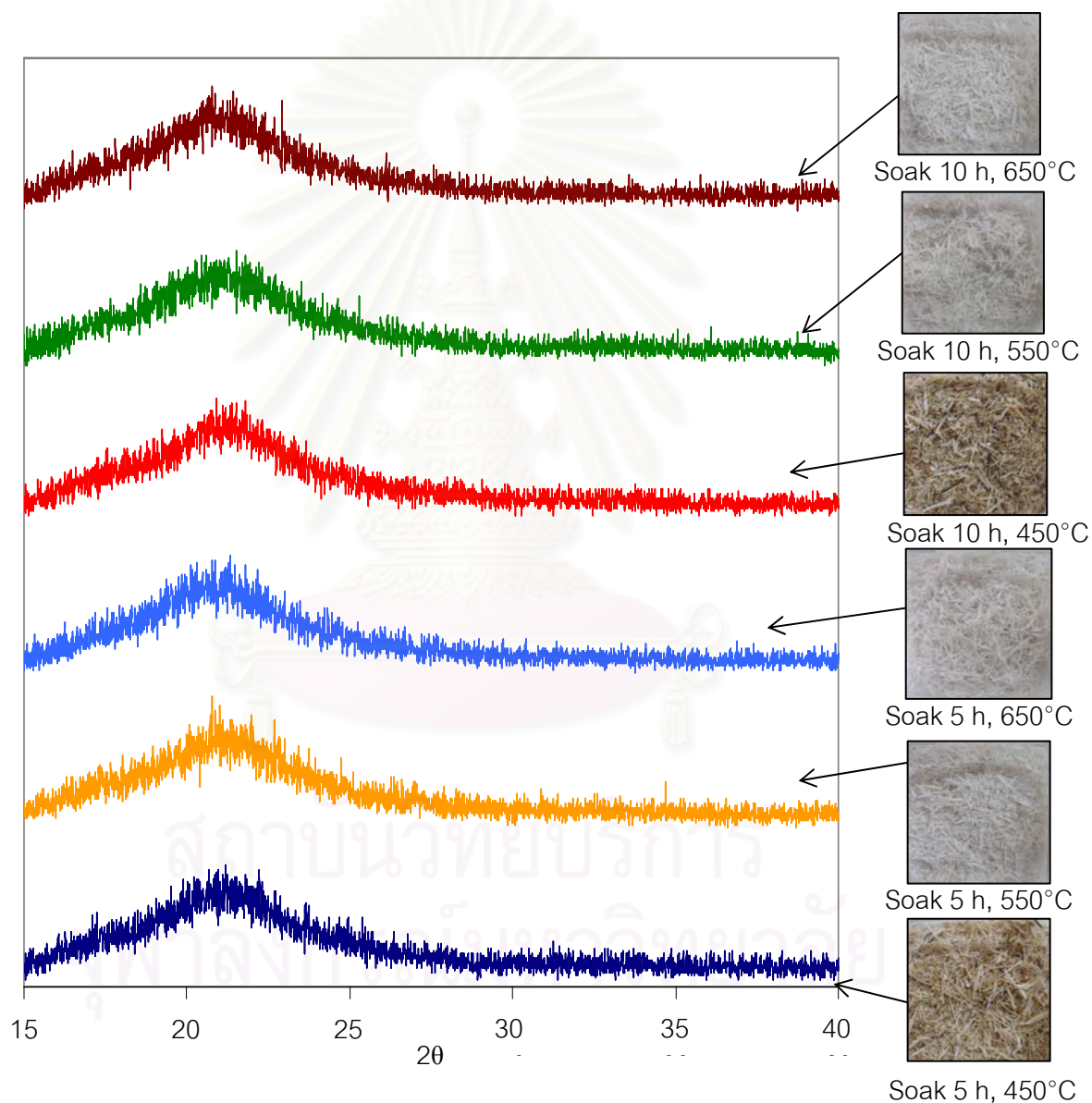


Figure 4.38 XRD patterns of RHA of Nakhonratchasima province calcined at 450, 550 and 650°C

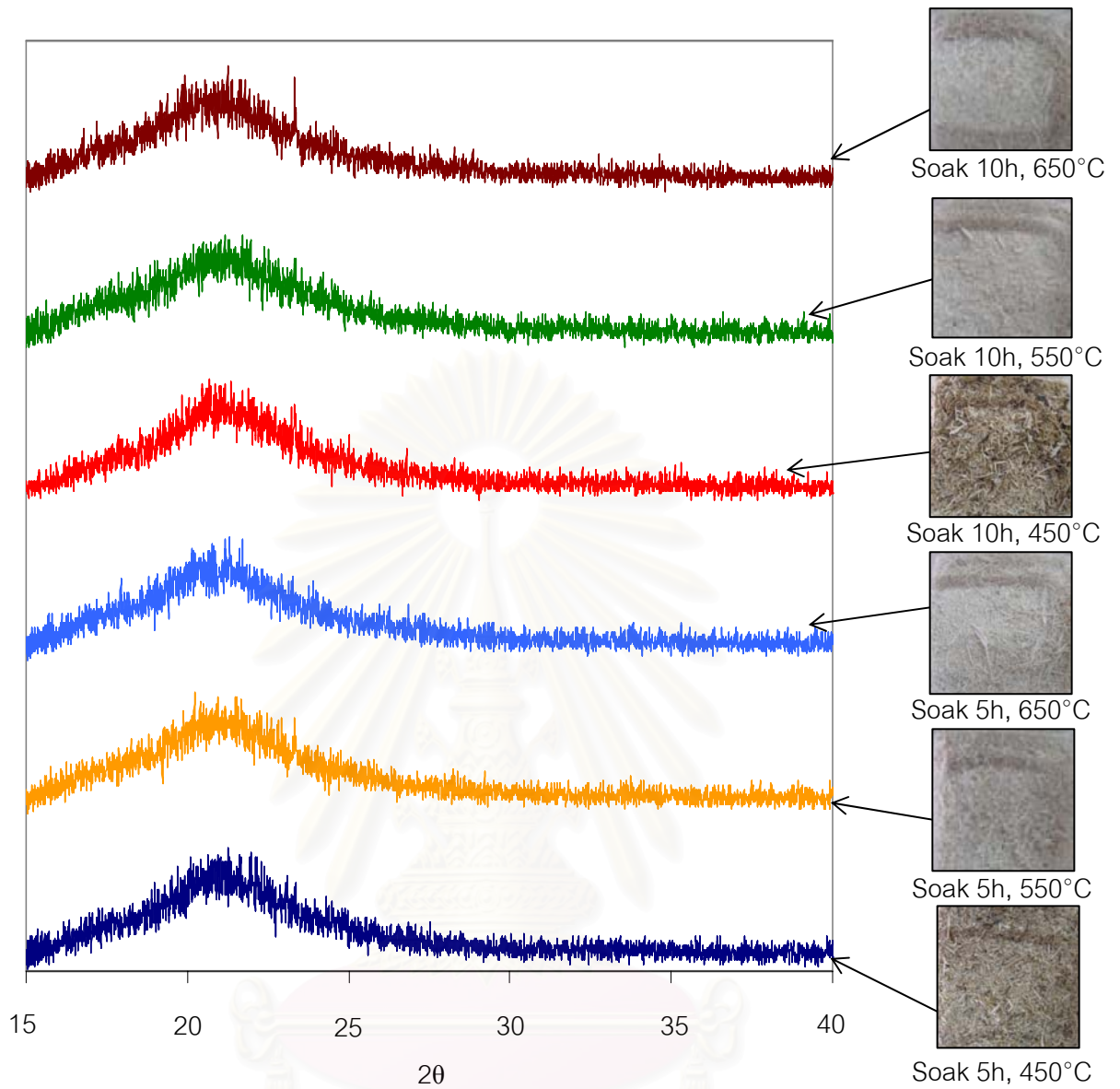


Figure 4.39 XRD patterns of RHA of Ratchaburi province
calcined at 450, 550 and 650°C

สถาบันวิจัยบริการ
จุฬาลงกรณ์มหาวิทยาลัย

CHAPTER V

CONCLUSIONS

The conclusions of results and observations from this study are as follows:

1. The content of K_2O strongly affected the crystallization temperature of amorphous silica in rice husk. K_2O content can be decreased effectively after washing by water.
2. The soaking of process in water for 5 hours, followed by washing in a washing machine for 15 minute can decrease K_2O to less than 0.5 wt%.
3. Cristobalite and amorphous silica from rice husk ash have potentials to be applied as anti-blocking additives for LLDPE films.
4. Crystal phase of RHA from factories and power plants is dependent on the type of furnaces and operating conditions. It was found that rice husk ash samples from Stoker furnace are cristobalite phase, while rice husk ash sample from Fluidized bed, gasification, and suspension furnaces are amorphous phases.
5. Rice husk ash from gasification furnace becomes to almost white ash (SiO_2) after being calcined at 500 – 800°C for 2 hours.

สถาบันวิทยบริการ
จุฬาลงกรณ์มหาวิทยาลัย

CHAPTER VI

FUTURE WORK

Recommendations for future work are as follows:

1. RHA from gasification furnace has potential to be applied as raw materials of water glass and anti-blocking powder for LLDPE film.

However, the RHA did not change to white color perfectly. It is important to know the reason why some particle did not change to white after heat treatment.

The research and development to use RHA from gasification furnace for real application should be performed hereafter.

2. Cristobalite waste from small rice mill factory should be concerned and the furnace and technology for burning rice husk to amorphous state should be developed.



สถาบันวิทยบริการ
จุฬาลงกรณ์มหาวิทยาลัย

REFERENCES

- [1] "Rice export," Prachachat Business (18 – 21 May 2006):19.
- [2] Martin, J. I., "The desilication of rice hulls and a study of the products obtained", (Master's thesis, Louisiana State University, 1938).
- [3] Lanning, F. C., "Silicon in rice," J. Agric. Food. Chem 11 (1963): 435-437.
- [4] Shigetaka Wada, "Survey of the research on the utilization of rice husk and rice husk silica," Paper present at the 1st Conference Workshop on the Utilization of Rice Husk and Rice Husk Silica, Faculty of Science, Department of Materials science, Chulalongkorn University, Bangkok, Thailand, 19th September 2005.
- [5] Rice husk ash market study 2003, (UK, Crown copyright 2003).
- [6] Kachin Saiintawong, "Low Cost Process for Producing Mullite from Industrial Wastes," 28th Annual International Conference & Exhibition on Advanced Ceramics & Composites, held at Doubletree and Hilton Hotels, Cocoa Beach, Florida, USA, 25-30th January, 2004.
- [7] Chittinannun Kunsawat, "Use of silica from rice husk as antiblocking-agent in low density polyethylene films," (Master's thesis, Department of Materials science, Faculty of Science, Chulalongkorn University, 1996).
- [8] Michel W. Barsoum, "Phase Equilibria," in Fundamental of Ceramics, (New York, McGraw-Hill Companies Inc., 1997), p 270.
- [9] W. D. Kingery, H. K. Bowen and D. R. Uhlmann, "Polymorphism," in Introduction to Ceramics, (New York, John Wiley & Sons, Interscience Publication, 1976), p 84.
- [10] Uraivan Leelaadisorn, "Preparation and Characterization of High-Grade Silica from Rice Husk," (Master's Thesis, Department of Material science, Faculty of Science, Chulalongkorn University, 1992).
- [11] A. M. Venezia, V. La Parola., "Effect of Alkali Ions on the Amorphous to Crystalline Phase Transition of Silica", Journal of Solid State Chemistry 161 (2001): 373-378.
- [12] Yasushi SHINOHARA and Norihiko KOHYAMA., "Quantitative Analysis of Tridymite and Cristobalite Crystallized in Rice Husk Ash by Heating." Industrial Health 42 (2004): 277–285.

- [13] Sheng-Wei Wu, David Shan Hill Wong, and Shih-Yuan Lu., "Size Effects on Silica Polymorphism," J.Am. Ceram. Soc. 85 10 (2002): 2590-2592.
- [14] R.V. Krishnarao , J. Subrahmanyam, T. Jagadish Kum car, "Studies on the formation of black particles in rice husk silica ash," Journal of the European Ceramic Soc 21 (2001): 99-104.
- [15] A. Prasad, "Polyethylene, metallocene linear low-density," in Polymer Data Handbook, James E Mark, (Oxford University Press, Inc., 1999), pp 529 – 539.
- [16] "Crystalline Silica in the Workplace," Chemical Hazards, CH059 (July 2004): 1-10.
- [17] "Silica, Cristobalite," Hazardous substance fact sheet, No. 1657 (April 2002): 1-6.



สถาบันวิทยบริการ
จุฬาลงกรณ์มหาวิทยาลัย



APPENDICES

สถาบันวิทยบริการ
จุฬาลงกรณ์มหาวิทยาลัย

APPENDIX A

Table 1 Rice paddy, rice husk and ash production in the 20 major countries in 2002

	Rice, Paddy Production in 2002 (t)	Percentage of Total Paddy Production	Husk Produced (20% of total) (t)	Potential Ash Production (18% of husk) (t)
China	177,589,000	30.7%	35,517,800	6,393,204
India	123,000,000	21.2%	24,600,000	4,428,000
Indonesia	48,654,048	8.4%	9,730,810	1,751,546
Bangladesh	39,000,000	6.7%	7,800,000	1,404,000
Viet Nam	31,319,000	5.4%	6,263,800	1,127,484
Thailand	27,000,000	4.7%	5,400,000	972,000
Myanmar	21,200,000	3.7%	4,240,000	763,200
Philippines	12,684,800	2.2%	2,536,960	456,653
Japan	11,264,000	1.9%	2,252,800	405,504
Brazil	10,489,400	1.8%	2,097,880	377,618
USA	9,616,750	1.7%	1,923,350	346,203
Korea	7,429,000	1.3%	1,485,800	267,444
Pakistan	5,776,000	1.0%	1,155,200	207,936
Egypt	5,700,000	1%	1,140,000	205,200
Nepal	4,750,000	0.8%	950,000	171,000
Cambodia	4,099,016	0.7%	819,803	147,565
Nigeria	3,367,000	0.6%	673,400	121,212
Sri Lanka	2,794,000	0.5%	558,800	100,584
Colombia	2,353,440	0.4%	470,688	84,724
Laos	2,300,000	0.4%	460,000	82,800
Rest of the World	29,091,358	5.0%	5,818,272	1,047,289
Total (World)	579,476,722	100%	115,895,344	20,861,162

APPENDIX B

Original XRD patterns of heat treated RHA

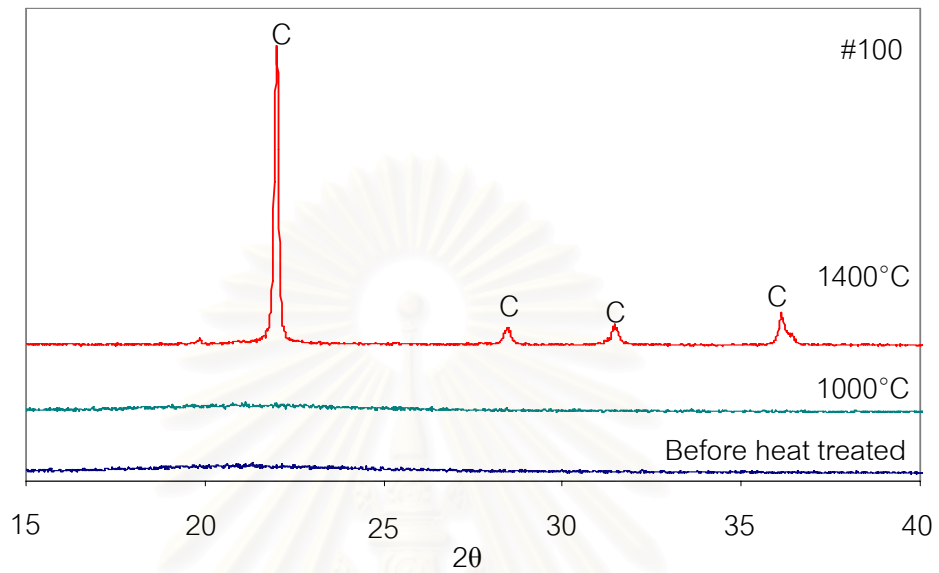


Figure 1 XRD patterns of silica glass sieved through a 100-mesh brass screen and heat treated at 1000°C and 1400°C for 2 h

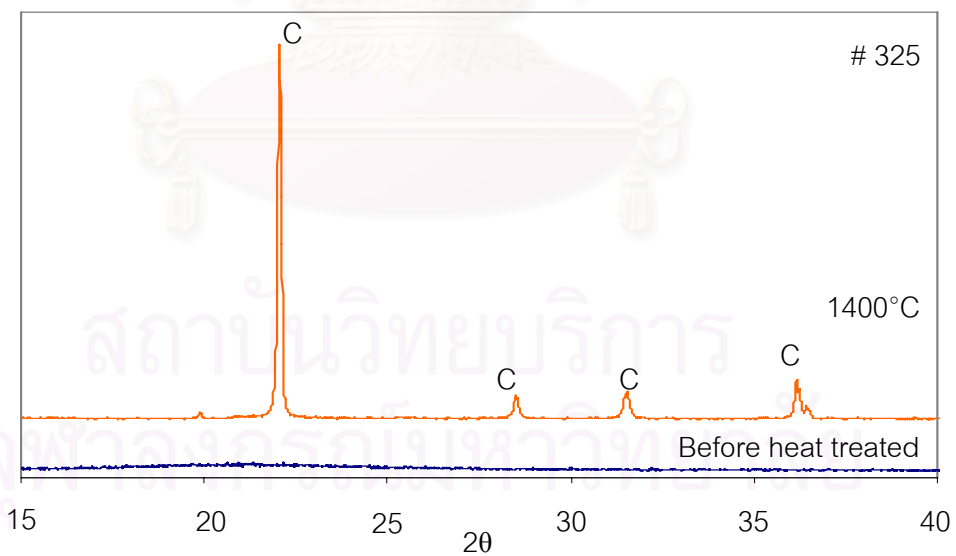


Figure 2 XRD patterns of silica glass sieved through a 325-mesh brass screen and heat treated at 1400°C for 2 h

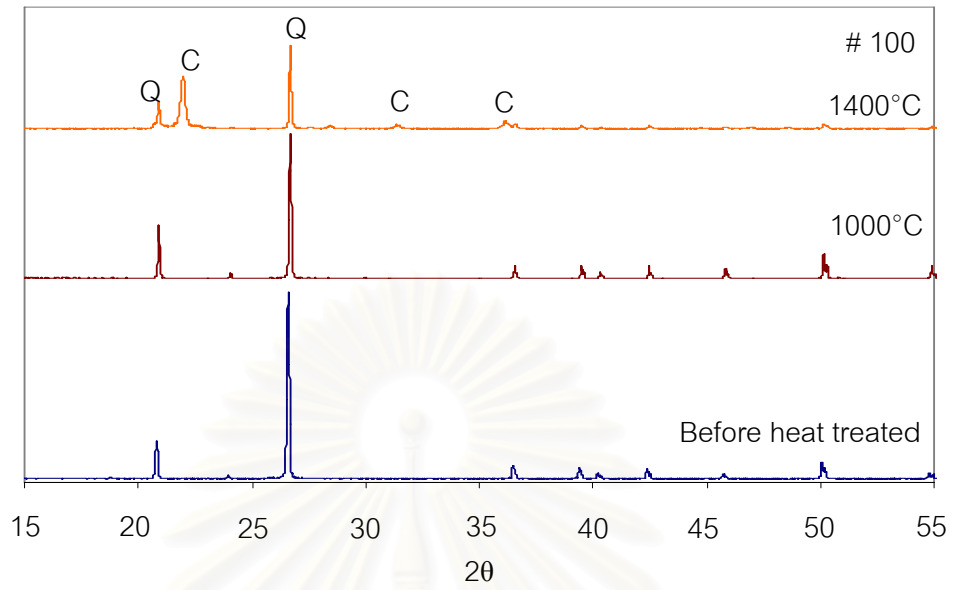


Figure 3 XRD patterns of quartz sieved through a 100-mesh brass screen and heat treated at 1400°C for 2 h

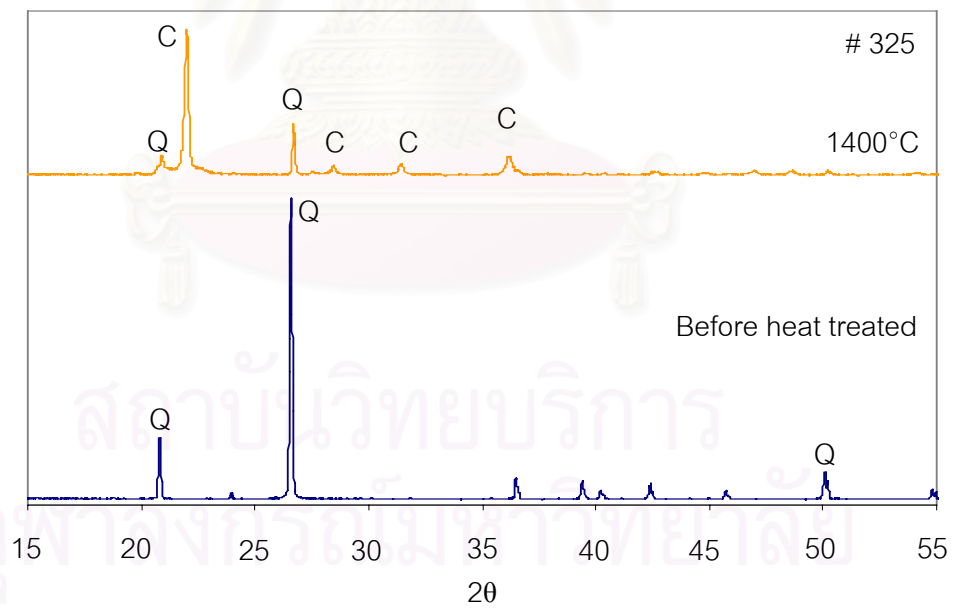


Figure 4 XRD patterns of quartz sieved through a 325-mesh brass screen and heat treated at 1400°C for 2 h

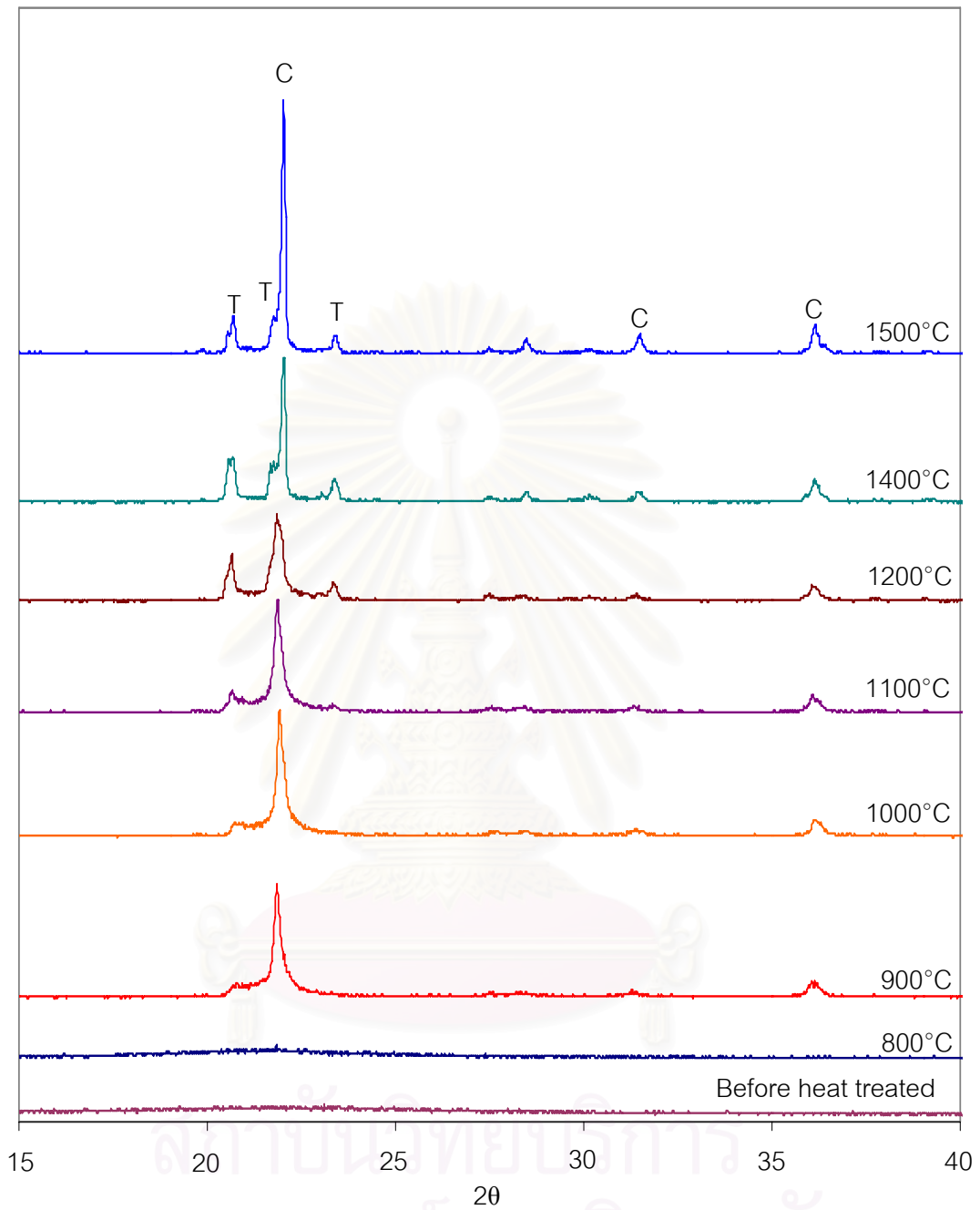


Figure 5 XRD patterns of RHA of untreated RH, not sieved and heat treated at 800°C, 900°C, 1000°C, 1100°C, 1200°C, 1400°C and 1500°C for 2 h

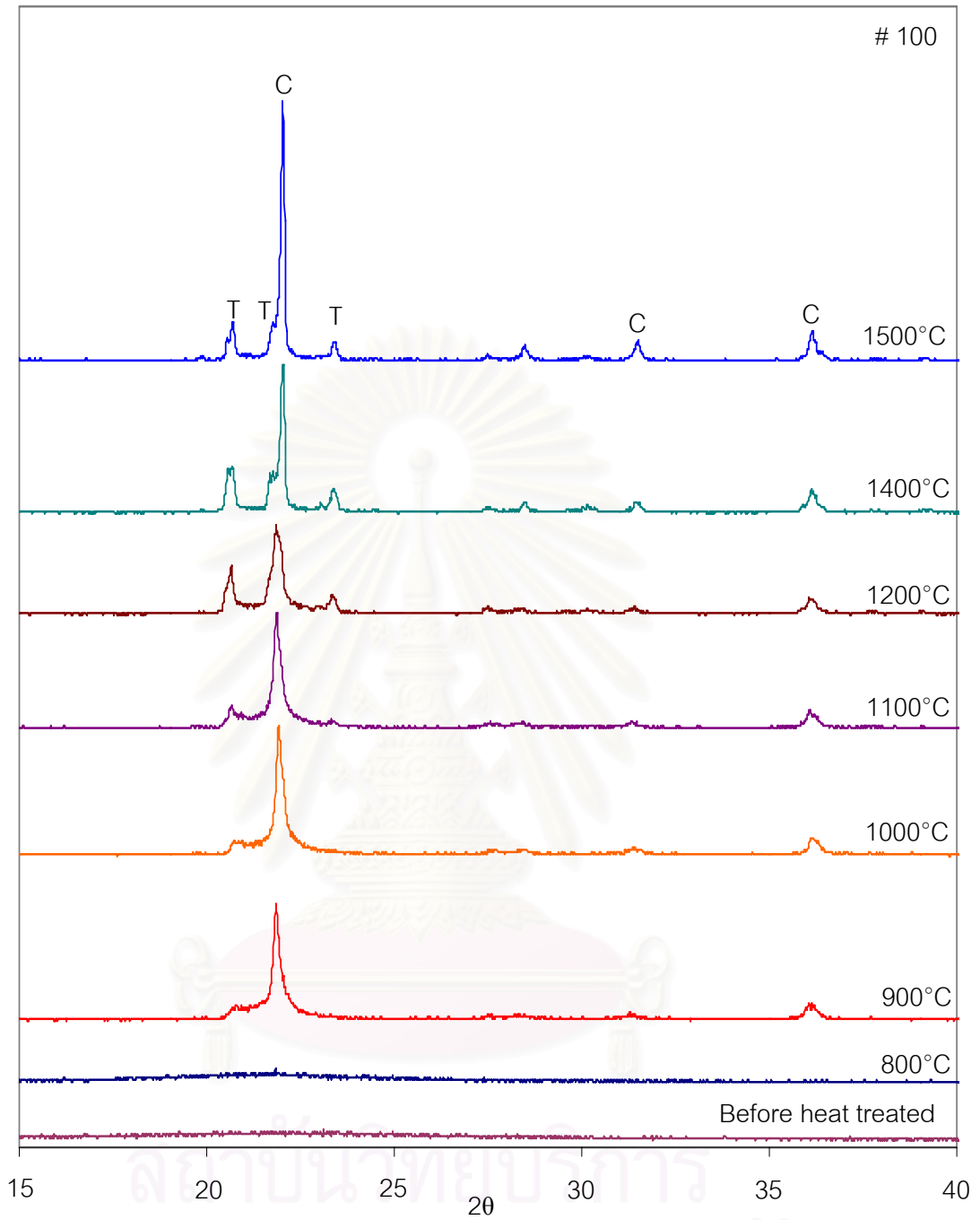


Figure 6 XRD patterns of RHA of untreated RH, sieved through a 100-mesh brass screen and heat treated at 800°C, 900°C, 1000°C, 1100°C, 1200°C, 1400°C and 1500°C for 2 h

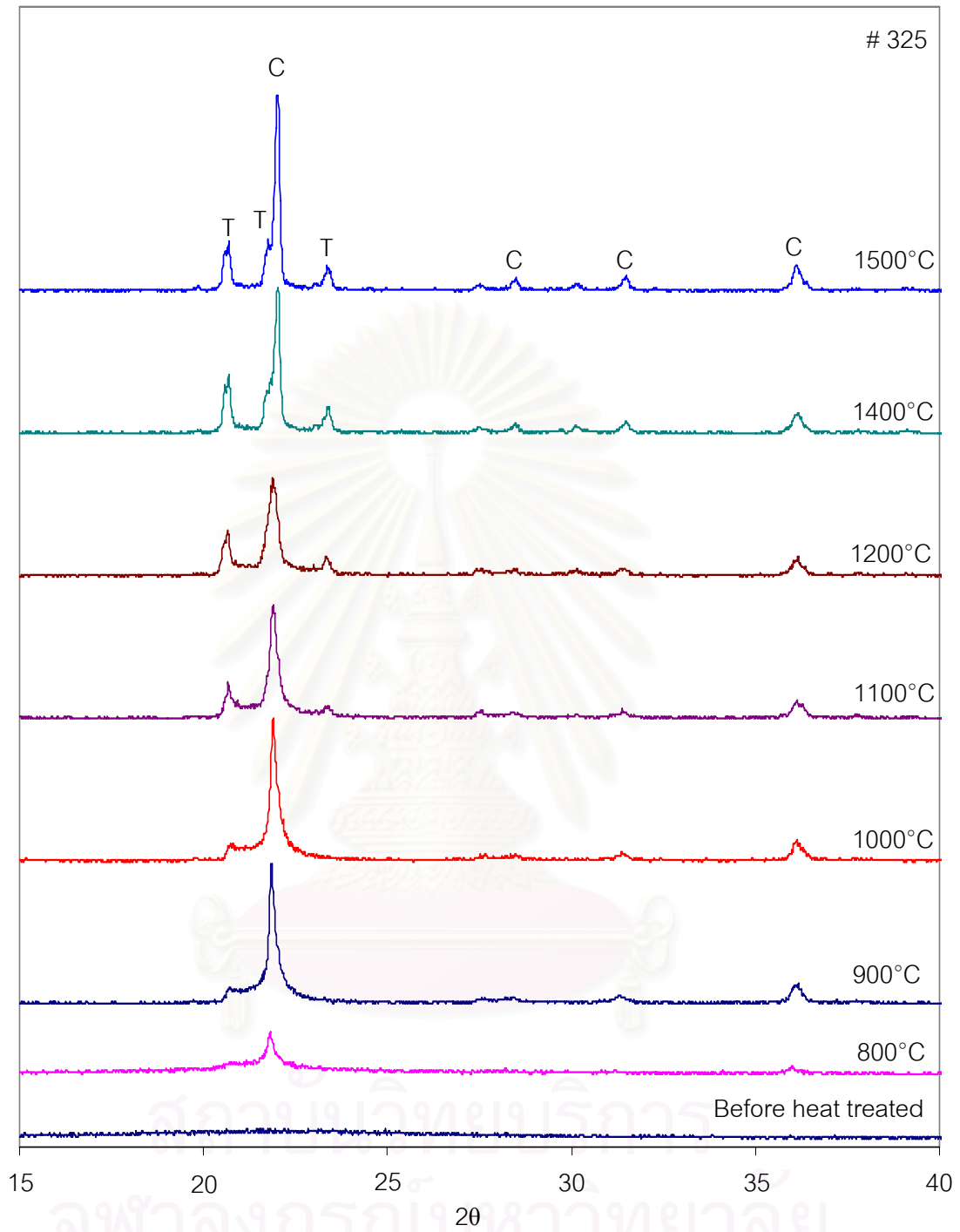


Figure 7 XRD patterns of RHA of untreated RH, sieved through a 325-mesh brass screen and heat treated at 800°C, 900°C, 1000°C, 1100°C, 1200°C, 1400°C and 1500°C for 2 h

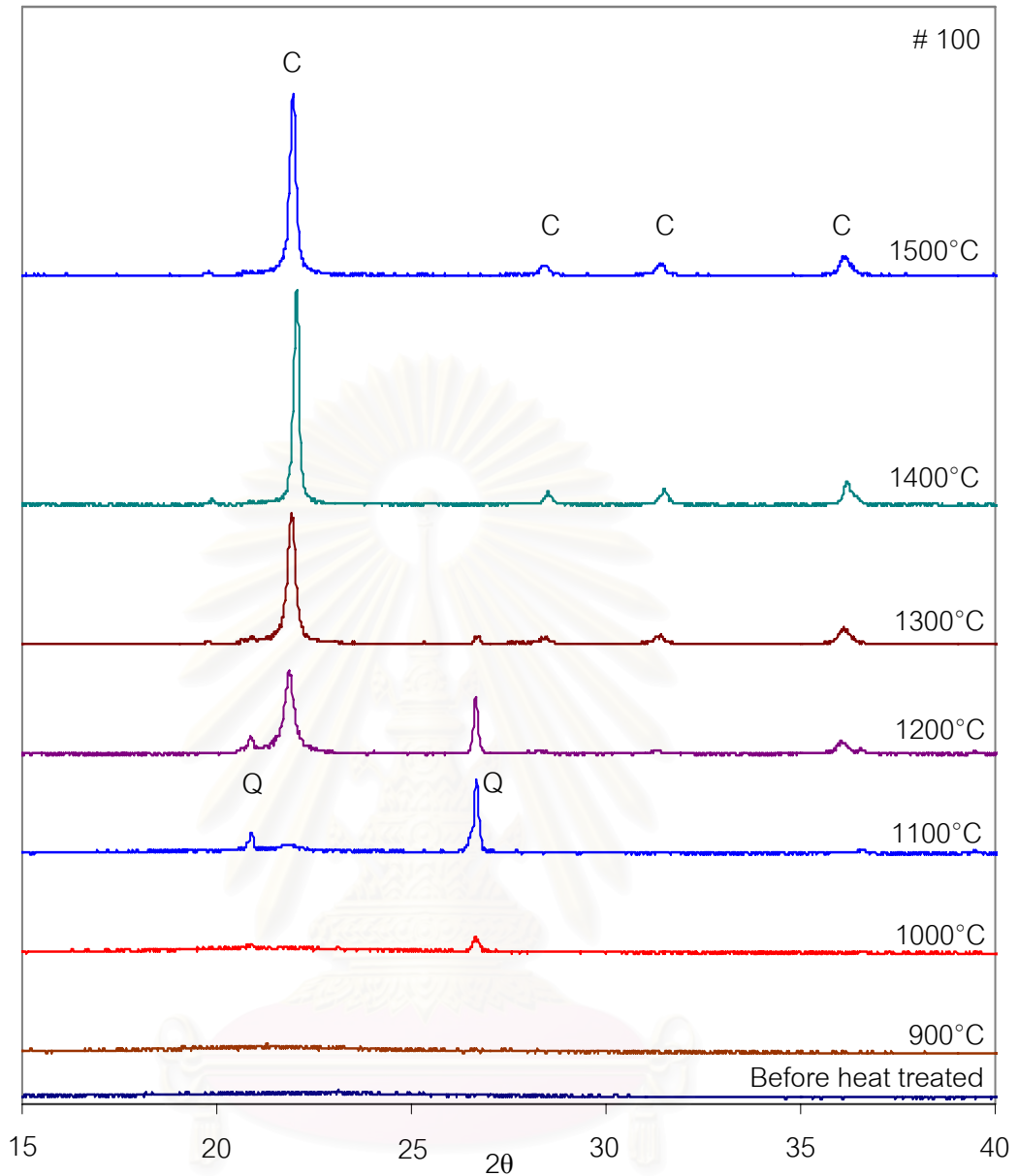


Figure 8 XRD patterns of RHA water treated RH, sieved through a 100-mesh brass screen and heat treated at 900°C, 1000°C, 1100°C, 1200°C, 1300°C, 1400°C and 1500°C for 2 h

จุฬาลงกรณ์มหาวิทยาลัย

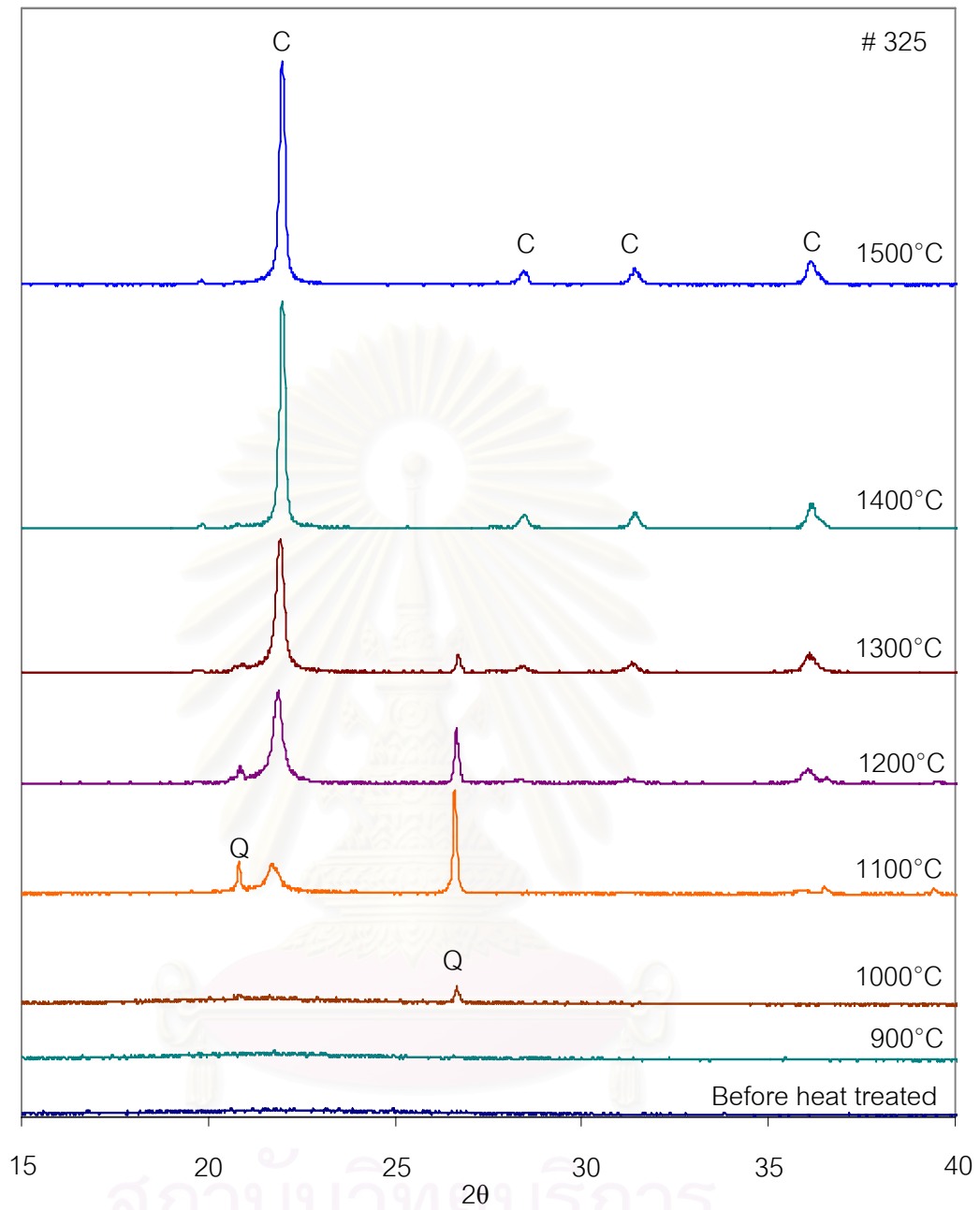


Figure 9 XRD patterns of RHA water treated RH, sieved through a 325-mesh brass screen and heat treated at 900°C, 1000°C, 1100°C, 1200°C, 1300°C, 1400°C and 1500°C for 2 h

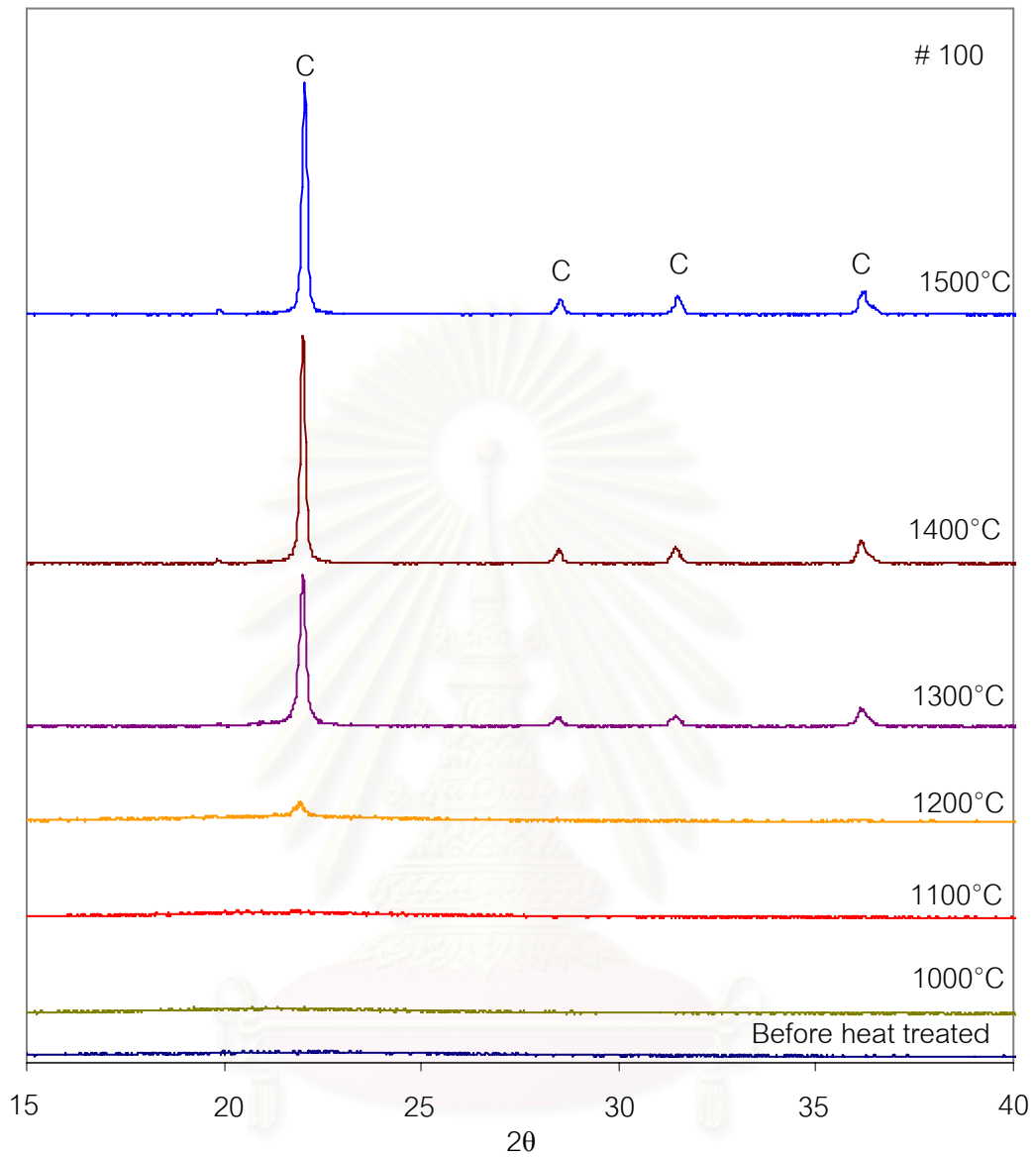


Figure 10 XRD patterns of RHA HCl treated RH, sieved through a 100-mesh brass screen and heat treated at 1000°C, 1100°C, 1200°C, 1300°C, 1400°C and 1500°C for 2 h

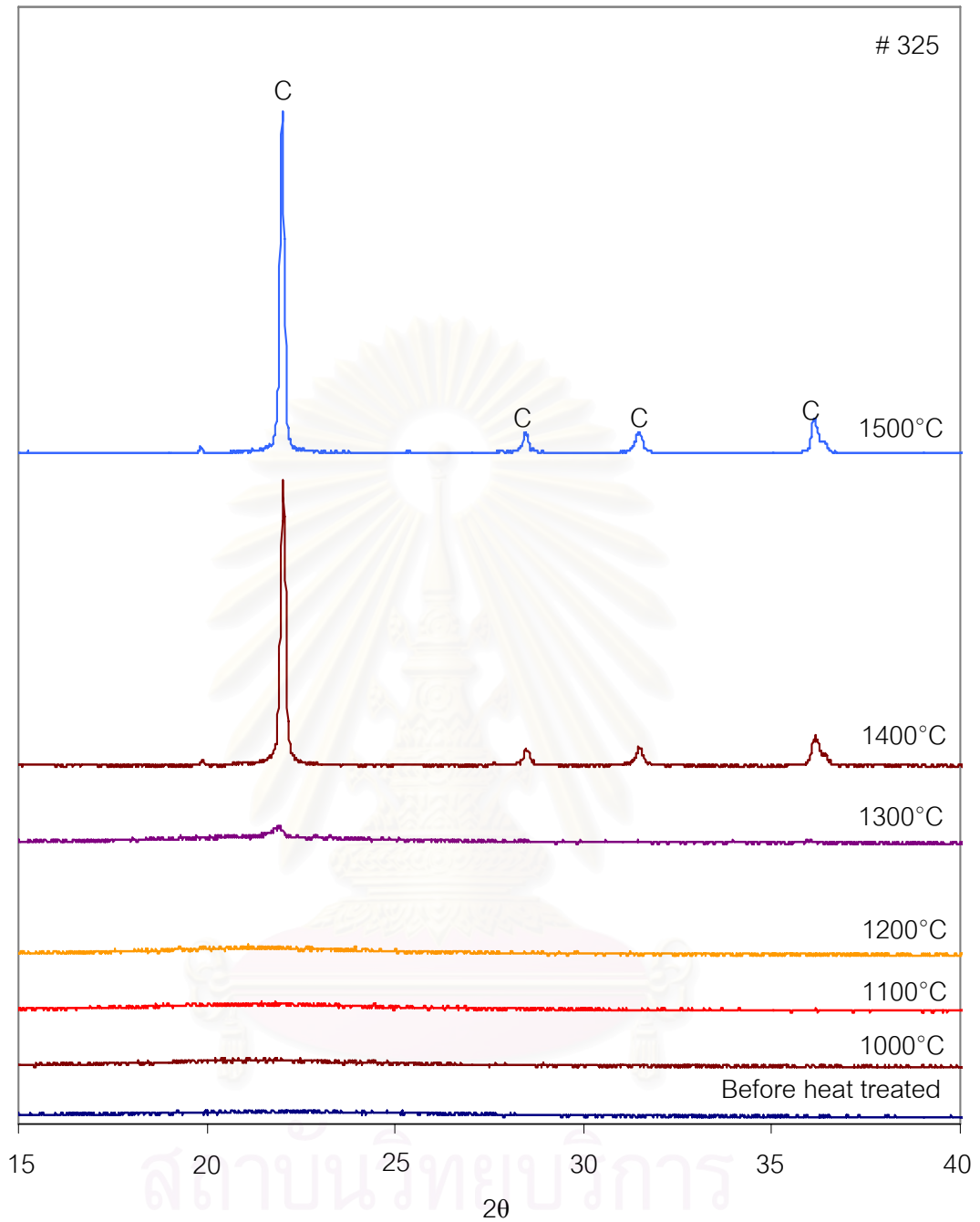


Figure 11 XRD patterns of RHA HCl treated RH, sieved through a 325-mesh brass screen and heat treated at 1000°C, 1100°C, 1200°C, 1300°C, 1400°C and 1500°C for 2 h

APPENDIX C

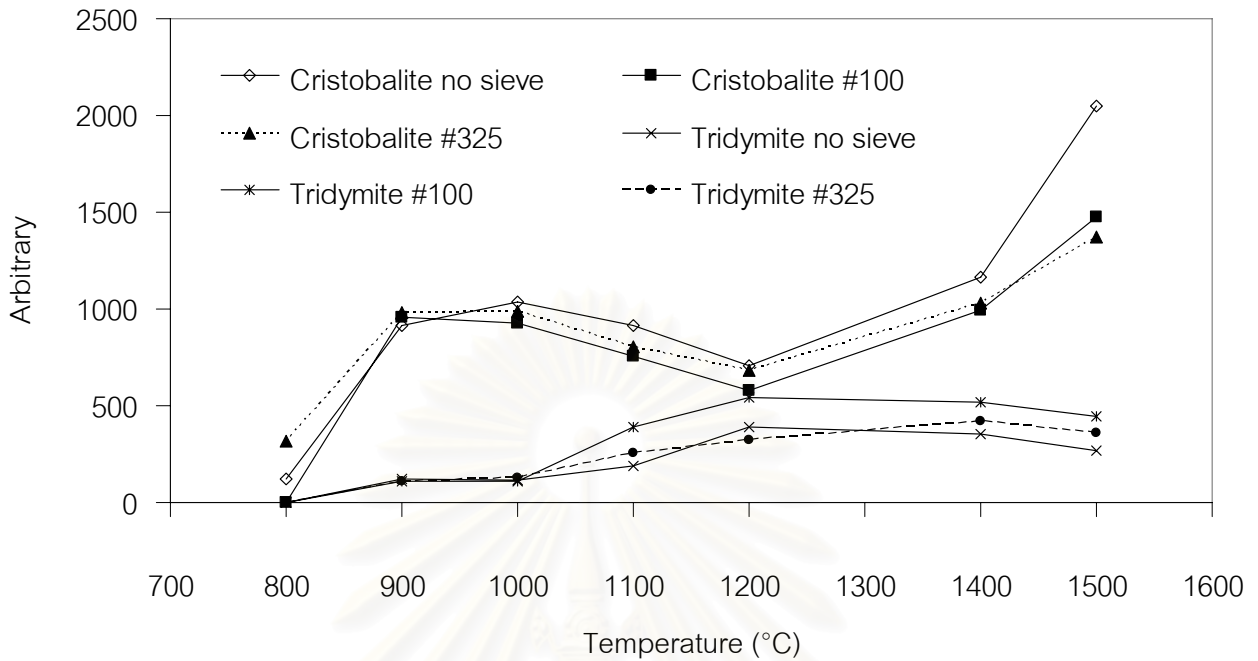


Figure 12 The relationship between heat treatment temperature and the peak intensity of cristobalite, tridymite at $2\theta = 22.025, 20.586$, respectively, of untreated RHA

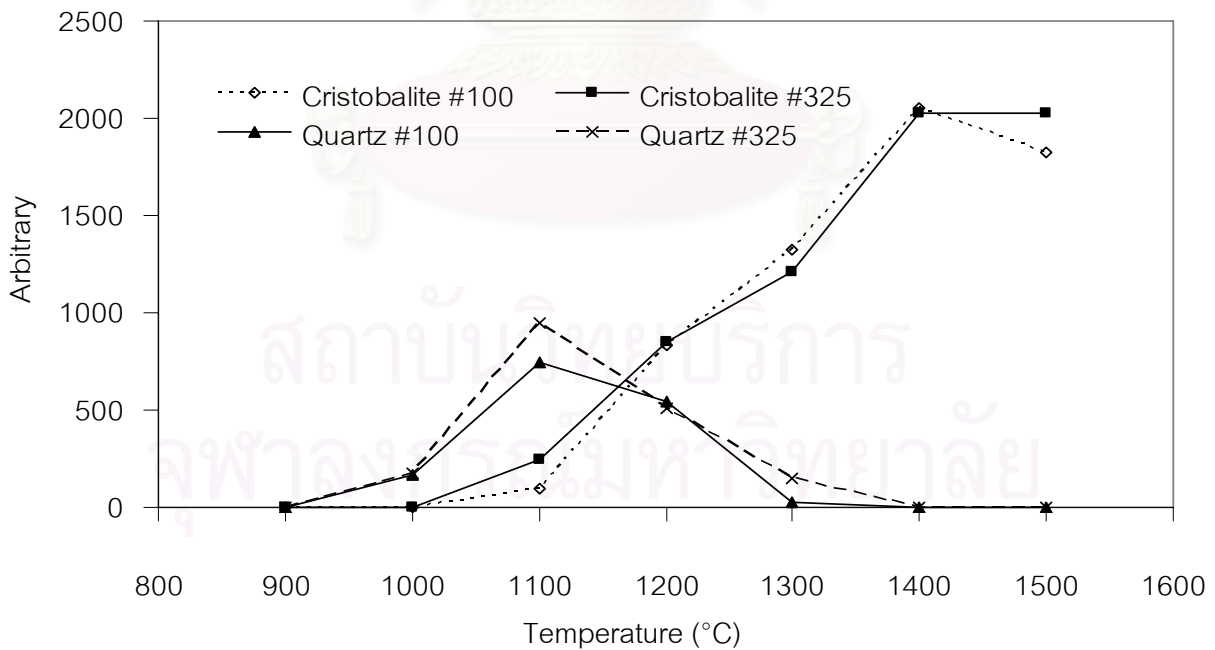


Figure 13 The relationship between the heat treatment temperature and the peak intensity of cristobalite, quartz at $2\theta = 22.025, 26.685$, respectively, of water treated RHA

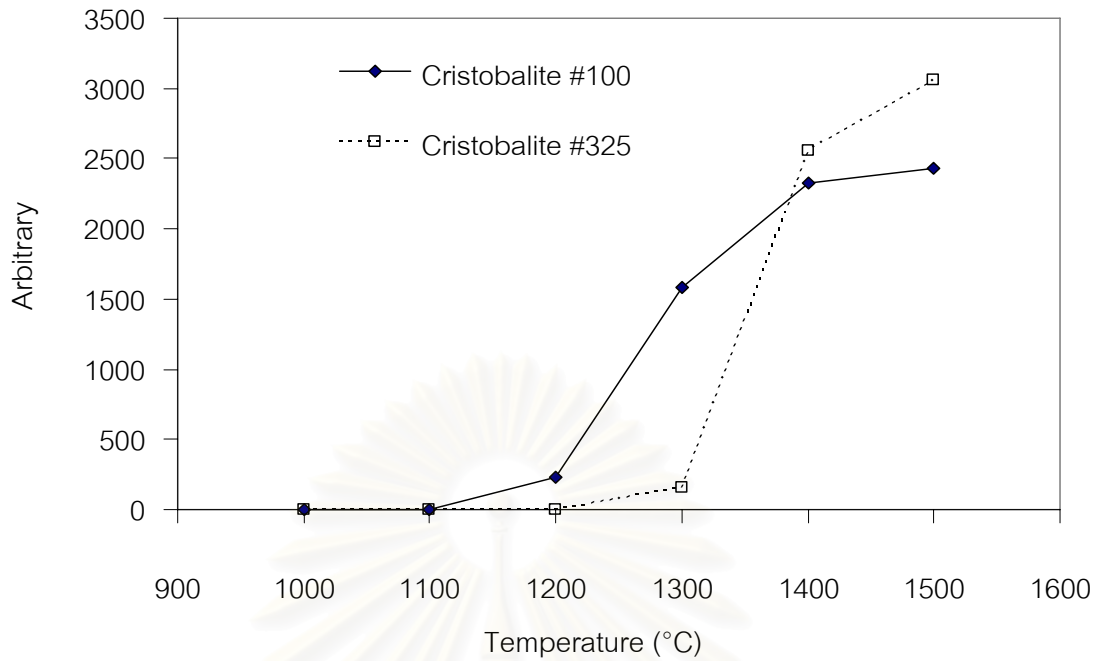


Figure 14. The relationship between the heat treatment temperature and the peak intensity of cristobalite at $2\theta = 22.025$ of HCl treated RHA

APPENDIX D

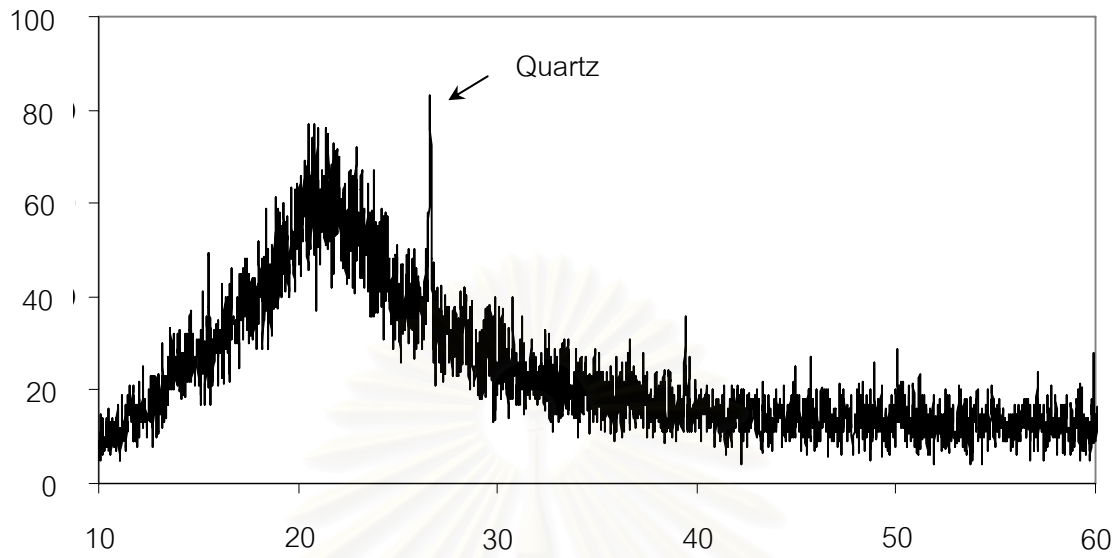


Figure 15 Rice husk ash from A.T. Biopower Co.,Ltd., Pichit Province

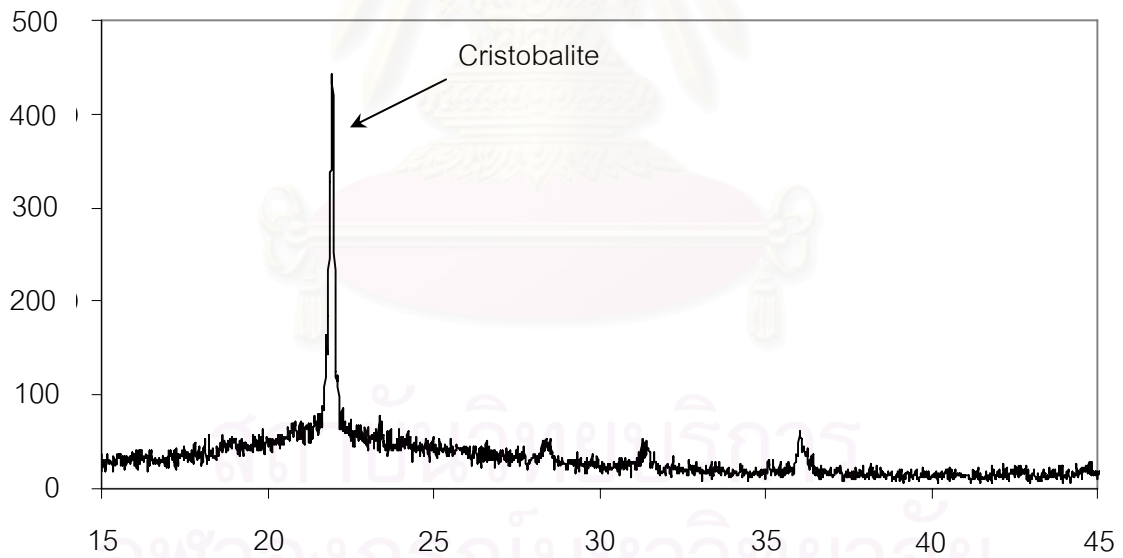


Figure 16 Thai Power Supply (3 MW plant, Rice husk only)

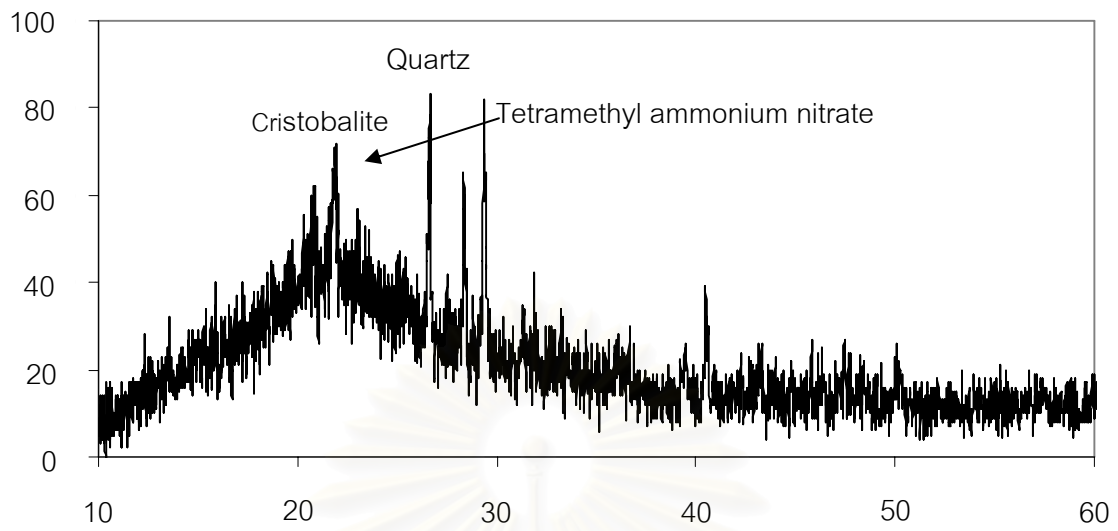


Figure 17 Thai Power Supply (Mixed biomass 10 MW plant)

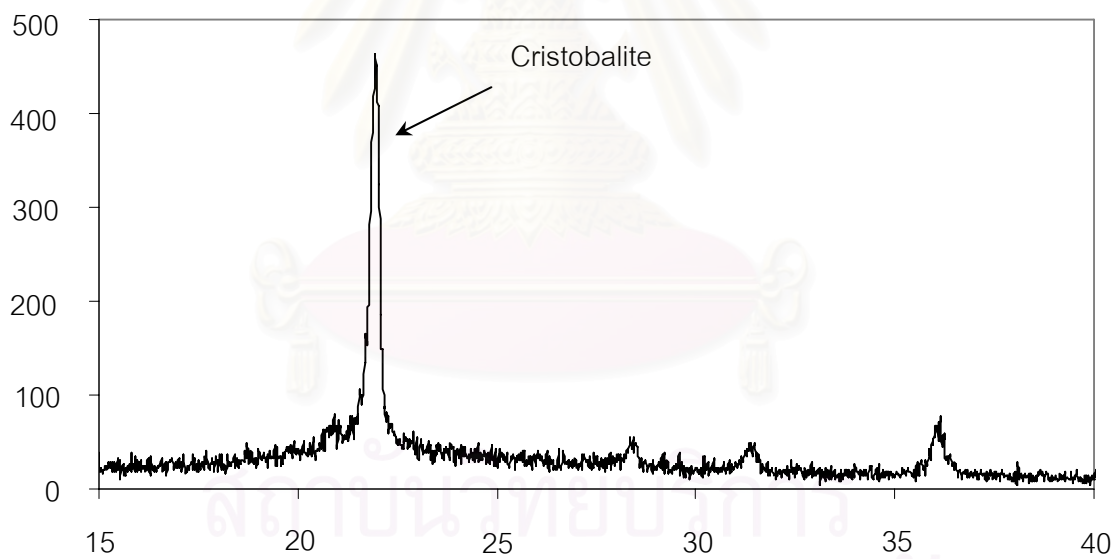


Figure 18 Mahaphant Fiber cement Industry

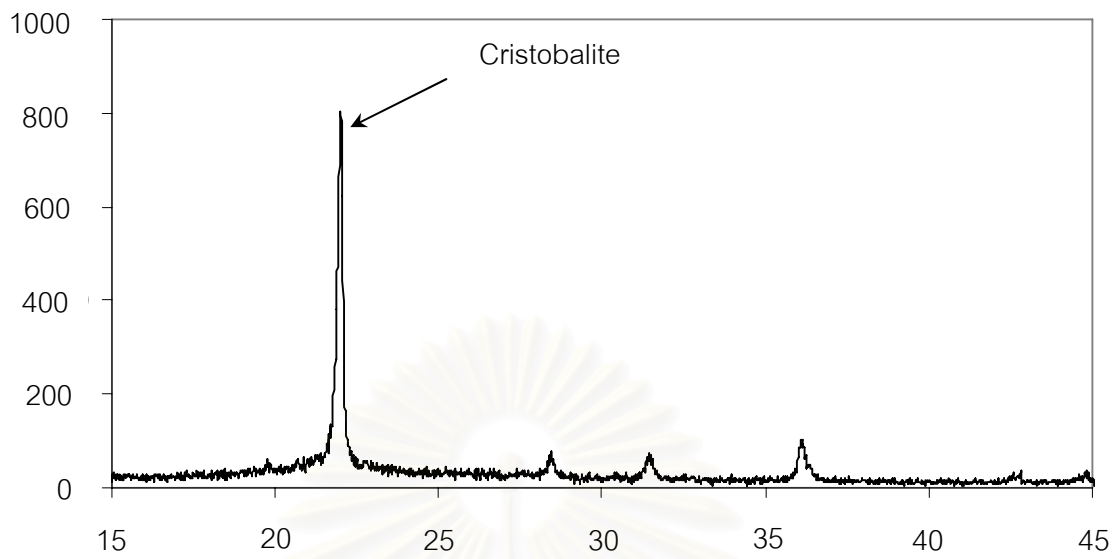


Figure 19 5 Company's names Kong Thai Fong Ltd., Saraburi Province Cooperative Ltd., P. Saengwattana 4 Fire Rice Mill Ltd., Jun Kai Seng Ltd. And Song Phee Nong Rice Mill Ltd.

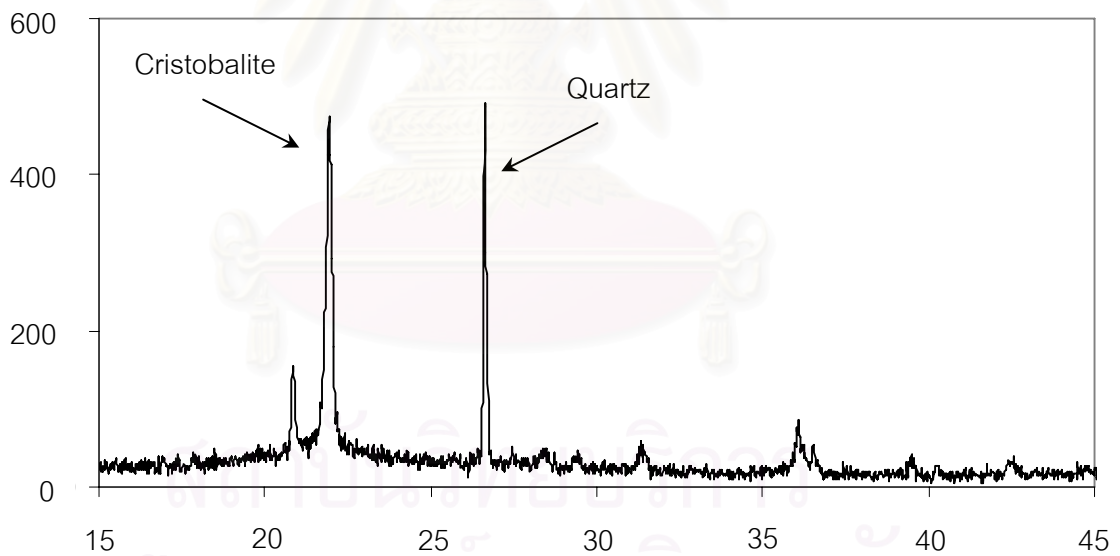


Figure 20 P. Saengwattana 3 Fire Rice Mill Ltd.

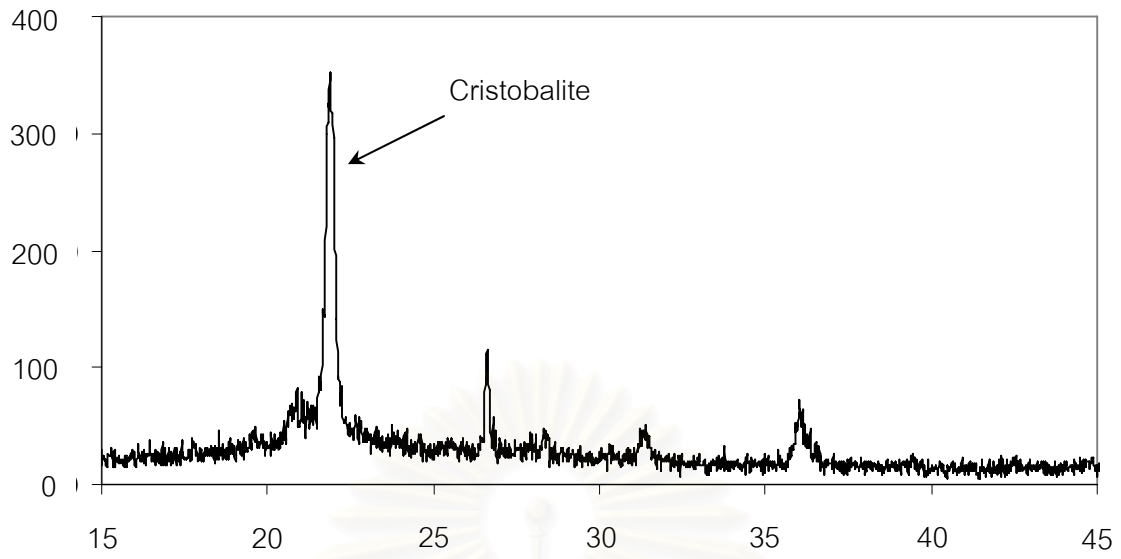


Figure 21 SATAKE CORPRATION (Suranare university plant, Pakestan Plant)

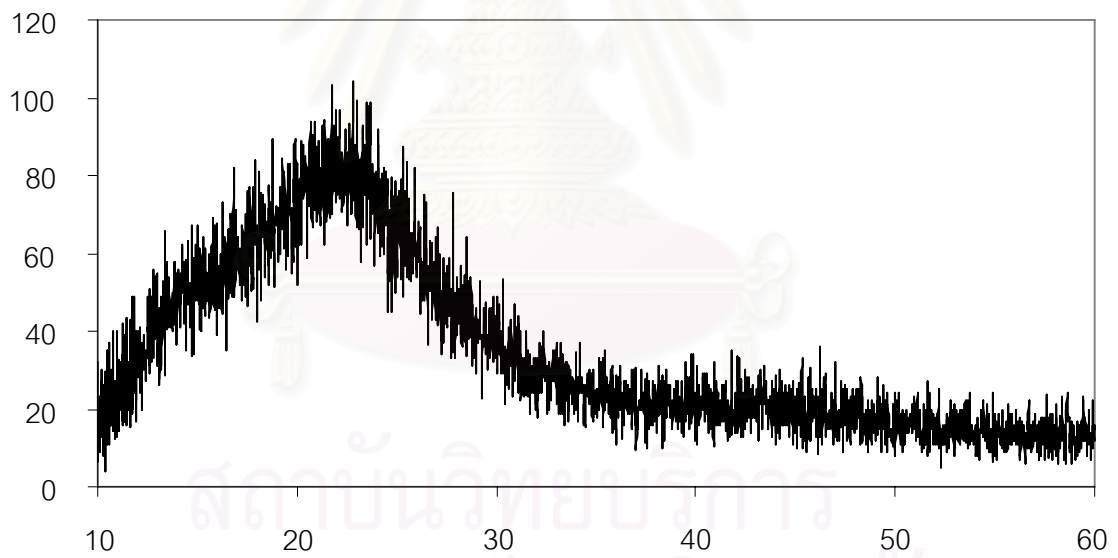


Figure 22 SMG 500 (KANSAI CORPORATION, JAPAN)

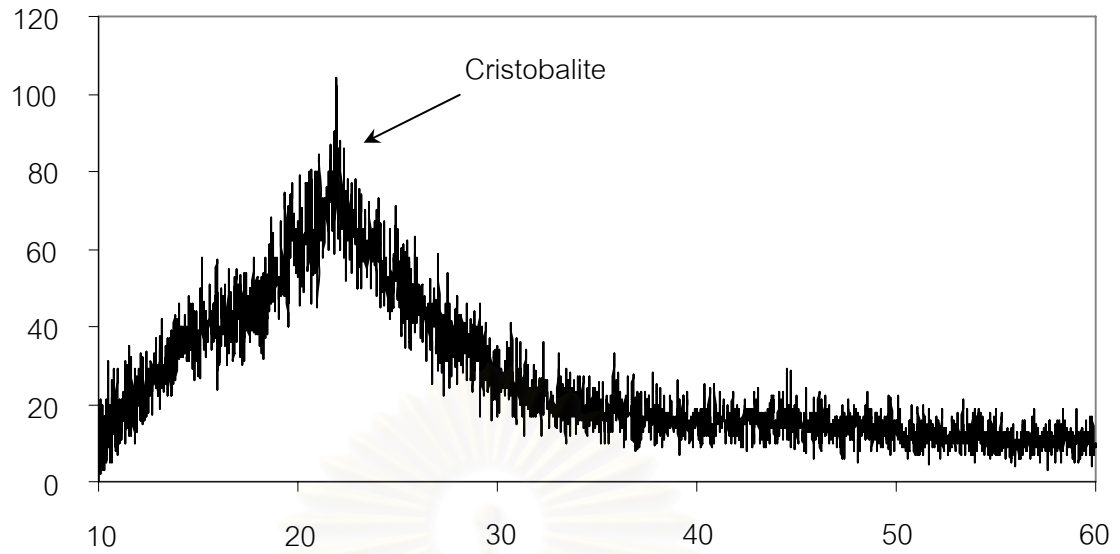


Figure 23 CE-LM 600 (KANSAI CORPORATION, JAPAN)

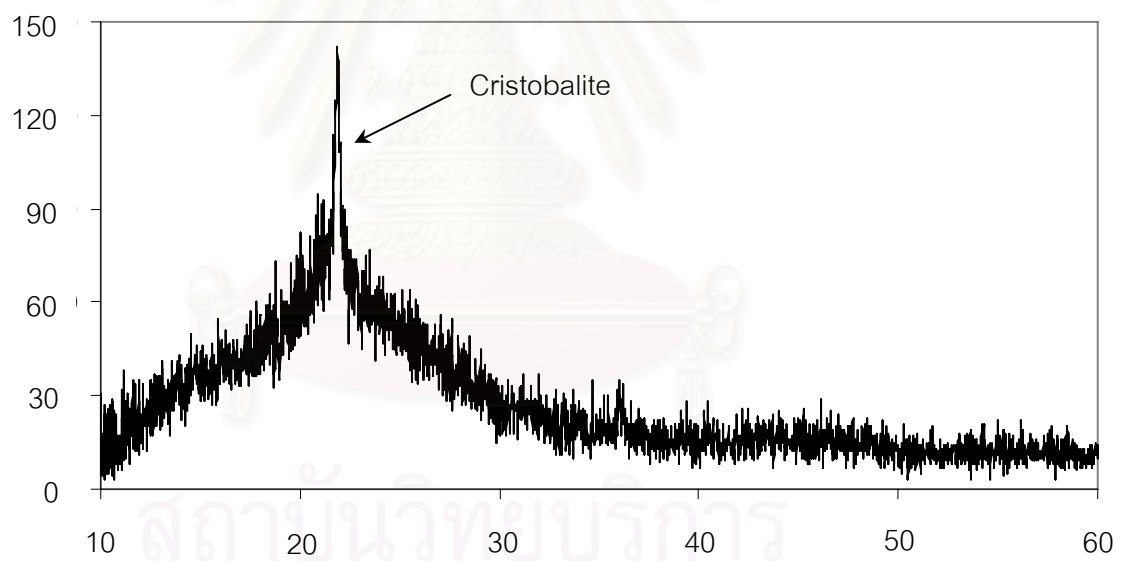


Figure 24 RC-DK/750 (KANSAI CORPORATION, JAPAN)

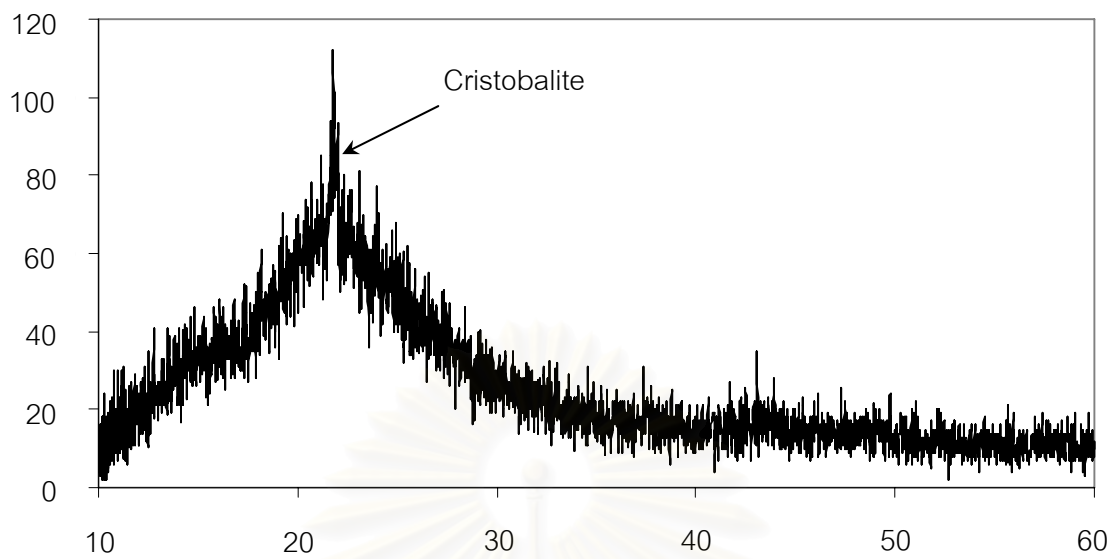


Figure 25 CE-DK/750 (KANSAI CORPORATION, JAPAN)

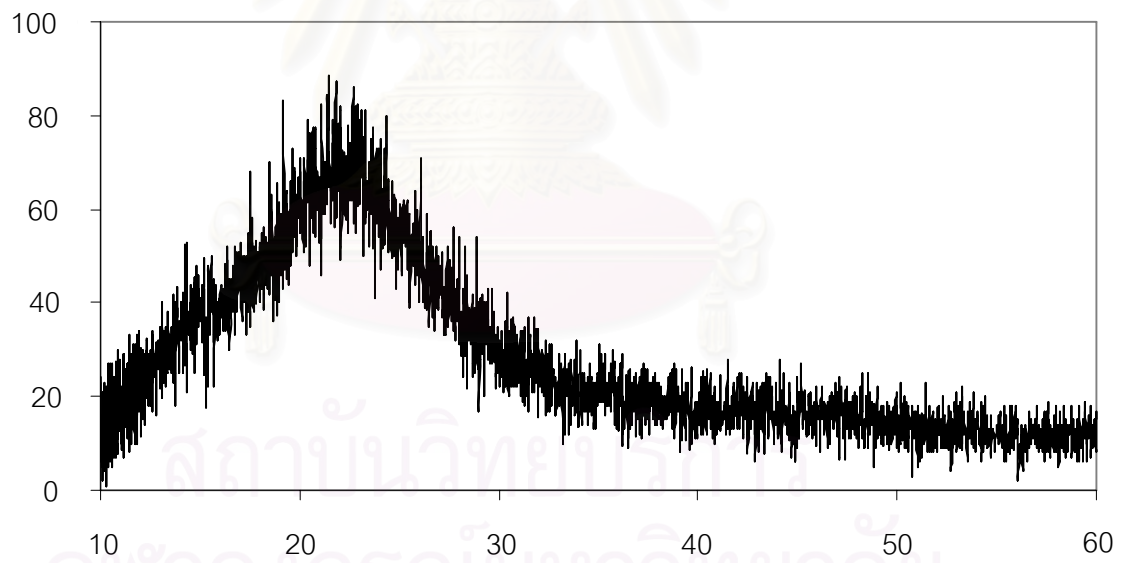


Figure 26 LM-900 Black (KANSAI CORPORATION, JAPAN)

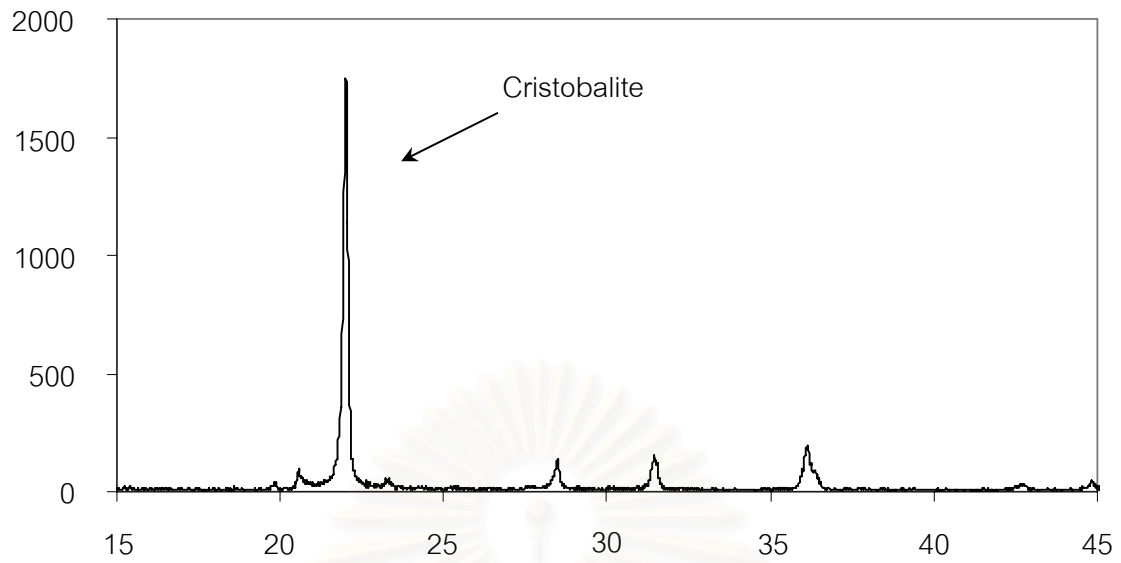


Figure 27 LM-900 White (KANSAI CORPORATION, JAPAN)

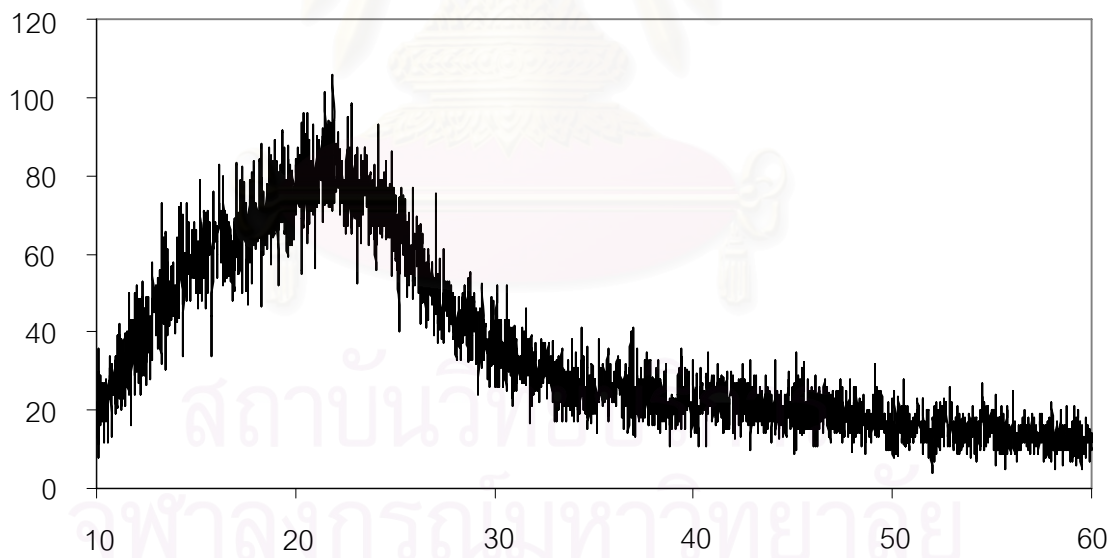


Figure 28 Outer heat 400 (MEIWA CORPORATION, JAPAN)

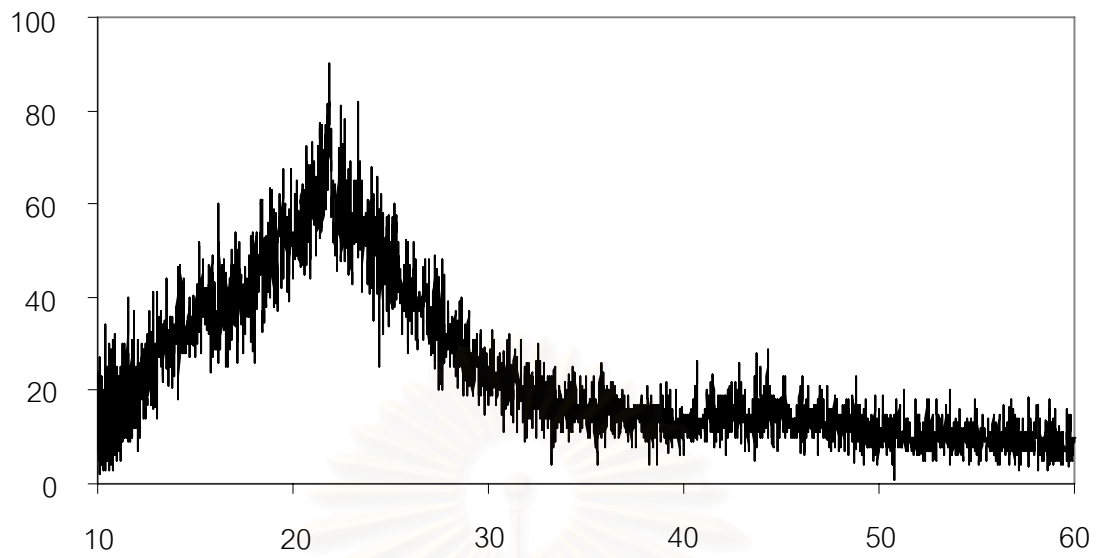


Figure 29 Inter heat (MEIWA CORPORATION, JAPAN)

สถาบันวิทยบริการ
จุฬาลงกรณ์มหาวิทยาลัย

APPENDIX E

Tensile strength data of plastic films including 1-2% of Cristobalite

Table 2 1% M4000 MD

	Tensile stress at Break (MPa)	Elongation at break (%)	Gauge Length (mm)	Thickness (mm)	Width (mm)
1	26.7	492	50.0	0.03	19.5
2	31.0	518	50.0	0.03	19.5
3	31.1	517	50.0	0.03	19.5
4	28.6	509	50.0	0.03	19.5
Mean	29.4	509			
STDV	2.01	12.3			

Table 3 1% M4000 TD

	Tensile stress at Break (MPa)	Elongation at break (%)	Gauge Length (mm)	Thickness (mm)	Width (mm)
1	38.9	616	50.0	0.03	19.5
2	39.0	596	50.0	0.03	19.5
3	39.7	619	50.0	0.03	19.5
4	38.2	604	50.0	0.03	19.5
5	37.2	591	50.0	0.03	19.5
Mean	38.6	605			
STDV	0.94	12.1			

Table 4 2% M4000 MD

	Tensile stress at Break (MPa)	Elongation at break (%)	Gauge Length (mm)	Thickness (mm)	Width (mm)
1	32.6	511	50.0	0.03	19.5
2	33.9	531	50.0	0.03	19.5
3	33.3	529	50.0	0.03	19.5
4	33.3	532	50.0	0.03	19.5
5	33.3	504	50.0	0.03	19.5
Mean	33.3	521			
STDV	0.47	13.0			

Table 5 2% M4000 TD

	Tensile stress at Break (MPa)	Elongation at break (%)	Gauge Length (mm)	Thickness (mm)	Width (mm)
1	33.4	559	50.0	0.03	19.5
2	31.3	559	50.0	0.03	19.5
3	33.2	571	50.0	0.03	19.5
4	30.6	541	50.0	0.03	19.5
5	31.1	559	50.0	0.03	19.5
Mean	31.8	558			
STDV	1.41	10.8			

Table 6 1% R3CY MD

	Tensile stress at Break (MPa)	Elongation at break (%)	Gauge Length (mm)	Thickness (mm)	Width (mm)
1	31.9	570	50.0	0.04	19.5
2	34.7	590	50.0	0.04	19.5
3	30.1	545	50.0	0.04	19.5
4	33.0	591	50.0	0.04	19.5
Mean	32.4	574			
STDV	1.94	21.6			

Table 7 1% R3CY TD

	Tensile stress at Break (MPa)	Elongation at break (%)	Gauge Length (mm)	Thickness (mm)	Width (mm)
1	27.8	575	50.0	0.03	19.5
2	27.1	568	50.0	0.03	19.5
3	28.9	607	50.0	0.03	19.5
4	28.0	592	50.0	0.03	19.5
5	27.8	590	50.0	0.03	19.5
Mean	27.9	586			
STDV	0.65	15.3			

Table 8 2% R3CY MD

	Tensile stress at Break (MPa)	Elongation at break (%)	Gauge Length (mm)	Thickness (mm)	Width (mm)
1	35.9	536	50.0	0.03	19.5
2	36.2	550	50.0	0.03	19.5
3	35.2	554	50.0	0.03	19.5
4	33.0	533	50.0	0.03	19.5
5	35.2	530	50.0	0.03	19.5
Mean	35.1	541			
STDV	1.24	11.0			

Table 9 2% R3CY TD

	Tensile stress at Break (MPa)	Elongation at break (%)	Gauge Length (mm)	Thickness (mm)	Width (mm)
1	39.3	622	50.0	0.04	19.5
2	37.9	604	50.0	0.04	19.5
3	36.8	585	50.0	0.04	19.5
4	37.3	600	50.0	0.04	19.5
Mean	37.8	603			
STDV	1.07	15.3			

Table 10 1% R4CY MD

	Tensile stress at Break (MPa)	Elongation at break (%)	Gauge Length (mm)	Thickness (mm)	Width (mm)
1	37.2	557	50.0	0.03	19.5
2	37.1	550	50.0	0.03	19.5
3	38.2	575	50.0	0.03	19.5
4	35.0	550	50.0	0.03	19.5
5	38.8	566	50.0	0.03	19.5
Mean	37.3	559			
STDV	1.43	10.9			

Table 11 1% R4CY TD

	Tensile stress at Break (MPa)	Elongation at break (%)	Gauge Length (mm)	Thickness (mm)	Width (mm)
1	34.7	581	50.0	0.03	19.5
2	31.6	584	50.0	0.03	19.5
3	35.1	578	50.0	0.03	19.5
4	31.8	564	50.0	0.03	19.5
5	34.7	590	50.0	0.03	19.5
Mean	33.6	579			
STDV	1.72	9.70			

Table 12 2% R4CY MD

	Tensile stress at Break (MPa)	Elongation at break (%)	Gauge Length (mm)	Thickness (mm)	Width (mm)
1	27.4	479	50.0	0.03	19.5
2	26.0	480	50.0	0.03	19.5
3	26.8	476	50.0	0.03	19.5
4	26.3	481	50.0	0.03	19.5
Mean	26.6	479			
STDV	0.62	2.00			

Table 13 2% R4CY TD

	Tensile stress at Break (MPa)	Elongation at break (%)	Gauge Length (mm)	Thickness (mm)	Width (mm)
1	28.1	547	50.0	0.03	19.5
2	29.8	576	50.0	0.03	19.5
3	31.1	551	50.0	0.03	19.5
4	31.1	558	50.0	0.03	19.5
Mean	30.0	558			
STDV	1.43	12.7			

Table 14 1% R5CY MD

	Tensile stress at Break (MPa)	Elongation at break (%)	Gauge Length (mm)	Thickness (mm)	Width (mm)
1	15.3	391	50.0	0.03	19.5
2	14.2	358	50.0	0.03	19.5
3	14.0	346	50.0	0.03	19.5
4	14.1	353	50.0	0.03	19.5
5	14.6	360	50.0	0.03	19.5
Mean	14.4	362			
STDV	0.55	17.4			

Table 15 1% R5CY TD

	Tensile stress at Break (MPa)	Elongation at break (%)	Gauge Length (mm)	Thickness (mm)	Width (mm)
1	17.5	471	50.0	0.03	19.5
2	18.3	470	50.0	0.03	19.5
3	19.2	466	50.0	0.03	19.5
4	18.4	468	50.0	0.03	19.5
5	17.3	474	50.0	0.03	19.5
Mean	18.1	470			
STDV	0.78	3.06			

Table 16 2% R5CY MD

	Tensile stress at Break (MPa)	Elongation at break (%)	Gauge Length (mm)	Thickness (mm)	Width (mm)
1	14.8	376	50.0	0.04	19.5
2	14.8	386	50.0	0.04	19.5
3	14.3	385	50.0	0.04	19.5
4	15.8	403	50.0	0.04	19.5
Mean	14.9	388			
STDV	0.64	11.2			

Table 17 2% R5CY TD

	Tensile stress at Break (MPa)	Elongation at break (%)	Gauge Length (mm)	Thickness (mm)	Width (mm)
1	13.9	373	50.0	0.04	19.5
2	11.9	401	50.0	0.04	19.5
3	12.5	390	50.0	0.04	19.5
4	13.4	368	50.0	0.04	19.5
Mean	13.0	383			
STDV	0.89	15.3			

Low data tensile strength of plastic films included 1-2% of Amorphous silica

Table 18 LLDPE Control MD

	Tensile stress at Break (MPa)	Elongation at break (%)	Gauge Length (mm)	Thickness (mm)	Width (mm)
1	39.4	589	50.0	0.04	19.5
2	37.1	563	50.0	0.04	19.5
3	38.1	578	50.0	0.04	19.5
4	37.1	594	50.0	0.04	19.5
5	35.6	587	50.0	0.04	19.5
Mean	37.5	582			
STDV	1.42	12.05			

Table 19 LLDPE Control TD

	Tensile stress at Break (MPa)	Elongation at break (%)	Gauge Length (mm)	Thickness (mm)	Width (mm)
1	31.1	596	50.0	0.04	19.5
2	33.6	626	50.0	0.04	19.5
3	30.1	596	50.0	0.04	19.5
4	28.5	587	50.0	0.04	19.5
5	-	633	50.0	0.04	19.5
Mean	30.8	607			
STDV	2.16	20.4			

Table 20 1% Unwashed MD

	Tensile stress at Break (MPa)	Elongation at break (%)	Gauge Length (mm)	Thickness (mm)	Width (mm)
1	29.6	520	50.0	0.04	19.5
2	28.4	501	50.0	0.04	19.5
3	31.4	549	50.0	0.04	19.5
4	27.6	518	50.0	0.04	19.5
5	27.6	508	50.0	0.04	19.5
Mean	28.9	519			
STDV	1.60	18.8			

Table 21 1% Unwashed TD

	Tensile stress at Break (MPa)	Elongation at break (%)	Gauge Length (mm)	Thickness (mm)	Width (mm)
1	27.2	369	50.0	0.04	19.5
2	29.8	375	50.0	0.04	19.5
3	29.2	365	50.0	0.04	19.5
4	28.5	388	50.0	0.04	19.5
5	25.9	377	50.0	0.04	19.5
Mean	28.1	375			
STDV	1.59	8.86			

Table 22 2% Unwashed MD

	Tensile stress at Break (MPa)	Elongation at break (%)	Gauge Length (mm)	Thickness (mm)	Width (mm)
1	27.9	508	50.0	0.04	19.5
2	27.1	506	50.0	0.04	19.5
3	34.0	557	50.0	0.04	19.5
4	27.9	495	50.0	0.04	19.5
5	29.2	526	50.0	0.04	19.5
Mean	29.2	519			
STDV	2.76	24.3			

Table 23 2% Unwashed TD

	Tensile stress at Break (MPa)	Elongation at break (%)	Gauge Length (mm)	Thickness (mm)	Width (mm)
1	31.9	595	50.0	0.04	19.5
2	29.1	573	50.0	0.04	19.5
3	27.8	590	50.0	0.04	19.5
4	28.8	577	50.0	0.04	19.5
5	30.3	581	50.0	0.04	19.5
Mean	29.6	583			
STDV	1.60	9.36			

Table 24 1% Water MD

	Tensile stress at Break (MPa)	Elongation at break (%)	Gauge Length (mm)	Thickness (mm)	Width (mm)
1	25.5	496	50.0	0.04	19.5
2	29.7	519	50.0	0.04	19.5
3	29.1	505	50.0	0.04	19.5
4	28.4	498	50.0	0.04	19.5
Mean	28.2	505			
STDV	1.87	10.7			

Table 25 1% Water TD

	Tensile stress at Break (MPa)	Elongation at break (%)	Gauge Length (mm)	Thickness (mm)	Width (mm)
1	21.7	525	50.0	0.04	19.5
2	26.3	556	50.0	0.04	19.5
3	24.4	539	50.0	0.04	19.5
4	24.6	549	50.0	0.04	19.5
5	22.8	520	50.0	0.04	19.5
Mean	23.9	538			
STDV	1.75	15.5			

Table 26 2% Water MD

	Tensile stress at Break (MPa)	Elongation at break (%)	Gauge Length (mm)	Thickness (mm)	Width (mm)
1	24.3	475	50.0	0.04	19.5
2	26.8	473	50.0	0.04	19.5
3	23.2	491	50.0	0.04	19.5
4	24.8	458	50.0	0.04	19.5
5	22.9	454	50.0	0.04	19.5
Mean	24.4	470			
STDV	1.55	14.7			

Table 27 2% Water TD

	Tensile stress at Break (MPa)	Elongation at break (%)	Gauge Length (mm)	Thickness (mm)	Width (mm)
1	21.7	521	50.0	0.04	19.5
2	23.2	521	50.0	0.04	19.5
3	25.7	551	50.0	0.04	19.5
4	22.6	514	50.0	0.04	19.5
5	25.1	544	50.0	0.04	19.5
Mean	23.7	530			
STDV	1.71	16.3			

APPENDIX F

Table 28 Chemical compositions of rice husk ash from various washed condition

Oxide	unwashed	S1-15	S1-30	S1-45	S2-24	S2-48	S2-72
SiO ₂	94.00	95.65	96.18	95.96	96.09	96.02	95.76
K ₂ O	2.21	1.14	0.55	0.33	0.55	0.24	0.22
Na ₂ O	0.20	0.20	0.23	0.22	0.15	0.16	0.15
MgO	0.56	0.50	0.47	0.46	0.38	0.32	0.33
Al ₂ O ₃	0.49	0.23	0.12	0.12	0.56	0.90	0.81
P ₂ O ₅	0.67	0.43	0.32	0.26	0.30	0.19	0.19
SO ₃	0.21	0.38	0.40	0.39	0.36	0.37	0.38
Cl	0.27	0.15	0.17	0.16	0.16	0.17	0.15
Fe ₂ O ₃	0.16	0.04	0.02	0.00	0.18	0.30	0.28
B ₂ O ₃	0.11	0.04	0.00	0.51	0.00	0.00	0.38
CaO	0.94	1.10	1.39	1.45	1.10	1.18	1.19
TiO ₂	0.03	0.01	0.01	0.01	0.03	0.06	0.06
MnO	0.16	0.14	0.14	0.13	0.14	0.10	0.10
	100.01	100.01	99.99	99.99	100.00	100.00	99.99

* Ratchaburi source

สถาบันวิทยบริการ
จุฬาลงกรณ์มหาวิทยาลัย

Table 29 Chemical compositions of RHA for 2 different sources of rice husk and various calcined temperatures at 450, 550 and 650°C

Nakhonratchasima	Soak 5 h			Soak 10 h		
Oxide	450°C	550°C	650°C	450°C	550°C	650°C
SiO ₂	97.47	97.52	97.51	97.52	97.61	97.6
K ₂ O	0.26	0.26	0.26	0.23	0.21	0.2
Na ₂ O	0.08	0.09	0.1	0.08	0.09	0.08
CaO	1.28	1.27	1.3	1.35	1.34	1.33
Fe ₂ O ₃	-	-	-	-	-	-
Al ₂ O ₃	0.12	0.06	0.05	0.07	0.03	0.05
P ₂ O ₅	0.14	0.15	0.15	0.16	0.14	0.13
SO ₃	0.25	0.26	0.24	0.23	0.24	0.24
Cl	0.02	0.02	0.01	0.03	0.01	0.01
MgO	0.24	0.24	0.25	0.23	0.24	0.24
MnO	0.11	0.1	0.1	0.08	0.08	0.08
Sum	99.97	99.97	99.97	99.98	99.99	99.96
Ratchaburi	Soak 5 h			Soak 10 h		
Oxide	450°C	550°C	650°C	450°C	550°C	650°C
SiO ₂	96.43	96.49	96.49	96.42	96.26	96.36
K ₂ O	0.45	0.41	0.42	0.46	0.48	0.42
Na ₂ O	0.11	0.12	0.12	0.1	0.11	0.12
CaO	1.72	1.72	1.7	1.8	1.86	1.84
Fe ₂ O ₃	0.02	0.01	0.02	0	0.02	0.01
Al ₂ O ₃	0.1	0.1	0.13	0.14	0.12	0.15
P ₂ O ₅	0.24	0.24	0.23	0.23	0.23	0.21
SO ₃	0.35	0.34	0.32	0.32	0.35	0.35
Cl	0.05	0.01	0.01	0.04	0.04	0.01
MgO	0.35	0.37	0.38	0.31	0.35	0.35
MnO	0.14	0.15	0.16	0.13	0.13	0.13
Sum	99.96	99.96	99.98	99.95	99.95	99.95

BIOGRAPHY

Mr. Verasak Mosungnoen was born in Nakhonratchasima on September 20th, 1976. In 2000, he finished his Bachelor's Degree in Chemistry Science from the Department of Chemistry, Faculty of Science, Ratchabhat Institute Nakhonratchasima. In the same year, he started working as an assistant researcher at the Siam Cement Group Industries. In 2004, he left to study for Master's Degree in the field of Ceramic Technology at Chulalongkorn University and graduate in 2007.



สถาบันวิทยบริการ
จุฬาลงกรณ์มหาวิทยาลัย